Doctoral Dissertation

Shibaura Institute of Technology

Topology Optimization for Nonlinear Material Structures based on Proportional Technique

September 2020

Suphanut Kongwat

SHIBAURA INSTITUTE OF TECHNOLOGY

Topology Optimization for Nonlinear Material Structures based on Proportional Technique

By

Suphanut Kongwat

A dissertation submitted in partial fulfillment
of the requirements for the degree of
Doctor of Philosophy

in the
Department of Functional Control Systems
Graduate School of Engineering and Science

September 2020

Declaration of Authorship

I, Suphanut KONGWAT, declare that this thesis titled, "Structural Optimization of Material Nonlinearities based on Topology Design by using Proportional Technique," and the work presented in it are my own. I confirm that:

- This work was done wholly or mainly while in candidature for a research degree at Shibaura Institute of Technology.
- Where any part of this thesis has previously been submitted for a degree or any other qualification at Shibaura Institute of Technology or any other institution, this has been clearly stated.
- Where I have consulted the published work of other, this is always clearly attributed.
- Where I have quoted from the work of others, the source is always given. With the exception of such quotations, this thesis is entirely my own work.
- I have acknowledged all main sources of help.

Signed: _____

Date: _____

"Our greatest weakness lies in giving up.

The most certain way to succeed is always to try just one more time."

…Thomas A. Edison

Acknowledgements

Firstly, I would like to express my sincere gratitude to my advisor Prof. Dr. Hiroshi Hasegawa for the continuous support of my Ph.D. study and related research, for his patience, motivation, and immense knowledge. His guidance helped me in all the time of research and writing of this thesis. I could not have imagined having a better advisor and mentor for my Ph.D. study.

Next, I would like to address my appreciation to Ministry of Education, Culture, Sports, Science and Technology on Japanese government for providing the scholarship under Monbukagakusho (MEXT) program. All transactions and financial supports are advanced to study in Doctoral course.

Last but not the least, I would like to thank my family, my parents and to my friends for providing me with unfailing support and continuous encouragement throughout my years of study and through the process of researching and writing this dissertation. This accomplishment would not have been possible without them.

Suphanut Kongwat

Dissertation Title	Topology Optimization for Nonlinear Material Structures based on Proportional Technique
Candidate	Suphanut Kongwat
Thesis Advisor	Prof. Dr. Hiroshi Hasegawa
Program	Doctor of Philosophy
Field of Study	Research in Topology Design for Mechanical Engineering
Department	Functional Control Systems
Faculty	Graduate School of Engineering and Science
Academic Year	2020

Abstract

Topology optimization is a preliminary process for the structural design to acquire an optimal layout based on each boundary condition. Moreover, the topology optimization is the most complex on the design process due to the optimal layout acquires from an unknown initial design. In automotive manufacturers, a nonlinear design is important for the safety of occupants to increase a deformation while keeping the transmitted load, such as a crashworthiness design. So, this research proposed the methodology and algorithm for topology optimization under material nonlinearities. Solid Isotropic Material with Penalization (SIMP) approach was employed for the optimization algorithm to determine the optimal layout. Element densities of design variables were updated based on a proportional algorithm, which is a non-sensitivity method for finding a suitable value of the element density in each iteration. The new proportional algorithm was introduced and formulated for updating the element densities by concerning the criteria of fully stressed design for topology optimization. The proportional topology optimization for nonlinear material behavior was first verified for investigating the performance of this algorithm by comparing it with the optimal layout on the gradient method. The optimal layout on the proportional technique showed significantly effective for the nonlinear optimization procedure.

Next, a characteristic of bilinear elastoplastic material was concerned for optimizing with the static load was applied. The objective of the optimization problem is to maximize the internal energy of the structure subjected to the maximum limit of the von mises stresses to avoid failure behavior. The results from the geometrical nonlinear structure were completely different when concerned with only elasticity structure. Besides, cyclic loading was applied to the structure for topology optimization under the material characteristic of isotropic and kinematic hardening. In this case, an unloading behavior was considered during the nonlinear optimization process to acquire the optimal layout. A common weight filtering factor cannot clearly obtain a final layout from topology design when the unloading behavior was concerned. Finally, a new weight filtering factor was introduced to acquire a clear layout from nonlinear topology design without the effect of unloading behavior and possesses all requirements for optimization constraint.

Keywords: Cyclic loading, Nonlinear structure, Structural design, Topology optimization, Weight filtering factor

Contents

List of Figures

List of Tables

Chapter 1

INTRODUCTION

1.1 Background and Signification of this Research

Structural optimization is a technique to find an optimal layout for the structure under various loading and boundary conditions. The final layout after the optimization procedure will be shown the suitable layout corresponding to the user-defined objective and optimization constraint. Generally, there are three types of structural optimization: size optimization, shape optimization, and topology optimization. The size optimization is the simplest technique of the structural optimization and applies for adjusting the size or thickness of the structural components. Figure 1.1a shows an example of the size optimization when a diameter of each rod is assigned to be the design variable. In shape optimization, the design variable can be an example of the diameter of holes, the radius of fillets or any other measure and will not result in new holes or split bodies apart (figure 1.1b). Both size and shape optimizations are acquired the final results when the preliminary design layout is already known. Topology optimization is the most common form for

structural optimization and usually applies to be the preliminary design process. Purpose of the topology optimization is to find an optimum material distribution inside the design domain by assigning the element density of each element to be the design variable. For topology optimization, the result will be shown a necessary area of material which should remain (solid element) or the useless area which should remove (void element). As mentioned above, only topology optimization has to determine the optimum distribution of material by not considering the layout of the initial design domain.

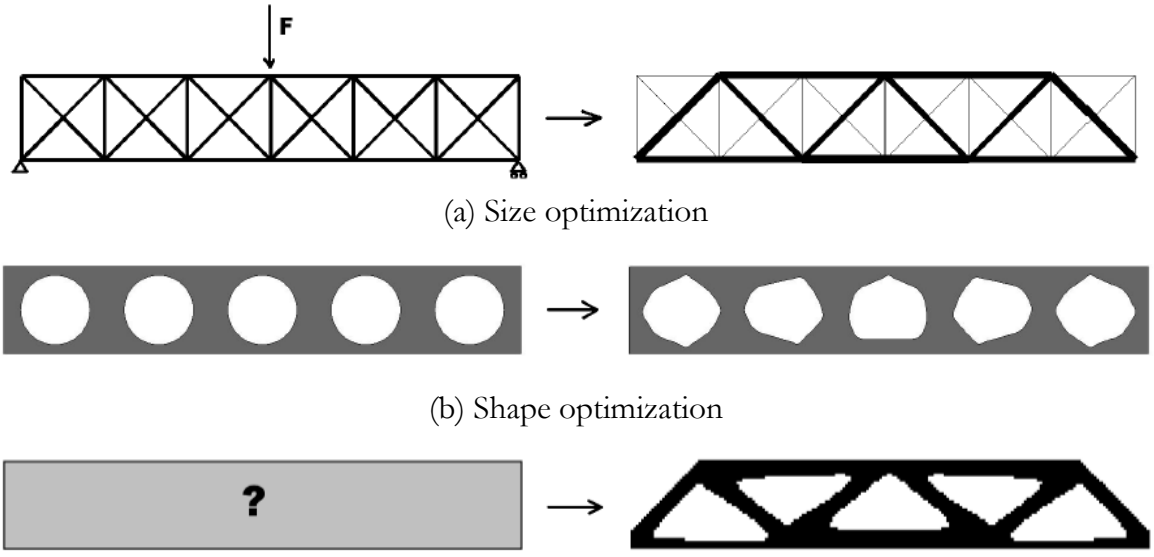

(a) Size optimization

(b) Shape optimization

(c) Topology optimization

Figure 1.1 Types and overview of structural optimization [1].

The most general problem for topology optimization is a structure subjected to the static load and assumed a small displacement to that problem. To optimize the structure, the objective for these cases usually define for two different problems: maximized stiffness of structure under volume constraint or minimized the mass of the given design area by concerning the stiffness or stress of the structure. The optimal distribution of material will be showed into difference layout and amount of element density based on the objective and optimization constraint of each problem. There is no efficient method for solving all

the optimization problems. Therefore, a number of optimization methods have been developed for solving various optimization problems in which the optimal seeking method is also known as a mathematical programming technique. For the topology optimization, there are also many optimization algorithms are employed for investigating the best result. In order to acquire the final layout, the optimization algorithms are integrated with a numerical analysis such as the meshfree method or finite element method (FEM).

The topology optimization always concerns for a linear problem or elastic material properties in which the structure can recover after deformed. However, when the external load is applied to the structure and causes large deformation, this case is necessary to consider the problem into nonlinearity. There are three categories for consideration the nonlinearities for mechanical structure: contact or friction problems, kinematics problems (large displacement, large rotation, etc.), and material nonlinearities problems. The technique for seeking the optimal layout under the nonlinear structure might be different and depended on the application of each problem. So, a methodology, algorithm, and the layout for topology optimization under nonlinear problems are also a difference from the elasticity.

Nonlinear topology optimization is a challenging problem to acquire an optimal layout due to the characteristic of material properties and nonlinear problems. An effective algorithm is necessary to suggest for optimization under nonlinear design due to the behavior of permanent deformation is completely different from the elasticity design. According to the application of automotive manufacturer, the structure is expected to increase a deformation via internal energy density while keeping the force transmitted to the occupants. Likewise, stiffness of the design area is also focused for increasing during the permanent deformation without failure. Since the characteristic of load-displacement curve of nonlinear geometry shows the value of compliance is not equal to two times of strain energy and complementary work. Therefore, the user needs to define the objective and optimization constraint according to the application of their problems. Moreover, an algorithm for nonlinear optimization also needs to implement and develop to obtain an effective method for topology technique.

To achieve the problem of nonlinear topology optimization, this dissertation aims to propose the proportional method for updating the element density during topology optimization under fully nonlinear analysis. The proportional algorithm is implemented by including the fully stress design criteria for topology design as a factor of the update function. The optimization method performs with Solid Isotropic Material with Penalization (SIMP) approach according to an application of crashworthiness design. A study on static and cyclic loads were conducted to acquire the optimal layout based on structural topology design in this dissertation. The optimal layout should clearly obtain for nonlinear topology optimization and different from the elastic behavior. A new weight filtering factor for cyclic loading of topology design also proposed in this research. Finally, numerical examples based on the nonlinear design with the proportional technique are also examined.

1.2 Objectives

1.2.1 Optimize a mechanical structure under topology optimization by concerning nonlinear problem based on nonlinear material geometries:

This dissertation aims to optimize the mechanical structure by using the topology optimization method under nonlinear behavior. A nonlinear analysis and nonlinear material geometries will be concerned during the optimization procedure. Therefore, the permanent deformation of the structure will be included for acquiring the final layout.

1.2.2 Implement an update function for nonlinear structural design for updating an element density of each design variable:

The update function is required for updating an element density of each iterative calculation during topology optimization. For nonlinear analysis, a stress behavior is not constant in the linear relationship for all analysis procedures. So, a technique for updating the element density will be developed in this research.

1.2.3 Design the structure based on topology technique with a static and cyclic loads are applied as an external load:

An external load is applied based on the characteristic of static and cyclic loads to the structure by concerning an unloading effect. For the cyclic load, an unloading point affects structural behavior when the permanent deformation is concerned. Therefore, an optimization procedure and structural behavior between static and cyclic load will be different and affects the final layout.

1.2.4 Propose a new weight filtering equation for designing the structure under topology optimization when unloading behavior is concerned:

To avoid a checkboard pattern problem during the optimization procedure, the weight filtering equation is used for investigating a neighbor element connectivity. Thus, the efficient filtering factor indicates the good final layout after topology optimization and performs a numerical analysis for all procedures.

1.3 Scopes of the Dissertation

1.3.1 Optimal layouts of a prescribed design domain are determined by investigating an element density of each design variable based on topology optimization procedure as the preliminary design process.

1.3.2 Nonlinear analysis is considered on the category of material characteristic of nonlinear behavior on two types: bilinear elastoplastic material property and isotropic and kinematic hardening material property.

1.3.3 Structural models are created and analyzed by finite element technique based on LS-DYNA software while the optimization performed on MATLAB coding to determine an element density and optimal layout of the structure.

1.3.4 Numerical examples are focused on shell element model (2D element) with concerned the material distribution for the optimization process on two-dimensional only. Shear stress, which causes along to direction of load, is assumed to be small and neglect in this study.

1.4 Dissertation Outline

This dissertation aims to present the methodology for nonlinear topology optimization under material nonlinearities. Therefore, the structure of this dissertation is organized as follows:

Chapter 1 introduced the background and signification of this study. The objectives and scopes was set to achieve the target of the current work. Moreover, related studies also reviewed for concerning on method and procedure of this research.

Chapter 2 explains on the theoretical issue of structural optimization and nonlinear finite element analysis. A general formulation of the optimization process and complements of the topology optimization problem are described to conduct the complete optimization problem before optimizing the structure. And the problem of nonlinear topology design is also explained in this chapter.

Chapter 3 describes on opportunities to apply the nonlinear topology optimization for application of crashworthiness design. A fully dynamic analysis by finite element always uses to investigate the structural strength and occupant's safety. Therefore, optimization on dynamic problem by finite element is a one choice for engineering design for automotive manufacturer.

Chapter 4 proposes a new proportional algorithm for updating element densities during topology optimization. The updated procedure of the proportional technique will display in this chapter until it obtains the optimal density of each design variable.

Chapter 5 shows a validation process on the new proportional algorithm with nonlinear

topology design. The optimal layout is compared with the results on the gradient approach to investigate an effective on this algorithm and procedure.

Chapter 6 investigates an optimal layout for nonlinear topology optimization by focusing on static analysis with the constant load. Over-relaxation factor uses for reducing a computation cost during the optimization procedure are also examined. The layout from the nonlinear analysis is compared with the elastic material property.

Chapter 7 shows an optimization process when the cyclic loading is applied. The optimal layout cannot acquire with a common weight filtering factor. So, the new weight filtering factor is proposed in this chapter for nonlinear topology optimization under cyclic loading.

Chapter 8 is a final chapter in this dissertation and concludes the study along with discussion regarding future works opportunities in this research.

1.5 Literature Review

Structural optimization is a process to design a suitable condition corresponding to each problem. There are three categories for structural optimization: size optimization, shape optimization, and topology optimization. Size and shape optimization is used for optimizing the structure when their initial design already obtained. On the other hand, the topology optimization applies to determine a preliminary layout from unknown shape and size of that structure. Therefore, topology optimization is the most complicated method and technique for the structural design process.

Topology optimization based on linear problem concerned a structure under elasticity or assuming to be a small deformation. Many optimization algorithms have been proposed for linear topology optimization in various applications and methodologies. The density approach is implemented to optimize a structure with maximizing the stiffness and defined an allowable mass of the design area [2]. A modified density approach has developed the algorithm by applying a penalization factor, so-called Solid Isotropic Material

with Penalization (SIMP) approach and employed to optimize the structure under the two-dimensional problem [3]. Likewise, a three-dimensional problem was also determined the final layout based on the regularized SIMP interpolation approach under stiffness and volume conditions [4]. The level set approach is one technique to acquire the optimal layout by using iso-surface of the level set function. A two-dimensional structure was optimized based on the level set method and combined with discrete function [5] and the reaction-diffusion equation [6] under linear problems. Moreover, the immersed interface method [7] and fictitious interface energy [8] also proposed for combining with the level set method for solving the topology optimization problem. The combination of the topological level set method, augmented Lagrangian algorithm, and assembly-free deflated finite element was suggested for solving multi-constraint on a three-dimensional topology problem [9]. As mentioned above, both SIMP and level set approaches are common schemes for seeking the optimal layout of the structure. Furthermore, a discrete method, which is a hard-killed approach (indicates only presence or absence materials), is also applied for finding the optimal layout under topology optimization. A genetic algorithm [10] or Ant colony optimization [11] were also adopted and acquired the suitable structure under linear problem. A commercial software was implemented for optimizing the structure under topology and multidisciplinary design [12, 13], and used that design process for application of engineering to design the vehicle structure based on the results from finite element analysis [14, 15]. Most studies usually seek a suitable layout based on maximizing stiffness under mass constraint and volume minimization under displacement constraint. However, both cases can generate the final layout-based material distribution, which sustains the best way for the applied load under user-defined boundary conditions [16].

When an external load is applied to the structure and causes a large deformation to the structure, the nonlinear analysis should be concerned for that condition. A high computational cost is required to calculate the optimal layout under nonlinear topology optimization. An evolutionary method [17] and a revised bi-directional evolutionary optimization (BESO) [18] method was used to maximize the structural stiffness for nonlinear topology design. A sequential piecewise linear programming (SPLP) is

mathematical programming which proposed to solve topology optimization under large displacement problem [19]. All subproblems of the SLPL method were converted into linear programming to speed up the algorithm on the nonlinear design. Nonlinear programming has investigated performance on the level set approach for topology optimization with methods of moving asymptotes (MMA) and a globally convergent modification under nonlinear problems [20]. Kreisselmeier-Steinhauser (KS) function was maximized for solving the geometrically nonlinear structure by using the level set method under volume constraint [21]. The results were effectively compared to the final layout from other criteria of stiffness problems. These problems were assumed for the large displacement of the structure under linear analysis for nonlinear behavior. A mesh-free particle technique was also proposed to determine the optimal structure under the geometrical nonlinearity problem by using the level set approach [22]. Reduced Order Model (ROM) was introduced to alleviate the heavy computational cost of nonlinear topology optimization [23]. The ROM can reduce a multiscale model for macroscopic structural design on stiffness problem using discrete level-set approach. A nature-inspired method, which imitates an animal behavior in nature, was a one optimization technique and developed for solving the problem on nonlinear topology optimization. Artificial bee colony algorithm (ABCA) was used with a rank-based method to improve the candidate solutions and results [24], while a modified ant colony optimization (ACO) was developed to obtain a stable robust design [25]. Both ABCA and ACO were adopted to optimize the structure under structural stiffness problems. Most studies focused on the stiffness of structure on nonlinear geometry due to compliance of the structure is not equal to two times of complementary work and strain energy [20], along to the typical of load-displacement cure of nonlinear structure (figure 1.2). Therefore, different results may be obtained if a different function is used in optimization process under geometrical nonlinearity.

Element distortion in finite element analysis often encountered when considering the large displacement. This problem is kind of a serious issue for topology optimization due to it caused a numerical instability during the optimization procedure. To avoid this

problem, a meshless method was employed to resolve the nonlinear topology problem, which formulated with the element-free Galerkin (EFG) method [26]. Element connectivity parameterization (ECP) was introduced to resolve an analytic sensitivity problem on nonlinear topology optimization when the commercial nonlinear finite element code is used for the two-dimensional problem [27]. In the same way as a three-dimensional problem, an internal ECP (I-ECP) also developed to substantially enhance computational efficiency on topology optimization under nonlinear material behaviors [28].

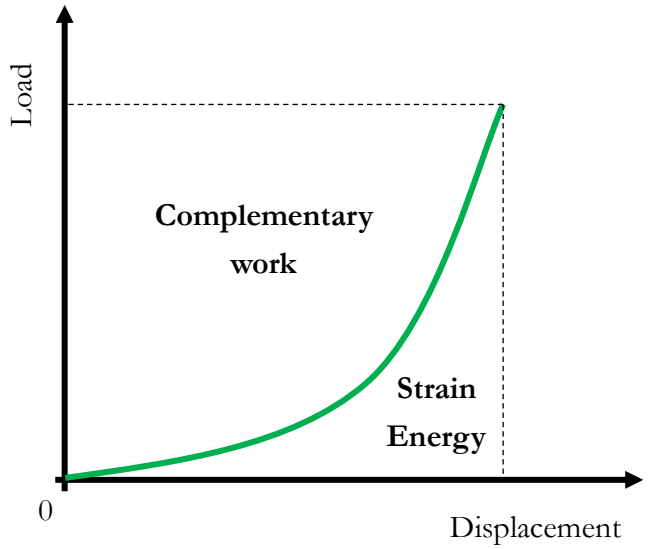

Figure 1.2 A load-displacement curve of geometrically nonlinear structure.

A sensitivity analysis is commonly required through the optimization process under nonlinear topology design. The sensitivities of the objective functions were derived and conformed to the adjoint method [18, 29, 30]. On the other hand, a non-sensitivity approach also proposed as a proportional method for optimizing the structure under the topology problem. Mechanical structures were optimized by manipulating the proportional method [31], and the results were significant compared to each optimization function. The proportional method was adopted to the robust topology design for solving the loading uncertainty problem [32]. Multi-material interpolation problem was solved by applying the proportional technique with the SIMP approach and effectively realize the polarization of

the intermediate-density elements [33]. Almost researchers concerned about the stress ratio at the current state of each element and on the summation of stress on the design area to be the update function through the proportional method. Furthermore, the optimization problem was also considered to a linear problem.

A density filtering technique is necessary for topology optimization with the density or SIMP approaches. The filtering density equation is useful to avoid the checkerboard pattern of the final layout which occurs during the optimization process and caused an instability of the numerical analysis. A gray-scale transition between solid and void elements of the final layout is eliminated by adopting a new morphology-based restriction scheme for the filtering technique [34] and combining it with the density algorithm. The regularized Heaviside projection method was employed to achieve a minimum length scale and the density solution nearly 0-1 for simple linear projection scheme and non-linear projection scheme [35]. Likewise, the Heaviside Projection Method (HPM) was also used for restricting the minimum length scale criterion of each material phase during the topology optimization process [36].

Chapter 2

THEORETICAL ISSUE

This chapter lectures on general technique for structural optimization, especially, methods for topology optimization. An algorithm of Solid Isotropic Material with Penalization (SIMP) approach which employed for the optimization procedure in this research. The procedure of nonlinear finite element analysis is also explained in this chapter.

2.1 Size Optimization

Sizes of each member or component inside the structure can be adjusted by applying the size optimization technique. For this method, a user needs to know the preliminary design or shape of the structure before applying this technique. After that, the objective and optimization constraints are defined in the optimization problem. Design variables are size or thickness of each element of the structural domain, such as a thickness of metal during sheet metal process or diameter of a rod of truss structure under static loading

condition. Figure 1.1a showed an example of size optimization by adjusting the diameter of structural elements.

2.2 Shape Optimization

This technique is similar to the size optimization because the preliminary design, such as number of holes, beams, etc., of the structure, needs to be decided before the shape optimization is applied to that structure. The design variables of this technique can be thickness distribution along with structural members, diameter of holes, radius of fillets, or any other measure inside the structural domain. Results from the shape optimization will not show a new hole, split the design domain, or new structural layout. However, an optimal dimension of each design variable (as mentioned above) will be resulted (as shown in figure 1.1b). To update the shape inside the design domain, the Perturbation vector approach [1] is a common method to employ with the shape optimization to change the shape to the discretized the finite element model.

2.3 Topology Optimization

The first step and most general process for structural design is the topology optimization technique. To design the structure based on size and shape optimization, the preliminary layout of the structure can be acquired by employing the topology technique for investigating an optimal layout, the number of holes, the direction of filet, etc., of the preferred design area under each loading condition. The topology optimization will result in optimal material distribution by deciding which area should be remain or remove areas (as in figure 1.1c).

To design by using the topology optimization, the structure is discretized by using the finite element method (FEM) for dividing the design area into a discrete element or mesh (figure 2.1). Each element of the design domain is assigned to be one dimensionless

of the design variable. The process of topology optimization will find the optimal location for overall design variables by identifying the number of 1 or 0 of each element for representing a solid or void element, respectively. The topology problem can be classified into two types: hard-killed and soft-killed problems. The hard-killed problem indicates a value of design variables into 0 or 1 only, while the value of each design variable during the optimization process can be continuous from 0 to 1 in case of the soft-killed problem.

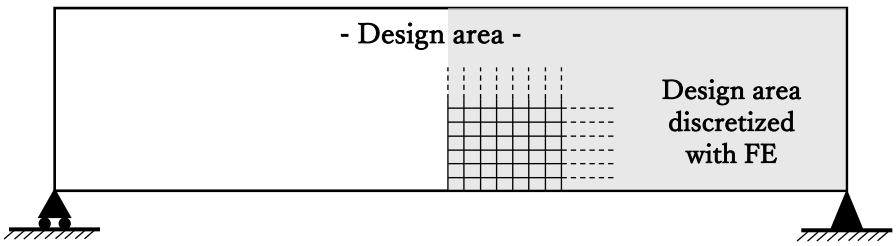

Figure 2.1 Discretization on design area by using finite element.

Many methods were proposed in order to update the design variables on the topology optimization process, or some methods also can be selected for the new design variables randomly. Thus, a selection and verification of procedure for updating the design variable based on topology design are important because the results may differ due to local or global optima. Moreover, the scheme for updating the design variable will affect the number of iterations until the global optimum is obtained. The common approaches for the topology optimization based on continuum structure are described in the following sub-section.

2.3.1 Homogenization Method

The effective material properties of the equivalent homogenized domain in a physical can be found by applying the homogenization method which it is an emergent by mathematical theory [37, 38]. This approach can be used in topology optimization as the structure to be optimized can be considered as a composite consisting of material and void. Bendsoe and Kikuchi [39] proposed the application of topology optimization based on the homogenization method by deriving the effective material properties for porous finite elements. Figure 2.2 showed the assumption of holes by rectangular shape, the porous

finite elements can be formulated based on three parameters of the rectangular geometrical of sizes and direction which represented by *a(x)*, *b(x)* and $\theta(x)$, respectively. All parameters were assigned to design variables and the density were varying from 0-1 on the porous region. The homogenization method has a rigorous theoretical basis which can provide a mathematical bound to the theoretical performance of the structures and faster to converge. On the other hand, a determination and evaluation of the optimal microstructures is cumbersome, and the solutions cannot be built directly since no definite length scale is associated with the microstructure [2].

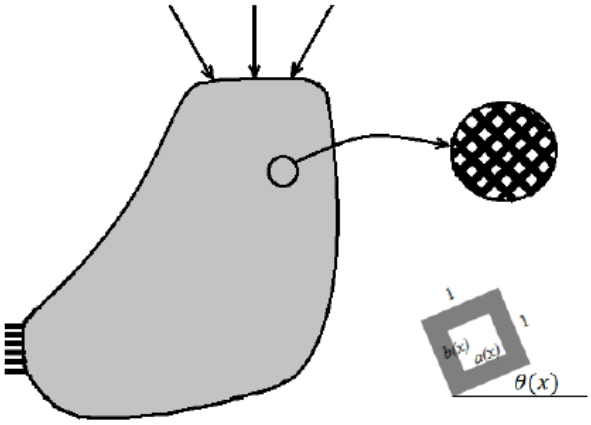

Figure 2.2 Rectangular microstructure [40].

2.3.2 Evolutionary Structural Optimization

Evolutionary structural optimization (ESO) is an optimization method that combines heuristic methods and gradient based approaches [41]. The ESO scheme is classified into the soft-killed method for topology optimization due to the varying density value of each design variable. This method started by finding the optimal solution from a bigger design space, which expected to obtain the final layout by removing an inefficient stress material. The ESO method was initially introduced an evolutional algorithm with two forms. The first form allows removal of the material from the surface or part; this produces a Min-Max situation where the maximum surface stress is reduced to a minimum. The

second form was the under-stressed material could be removed from anywhere in the allowable design space, and with compensation for checker-boarding; this produces an optimum topology under the prescribed environments. On the contrary, the element of the discretized design domain can be added to the structure where they are needed by using an additive evolutionary structural optimization (AESO) [42]. The AESO method was the opposite procedure from the original ESO, while the evolutionary process is similar. Moreover, a bi-directional evolutionary structural optimization (BESO) [42-44] was presented by combining the AESO and ESO to improve results and convergence time of both AESO and ESO. The BESO was an effective method for removing an unwanted design element in which stress was not affecting the design criteria from the structure iteratively and added the efficient material to the design area where the high stress occurred simultaneously.

The advantages of the ESO, AESO, and BESO are a reasonable computational cost and high quality of the solutions after the optimization process. The optimization algorithms of these schemes are also easy to implement and understand [45]. However, the evolutional methods are complicated to apply with the optimization problem for other constraints, such as displacement constraint, or multiple loading conditions. An investigation of the evolutionary methods [46] showed the BESO method resulted in a local optimum rather than non-local optimum, while the same results can be achieved by employing the density method, only using the high value of penalization factor and changing the initial density of the design domain.

2.3.3 Genetic Algorithms.

One typical method for a stochastic based approach in topology optimization problem is the genetic algorithms. The genetic algorithm operates by generating the population of potential solutions toward better solutions, rather than improving a particular solution. An evolutionary survival-of-the-fittest mechanism [47, 48] is used in the genetic algorithms for allowing the designs in a population to compete with each other to become parent designs. A swap portion of the generic code is then used to create the child

generation from the parent design. The child generation mutates until it reaches the limits of a random number, which expected to be a higher quality of the parent design and replaces the parent generation. This evolutionary process is repeated until the optimal design is reached [49, 50].

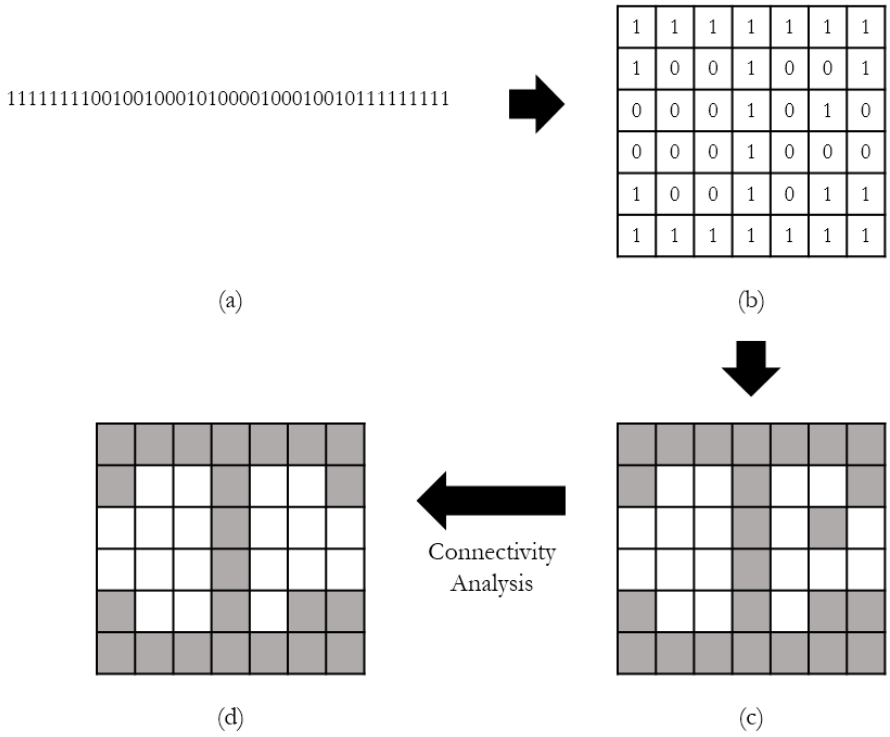

Figure 2.3 Overall process of the genetic algorithms (a) a chromosome (b) chromosome substitution in mesh (c) layout generation from the chromosome (d) an optimal layout from topology optimization.

Design variables in the genetic algorithm are expressed in a digital code (figure 2.3a), which is a character of a string and represented a gene of a chromosome. The new design variables can be generated by undergoing a genetic crossover, and the child generations have traits from both parents. To investigate a performance of the new design variables, a merit function is used to evaluate by giving a higher chance of creating offspring to the designs with higher merit and surviving into the next generation. Then, the new design

variables are substituted into the mesh for representing the structural layout with solid (equal to 1) and void (equal to 0) elements (figure 2.3b and 2.3c). The optimal layout (figure 2.3d) will obtain after a connectivity analysis, which expecting the result to void all unconnected elements [51, 52]. A single point crossover for the chromosome is the most basic method by selecting and the segments of the code after that are swapped randomly (figure 2.4). By the way, there are other methods that also possible for crossover the chromosome during the optimization procedure [52].

The genetic algorithms have disadvantaged by the high computational cost due to a large number of design variables and function evaluations. So, this method is suitable for optimizing the problems with little knowledge about the nature of the design domain [53]. However, the genetic algorithms are less chance to meet the local optimum by comparing to the gradient based methods.

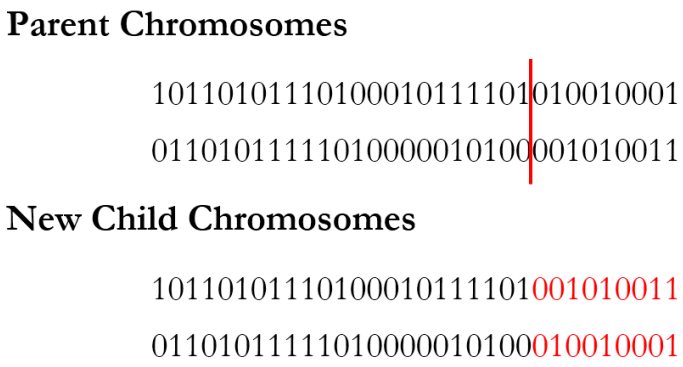

Figure 2.4 Crossover of the chromosomes based on the genetic algorithm.

2.3.4 Level Set Method

The first application of the level set method was introduced for tracking moving interface [54]; then, the level set method has been introduced and developed to many physical problems. This method is quite different from the other techniques of topology optimization for finding the final layout by removing or adding material. Nevertheless, the level set method uses an implicit description of boundaries to parameterize the geometrical

layout during the optimization process [55-60]. Thus, the level set function is necessary for the level set method because it uses to define the interface between material phases implicitly.

The two-phase material-void problem is the simplest for the level set method and often used for treading the case in structural optimization. The design domain (φ), void area (ϑ), and the interface area (γ) usually relate to the level set function (ξ) as follows:

$$\xi(X)=\begin{cases}\xi(X)>c & \rightarrow \quad X\in\varphi\\ \xi(X)=c & \rightarrow \quad X\in\gamma\\ \xi(X)<c & \rightarrow \quad X\in\vartheta\end{cases} \tag{2.1}$$

where X is a point of design domain and c is a constant value [55, 58]. For the level set function, most studied have been concerned the concerned the constant value (c) of equation 2.1 equal to zero. Changing of the level set function adjusts the level of design domain and possibility to topology the design material during the optimization process. To change the level set function, the Hamilton-Jacobi equation was frequently proposed for the level set method as follows:

$$\frac{\partial\xi(X)}{\partial t}+v_n(X)\left|\xi(X)\right|=0 \tag{2.2}$$

where $v_n(x)$ is a normal velocity by obtaining from the sensitivity analysis of the objective function with respect to the boundary variation. Thus, an updating of the level set function by moving the boundary along the normal direction is necessary to solve the equation 2.1. Moreover, the level set method requires a regularization technique to obtain a well-posted optimization problem to remove numerical instabilities and improve convergence behavior. The level set method is close to the shape optimization because the shape-sensitivity analysis is possible to apply with the level set method and alter only the boundaries of the

design domain [55, 56]. In the other hand, regularization technique [8] were also used for controlling the geometrical properties of the final design.

2.3.5 Solid Isotropic Material with Penalization

The Solid Isotropic Material with Penalization (SIMP) was introduced to the topology optimization process shortly after the homogenization method has been proposed. The SIMP or power-law approach suggested to be an easy optimization algorithm but can be artificial for reducing the complexity of the homogenization approach. Furthermore, the SIMP method also aimed to improve the convergence of the solutions by relaxing to the continuous problem, available the results vary in a range of 0 and 1 (not only 0 and 1) or material density from 0% to 100%, respectively.

A small lower bound of the element density ($\rho_{\min}$) is usually imposed as $0 < \rho_{\min} \le \rho$ for avoiding a singular finite element method problem. The relationship between element density and Young's modulus in the equilibrium calculation can be shown as follows:

$$E = E(\rho) = \rho^{p} E_0 \tag{2.3}$$

where E is the elastic properties, p is the penalization factor that is always greater than 1 and E_0 is initial stiffness matrix. The relationship between the relative stiffness (E/E_0) and the volume density or element density (ρ) was shown in figure 2.5 with various the penalization factor, and it can be illustrated for recommendation the suitable value of the penalization factor. There were some studies applied the penalization factor (p) equal to 1, that optimization problems corresponds to the so-called "variable-thickness-sheet". The variable-thickness-sheet problems usually are the convex problem with the unique solution [61, 62]. Selecting the penalization factor (p) too law or too high effects to the too much gray scale or too fast convergence of the optimal layout. Therefore, the recommendation of the penalization factor (p) is equate to 3 [63] as the magic number to ensure physical realizability of elements with intermediate densities. Microstructures of material and void

realizing the material properties of the SIMP model was shown in figure 2.6 by applying 3 for the penalization factor (p).

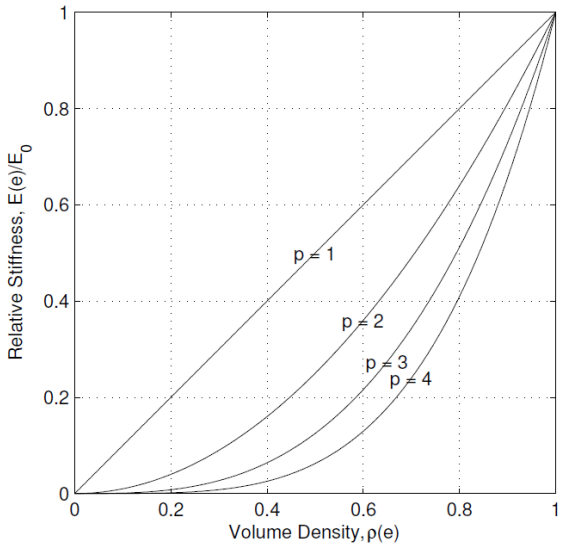

Figure 2.5 Relationship between the relative stiffness and the volume density [63].

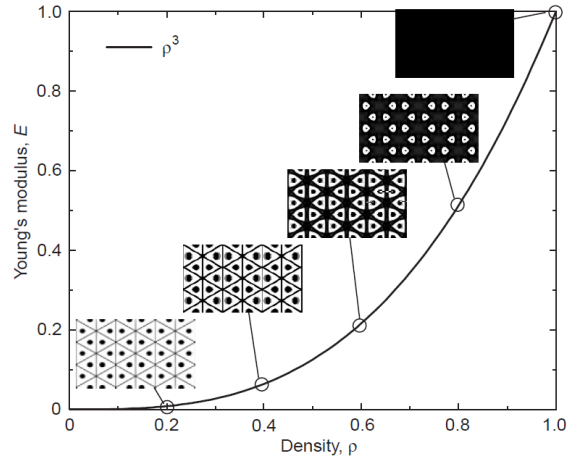

Figure 2.6 Microstructures of material and void realizing the material properties of the SIMP model with the penalization factor equal to 3 [64].

The element densities usually are assumed to the constant value on each design variable. Thus, a relationship of the density-stiffness can be simply implemented by scaling

the element stiffness matrices before assembling them into the global stiffness matrix as written as follows:

$$K_e = \rho_e^p K_e^0 \tag{2.4}$$

where K_e is stiffness matrix and K_e^0 represents real element stiffness matrix with initial stiffness matrix E_0 before assembling to global stiffness matrix. For the application to reduce the volume of the design area (Ω), the total volume (V) of the design area can be determined by:

$$V = \int_{\Omega} \rho d\Omega \tag{2.5}$$

In recent years, a numerical implementation of the SIMP method was developed by assigning the lower bound on element density value of the design variables as $\rho_{\min} \le \rho \le 1$ where $0 < \rho_{\min} \ll 1$ to avoid singularity of the stiffness. Moreover, these conditions can be ensured unique displacement vector for every state of the design variables in the design space. So, a modified SIMP method has been alternatively formulated as:

$$E = E(\rho) = E_{\min} + \rho^p \left(E_0 - E_{\min}\right) \tag{2.6}$$

where $0 < E_{\min} \ll 1$ is a small lower bound on the stiffness. Element density can be varied in the range of $\rho \in [0,1]$ by following the modified SIMP approach. Both the SIMP model and the modified SIMP model, void regions are represented by very compliant material. The advantages of the SIMP method (or density method) are any combination of the design constraints can be used. Furthermore, this method does not require too much extra memory for calculation. Only one free variable is needed per design element.

2.4 Mathematical Formulations for Structural Optimization

For the general problem of the structural optimization, the final layout is expected to search the minimum or maximum value of the objective function (*f(x)*). There are common three components for constructing the optimization problem: design variable, objective function and optimization constraint. The design variable (*x*) for the general optimization problem can be defined as:

$$X = \begin{Bmatrix} x_1 \\ x_2 \\ x_3 \\ \vdots \\ x_n \end{Bmatrix} \tag{2.7}$$

where *X* is an *N*-dimensional vector of the total number of design variable. The design domain usually discretized to each design element (meshing) by using finite element method. So, one element in the finite element model is assigned to one design variable. The optimization constraint usually defines for two types: inequality type and equality type. Both types of the optimization constraint can be generally written as:

$$\begin{aligned} g_j(X) &\le 0, \quad j = 1,2,3,\ldots,m \\ h_j(X) &= 0, \quad j = 1,2,3,\ldots,t \end{aligned} \tag{2.8}$$

where $g_j(X)$ represents the optimization constraint for the inequality type and $h_j(X)$ represents the optimization for the equality type. The number of constraints *m* and *t* and the number of design variable *N* are not needed to relate in any way. If the optimization

problem can be constructed with all three components, the problem so-called a constrained optimization problem. Some optimization problems do not involve any constraints, this case so-called an unconstrained optimization problem, and it can be state as only:

$$\text{Find} \quad X = \begin{Bmatrix} x_1 \\ x_2 \\ x_3 \\ \vdots \\ x_n \end{Bmatrix} \quad \text{which minimizes or maximizes } f(x) \tag{2.9}$$

As mentioned in the chapter 1, the most general problem for topology optimization based on static and linear load cases generally defined for two types of the problem: minimize compliance or volume of the design structure. So, the mathematical formulation of that two problems were showed in this dissertation as following the sub-section.

2.4.1 Mass Constrained with Compliance Minimization

This type of optimization problem is the most common for constructing the optimization problem based on the static load case with elastic structure. The objective is to minimize the compliance of the structure subject to a mass constraint. The goal of this formulation has distributed the material inside the design for maximizing the stiffness of the structure. The problem can be mathematically written as:

$$\text{Minimize:} \qquad C(X) = d^T K d \tag{2.10}$$

$$\text{Subject to:} \qquad \begin{aligned} & m(\rho) = \sum_{i=1}^{N} \rho_i \le m_0 \\ & 0 < \rho_{\min} \le \rho \le 1 \end{aligned} \tag{2.11}$$

where *d* is the global displacement vector and *K* is the global stiffness matrix. m_0 is the maximum allowable of weight on the final layout as define as the optimization constraint. $\rho_{\min}$ is the minimum allowable for the relative density of each design variable. This value typically set nearly to zero. The design element will be voided if the element density (ρ) equal to the minimum allowable value ($\rho_{\min}$). Otherwise, the solid element will be appeared in the given design domain.

2.4.2 Stress Constrained with Mass Minimization

The optimization of stiffness maximization was occasionally not representative of practical structural design requirements. Therefore, an implementation of the mathematical formulation in the sub-section 2.4.1 was required. One more useful problem for optimization is to determine a lightweight structure, and it does not fail. The essential criteria for investigating the failure of the structure is the Von Mises stress. The stress distribution inside the structure should not exceed the yield stress for the elastic structure and avoiding the permanent deformation. So, the optimization problem for minimizing the mass of the structure with stress constraint can be mathematically formulated as:

$$\text{Minimize:} \qquad m(\rho) = \sum_{i=1}^{N} \rho_i \tag{2.12}$$

$$\text{Subject to:} \qquad \frac{\sigma_i}{\sigma_{all}} \le 1, \quad 0 < \rho_{\min} \le \rho \le 1 \tag{2.13}$$

where σ_i is an elemental stress at element i^{th} and σ_{all} is the allowable stress of the structure. Value of the allowable stress depends on the problem and goals of that optimization case. For linear structural design, the yield stress is assigned to this parameter. For the nonlinear problem, this value is depended on the characteristic of the material behavior and material properties.

2.5 Numerical Instabilities

For topology optimization with continuum structures, there are commonly three types of numerical instabilities associated with the calculation process. That is local optima, mesh-dependence, and checkerboard [65]. The following sub-section will describe the effect of each case on numerical instability for the topology optimization process.

2.5.1 Local Optima

The final layout from topology optimization can be differently obtained, depending on the optimization approach and initial parameters [66]. The difference between local and global optimum point for the optimization process was shown in figure 2.7 where *a* and *b* are the lower bound and upper bound of the design variable, respectively. Therefore, it can be concluded that there exist many local optima for the topology optimization problem of a continuum structure. The topology optimization with a single optimization formulations that produce a result in 0 or 1 (void or solid element, respectively) design are nonconvex and subject to converge into a local optima [65].

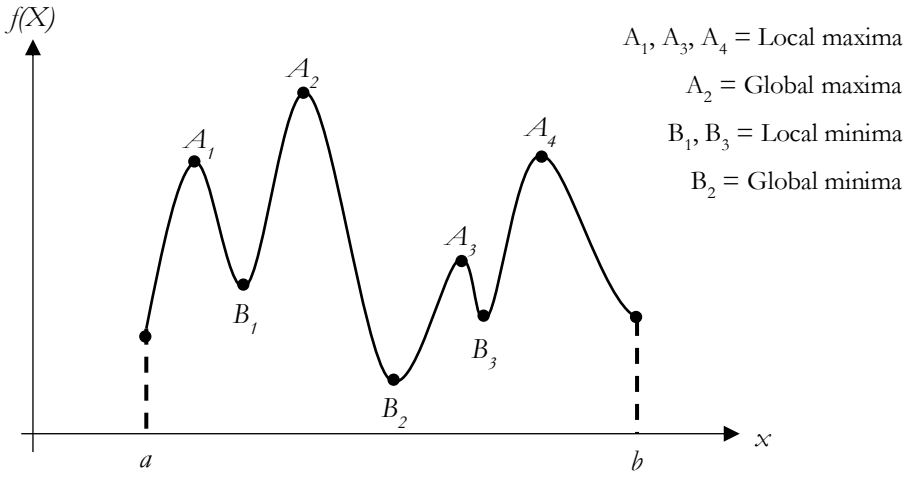

Figure 2.7 Local and global optima.

2.5.2 Mesh-dependence

The design domain has to discretize by using the finite element method (meshing) for assigning the design variable. The size of the meshing also affects the shape of the final layout. Thus, the mesh-dependence refers to the problem when achieving the different optimal layout from the topology optimization process because the size of the mesh is the difference. Figure 2.8a and 2.8b showed the example of the final layout from topology optimization by discretizing 600 and 5,400 finite elements, respectively.

(a) 600 finite elements model

(b) 5,400 finite elements model

Figure 2.8 Optimal solutions from the SIMP method [65].

The final layout obtained in much more detail by using a higher number of elements in the finite element model. Nevertheless, the high number of finite elements also requires high computational costs in both the analysis and optimization process. By using the finer mesh in the finite element, the model is expected to obtain the same optimal results ideally. However, implementation on the finer mesh of the topology optimization increases the complexity of the final solutions such as more members in the given design domain when the smaller size of mesh is used. In the additive manufacturing process, the complex layout may affect the production cost. However, high-performance solutions with more complexity are also preferred sometimes.

2.5.3 Checkerboard

The checkerboard problem is the most common type of the numerical instability on topology optimization, which usually occurs when optimizing the structure with homogenization, ESO/BESO and SIMP approaches. The checkerboard problem causes the final layout in formation of alternating void and solid elements, seem like a block pattern and it looks like a checkerboard (figure 2.9). However, it found that the optimal structure with the checkerboard configuration had artificially high stiffness values when compared with the normal structure [67]. Even though the high stiffness of the structure can be acquiring from the checkerboard layout, it was terrible for the numerical calculation based on the finite element analysis. There are many techniques such as patch technique, perimeter control, higher-order finite element method, which proposed to prevent the checkerboard pattern from topology optimization technique.

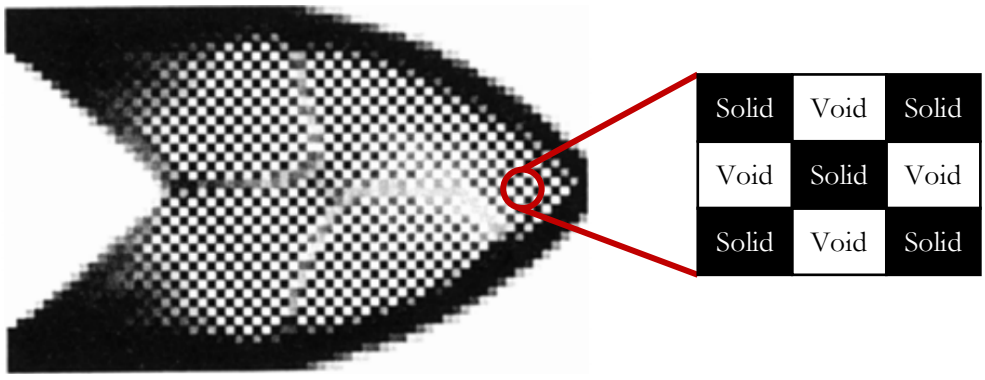

Figure 2.9 An example of the checkerboard pattern [67].

One technique based on image processing filtering techniques also proposed to prevent the checkerboard pattern by using the sensitivity filtering scheme. An estimation of the design sensitivity of specific elements from the weighted average of the element itself and the neighboring elements was an idea for suggesting this technique. In this technique, the sensitivity of an element was being modified by weighted averaging of the sensitivities of the elements in a fixed neighborhood of minimum radius of the neighbor.

2.6 Crashworthiness Design for Nonlinear Material Structure

In the crashworthiness design, an absorb maximum energy while keeping the peak loads is usually defined as the goal of the optimization process for transmitting minimum damage to occupants. This is a common objective function that automotive manufacturers require for imposing as part of government regulations for the crashworthiness design. Structural integrity can be measured in terms of total deformation, and it should show as well as characteristics of energy absorption. To maximize both energy absorption and structural integrity, maximizing an area under the load-displacement curve (an example was showed in figure 1.2) is the most common way for increasing the characteristics of the structure.

Metal is usually used as the main material for producing many types of vehicles in automotive manufacturers. An energy absorption achieves the metal by permanent deformation. As a design domain has to discretize before doing the topology optimization, the energy absorbed by each design variable (each element) can be measured by integrating the load transmitted based on the resulting displacement. When the structure under applied loading reaches the yield stress, the plastic strain (plastic deformation) will occur on that structure. The total strain of the structure can be determined by summation of elastic and plastic strain. An equation for calculating the total strain can be expressed as following in equation 2.14 where ε is the total strain, ε_e is the elastic strain, and ε_p is the plastic strain.

$$\varepsilon = \varepsilon_e + \varepsilon_p \tag{2.14}$$

The energy absorption can be calculated by considering only the elastic strain, and it occurs only elastic deformation (structure can recover by itself) in case of a purely elastic

structure. The elastic strain energy is used to measure the energy absorption in case of the purely elastic structure which is expressed by

$$U^e = \int_{\varepsilon_i^e}^{\varepsilon_f^e} \sigma \, d\varepsilon^e \tag{2.15}$$

where U^e is the elastic strain energy and ε^e is the elastic strain based on applied loading with subscript *i* and *f* mean the initial and final elastic strain, respectively.

The structure under high external loading or impact loading is involved in a large displacement, the behavior of plastic material properties is necessary to consider during analysis and optimization process. In this case, the plastic strain energy or plastic work is used for calculating the energy absorption during the permanent deformation. The equation of plastic strain energy is expressed as follows:

$$U^p = \int_{\varepsilon_i^p}^{\varepsilon_f^p} \sigma \, d\varepsilon^p \tag{2.16}$$

where U^p is the plastic strain energy and ε^p is the plastic strain based on applied loading with subscript *i* and *f* mean the initial and final plastic strain, respectively. Therefore, the total energy absorption including elastic and inelastic deformations can be calculated based in the internal energy density which is expressed as follows:

$$U = U^e + U^p = \int_0^{\varepsilon_f} \sigma \, d\varepsilon \tag{2.17}$$

where σ is the stress which is integrated since the undeformed shape before applied loading until occurs the final deformation (final strain state).

In the state of crashworthiness, the energy absorption can be represented by work done due to the deformation of the structure after it deformed. Thus, maximizing the area under the force-displacement curve effects by increasing the energy absorption directly (figure 2.10).

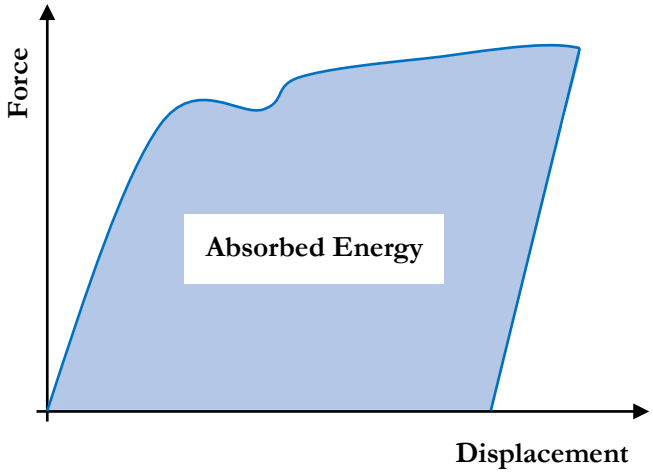

Figure 2.10 Area under force-displacement diagram represents the energy absorption.

2.7 Nonlinear Finite Element Analysis

The finite element method is widely used for solving many physical problems in engineering analysis and design. Initially, the finite element method was developed on a physical basis for analyzing the problems in the field of structural mechanics. After that, it was recognized for applying to heat transfer, and fluid flows problems. The finite element analysis solves the mathematical model which it requires the certain assumption that lead the differential equation for governing the mathematical model.

When the structure causes a small displacement and that material is linear elastic, the problem is assumed to a linear finite element analysis. In addition to the linear finite element analysis, the problem can be assumed that the nature of boundary conditions are not

changed during the analysis procedure. For this assumption, the equilibrium equation for linear finite element analysis with applied static load is expressed as follows:

$$Kd = F \tag{2.18}$$

where d is a displacement vector and F is the applied load vector. If the applied load is αF instead of F, which α is the constant load, and the structure causes a high deformation with the corresponding displacement vector is αd. When this case happens, the nonlinear analysis is performed to the finite element problem.

Types of nonlinear analyses can be classified in Table 2.1, and figure 2.11 illustrates the classification of analyses that are encountered as a list in Table 2.1. In the case of materially-nonlinear-only, the nonlinear behavior of the structure causes based on the nonlinear stress-strain relation. The displacements and strains are infinitesimally small. Thus, the engineering stress and strain can be employed in this type of nonlinear analysis. When the large displacements or large rotations are considered, but the strains are subjected to infinitesimally small strain, a body attached coordinate frame x', y' is used to measure the strain of the structure. Furthermore, this frame undergoes a large rigid body for displacements and rotations. The relationship between stress and strain can be linear or nonlinear material behavior. For the large displacements or large rotations, this is the most general problem and conditions for the nonlinear finite element analysis that in essence the material is subjected to large displacements and large strains. The stress-strain relation is usually nonlinear behavior.

In addition to nonlinear analyses which categorized in Table 2.1, there are another type of nonlinear analysis which displayed in figure 2.11 by changing the boundary conditions during the motion of body. This situation arises in the analysis on contact problem which occurs from two objects or more (figure 2.11e). The material can be linear or nonlinear properties which depending on the conditions on each problem.

In actual finite element analysis, the user needs to decide whether a problem falls into

one or another type of analysis. It is necessary for dictating the formulation to describe the actual physical problem. The large strain formulation will always be correct for the nonlinear analysis surely. However, the practical and compatible formulation can reduce the computational costs and also provide more insight into the response prediction.

Table 2.1 Classification of nonlinear analyses [68].

Type of analysis	Description	Typical formulation used	Stress and strain measured
Materially-nonlinear-only	Infinitesimal displacements and strains; the stress-strain relation is nonlinear	Materially-nonlinear-only (MNO)	Engineering stress and strain
Large displacements, large rotations, but small strain	Displacements and rotations of fibers are large, but fiber extensions and angle changes between fibers are small; the stress-strain relation may be linear or nonlinear	- Total Lagrangian (TL) - Updated Lagrangian (UL)	- Second Piola-Kirchhoff stress, Green-Lagrange strain - Cauchy stress, Almansi strain
Large displacements, large rotations, and large strain	Fiber extensions and angle changes between fibers are large, fiber displacements and rotations may also be large; the stress-strain relation may be linear or nonlinear	- Total Lagrangian (TL) - Updated Lagrangian (UL)	- Second Piola-Kirchhoff stress, Green-Lagrange strain - Cauchy stress, logarithmic strain

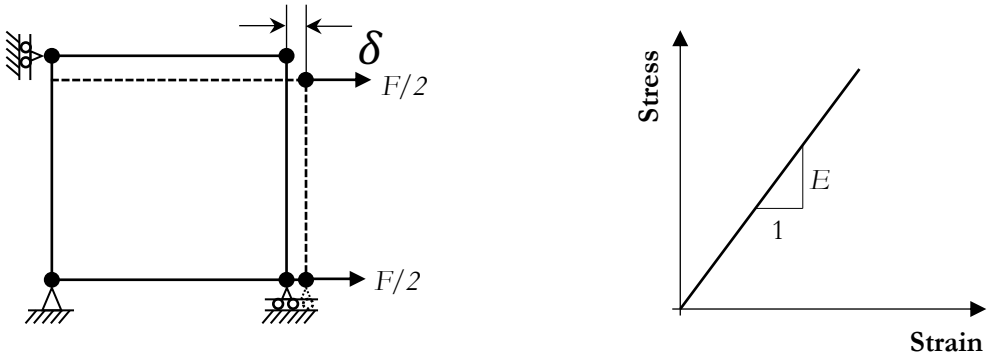

(a) Linear elastic (infinitesimal displacement)

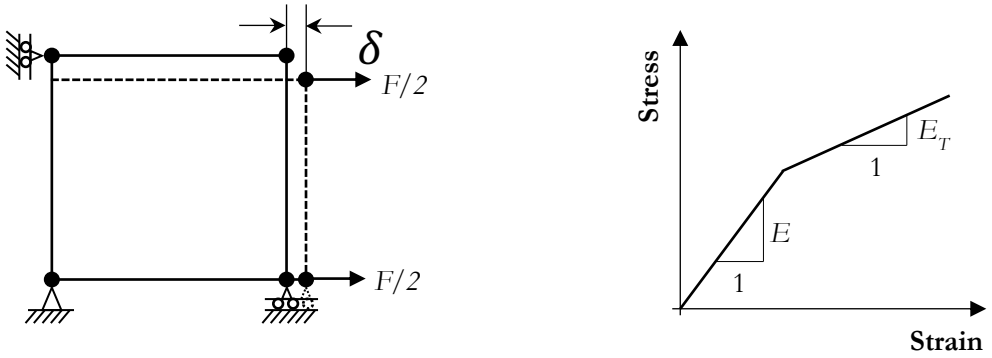

(b) Materially-nonlinear-only (infinitesimal displacement, but nonlinear material)

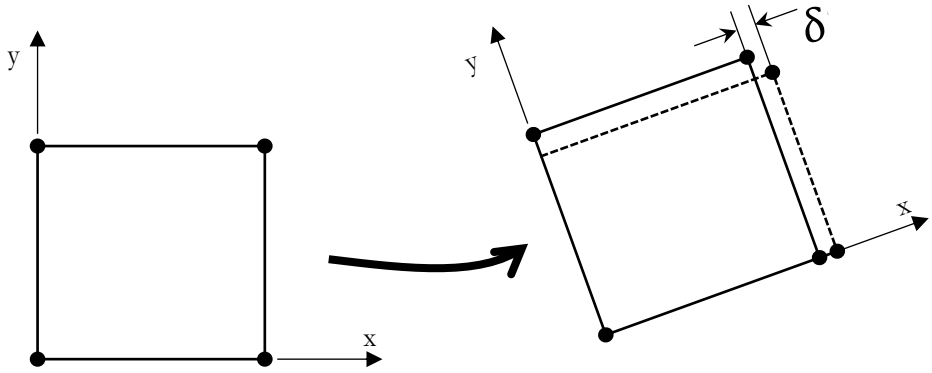

(c) Large displacements and large rotations but small strains, linear or nonlinear material behavior

Figure 2.11 Classification on analyses.

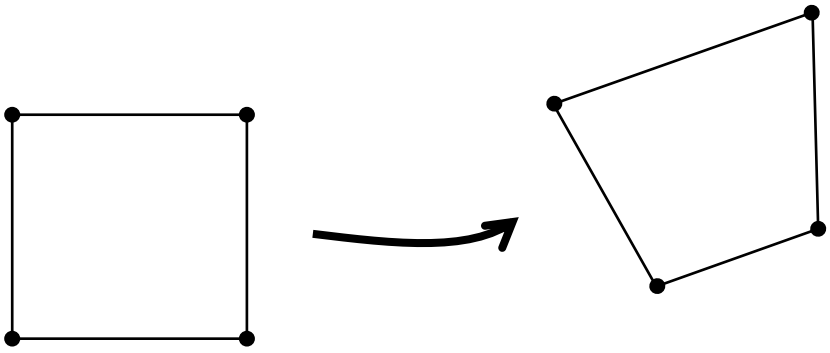

(d) Large displacements, large rotations, and large strain, linear or nonlinear material behavior

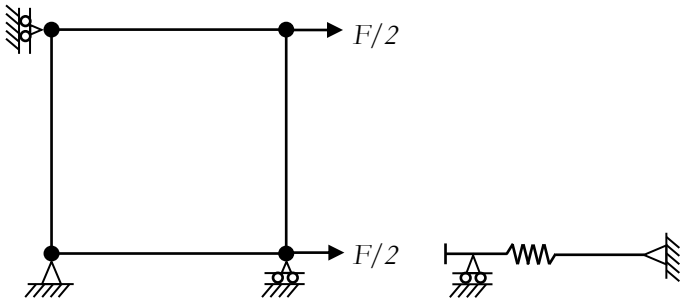

(e) Change in boundary conditions

Figure 2.11 Classification on analyses (*continued*).

2.7.1 Nonlinear Analysis

A problem in nonlinear analysis generally aims to find an equilibrium equation of the body corresponding to the applied load. There is one assumption for the nonlinear analysis, that is an external load, which is described as a function of time *t*. Thus, the equilibrium equation of the nonlinear finite elements representing the body under loading condition is expressed as follows [68]:

$$R^t - F^t = 0 \tag{2.19}$$

where R^t is a vector of externally applied nodal point forces which is configuration at the

time t and F^t is a vector of nodal point forces that corresponding to the elemental stress in the configuration at time t. According to equation 2.19, some nonlinear static analyses by this equilibrium equation and can be calculated based on the load level. However, when the problem includes path-dependence of nonlinear geometric or material geometry, or time-dependent, the equilibrium equation (equation 2.19) needs to calculate for complete in a range of the time interested. Therefore, a step-by-step incremental solution can carry out this nonlinear response, which reduces to a one-step analysis.

An approach of the incremental step-by-step solution aims to assume the solution for the calculation time t to the discrete time $t + \Delta t$, where Δt is the suitable time increment. Since the discrete time $t + \Delta t$ is considered, the equilibrium equation for nonlinear finite element analysis is modified as follows:

$$R^{t+\Delta t} - F^{t+\Delta t} = 0 \tag{2.20}$$

where $R^{t+\Delta t}$ is assumed to independent of the deformation at time $t + \Delta t$. Since the solution is known at time t, the vector of nodal point forces can be written as:

$$F^{t+\Delta t} = F^t + F \tag{2.21}$$

where F is the incremental nodal point forces corresponding to the increment in elemental stresses and displacements from time t to time $t + \Delta t$. The tangent stiffness matrix K^t is used to approximate the vector of incremental nodal point forces corresponding to the nonlinear geometric and material at time t as shown in equation 2.22 and 2.23 where d is the incremental nodal displacements.

$$F = K^t d \tag{2.22}$$

$$K^t = \frac{\partial F^t}{\partial d^t} \tag{2.23}$$

As following the above equations, the equations 2.21 and 2.22 can substitute in equation 2.20, and it is modified as equation 2.24 and the incremental nodal displacements can be calculated by using equation 2.25.

$$K^t d = R^{t+\Delta t} - F^t \tag{2.24}$$

$$d^{t+\Delta t} = d^t + d \tag{2.25}$$

An approximation procedure is necessary to employ to the nonlinear analysis for evaluating the displacements corresponding to time $t + \Delta t$ and then proceed to the next incremental calculation. The Newton-Raphson approach is widely used for iterative calculation process in finite element analysis. This method is an extension for the simple incremental technique, which calculated an increment nodal displacements. The process can repeatedly calculate the incremental solution based on the currently known displacements at time *t*. An iterative calculation based on the Newton-Raphson approach is shown as follows:

$$\begin{aligned} K_j^t d_{j+1} &= R^{t+\Delta t} - F_j^{t+\Delta t} \\ d_{j+1}^{t+\Delta t} &= d_j^{t+\Delta t} + d_j \end{aligned} \tag{2.26}$$

in which $j = 1, 2, 3, \ldots$ is the iteration index for the iterative calculation process under the Newton-Raphson approach.

2.7.2 Overview on Stress Update for Elastoplastic Materials

In the uniaxial tension test, the relationship between an engineering stress against uniaxial strain can generate as the curve in figure 2.12 under the applied load *P* and cross-sectional area *A* [69].

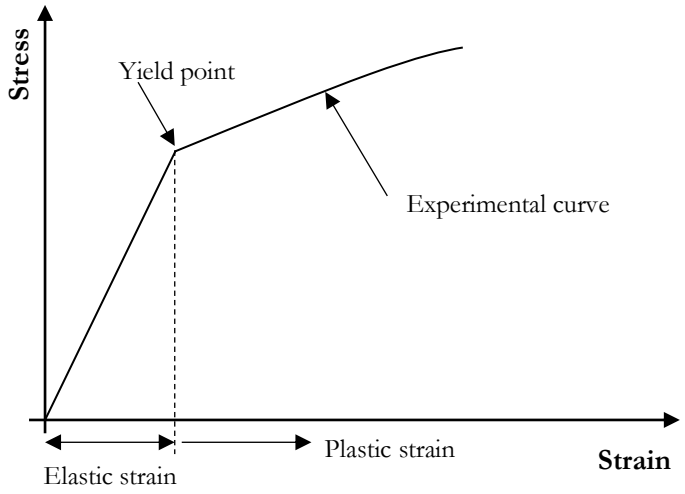

Figure 2.12 Plastic behavior is demonstrated from the uniaxial test.

Figure 2.13 illustrates a simple Von Mises stress model, and it shows the pressure independent and yield surface of yield stress, which is a space of cylindrical principal stress. The pressure independent of the yield surface can be categorized in term of a function of deviatoric stress tensor (s_{ij}) and yield stress function. So, the equation of the pressure independent yield surface (P) can be given in equation 2.27, where $f(s_{ij})$ is the function for determining the shape and $\sigma_Y(a_i)$ is the function for determining the translation and size.

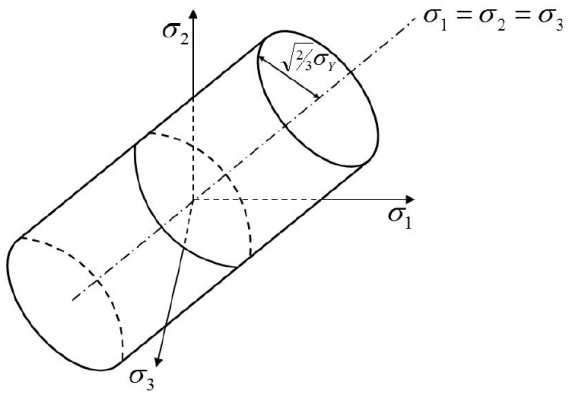

Figure 2.13 Yield surface in principal stress space in pressure independent [70].

$$P(s_{ij}, a_i) = f(s_{ij}) - \sigma_Y(a_i) = 0 \tag{2.27}$$

The plastic potential (g) is the existence of the potential function. The plastic potential can be assumed as in equation 2.28 and the stability and uniqueness is required in equation 2.29, which λ is a proportional constant.

$$g = g(s_{ij}) \tag{2.28}$$

$$d\varepsilon_{ij}^{p} = \lambda \frac{\partial g}{\partial s_{ij}} \tag{2.29}$$

The incremental plastic strains ($d\varepsilon_{ij}^{p}$) are normal to the plastic potential function as illustrated in figure 2.14. This is the normality rule of plasticity. The assumption of the plastic potential is identical with the yield condition as in equation 2.30. So, the incremental plastic strains can be rewritten as following in equation 2.31.

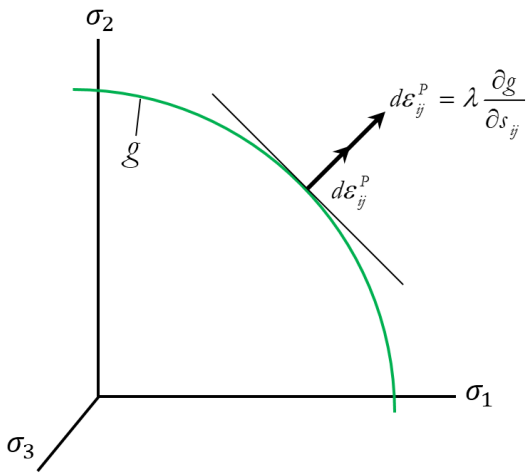

Figure 2.14 Plastic strain is normal to the yield surface.

$$g \equiv P \tag{2.30}$$

$$d\varepsilon_{ij}^{p} = \lambda \cdot \frac{\partial f}{\partial s_{ij}} = \lambda \cdot grad \cdot f \tag{2.31}$$

Moreover, the incremental stresses (ds_{ij}) are also normal to the plastic flow $\frac{\partial g}{\partial s_{ij}}$

Chapter 3

OPPORTUNITY FOR NONLINEAR DESIGN

This chapter describes on an opportunity for doing nonlinear structural optimization. An example of a bus rollover test according to ECE-R66 regulation is mentioned through the application of an automotive manufacturer for structural design process. The bus structure is led to the nonlinear design due to structural deformation behavior.

3.1 Problem Signification

Bus transportation is common for short and long-distance in worldwide. Although the bus transportation is not a primary and common vehicle for road traffic, the bus accident caused a high number of injuries and fatalities compared to other types of road accidents. National Highway Traffic Safety Administration (NHTSA) reported the bus accident of the United States of America on 2012 [71]. The bus rollover accidents occurred

only 2.2% compared with non-rollover accidents (Fig. 3.1a), but the number of fatalities showed one-third of all fatalities caused by the bus rollover accidents (Fig. 3.1b). Therefore, United Nations Economic Commission for Europe (UN/ECE) has been enforced regulation for the strength of the large bus structure: Economic Commission for Europe Regulation 66 (ECE-R66) [72] due to the serious status of rollover accidents. After the rollover test, the bus structure shall not be intruding into the residual space as defined by ECE-R66 regulation during and after the rollover test. To design with efficient process for the bus structure, the final bus model should pass all of the normal operation conditions, including to rollover test according to ECE-R66 requirements by taking into costs consideration, materials, and production processes.

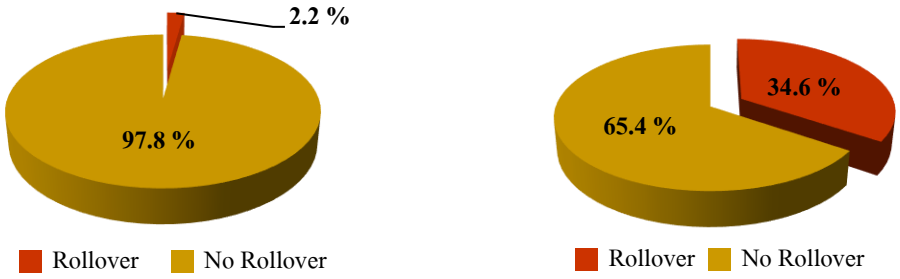

Figure 3.1 Bus accident in United States of America on 2012
(a) types of bus accident (b) number of fatalities from bus accidents.

3.2 Loading Conditions for Bus Optimization

Vehicle structural design is a process to determine an appropriate configuration and dimensions of members supporting the vehicle components such as occupant seats, air conditioning and lighting systems, power transmission, engines, etc. The bending stiffness condition concerns the strength of superstructure to carry passenger and facility loads. Torsion stiffness ensures the bus structural integrity when a torque occurs to the bus structure traveling on rough surface.

3.2.1 Bending Stiffness

The bending stiffness is the condition that required the bus structure should support and no failure occurs under the body weight. Furthermore, the bending stiffness analysis can be used to analyze the structural behavior for other cases as follows:

- Towing is a case which the support point is not the vehicle's axle but change to the end of front or back of the vehicle. This case is considered to be a severe case for the passenger since cause the maximum moment is higher than normal condition. Although this case may not be the general case but can be proof confidence to the passengers that the vehicle will not fail if this case is occurred.

- Dynamic loading is a case that caused by vehicle components are operated over the static condition. This case can simplify to static problem by using dynamic factor that equal to 2 times of gravitational load (2g) multiplied by the force and the moment that occur in the static state.

3.2.2 Torsion Stiffness

The torsion stiffness represents the condition where one-wheel falls into a ditch and become unsupported. The structure should recover its shape without plastic deformation at any parts of the structure. Structural investigation based on the torsion stiffness requirement is analyzed by applying the maximum torque to the structure in the part of chassis. So that the structure of the vehicle can be restored to its original state. A recommendation of the torsion stiffness of the bus structure ranges from 18,000 to 40,000 N.m/deg [73].

3.2.3 Rollover Test According to ECE-R66

The ECE-R66 regulation intends to ensure the strength of bus superstructure for protection of occupants with the condition that none of the bus structural parts intrudes into the residual space both during and after rollover test. For the testing process, the

complete vehicle is located on the tilting platform (Fig. 3.2) with blocked suspension. The bus structure is tilted by applying an angular velocity to the tilting platform slowly until its unstable equilibrium position. The rollover process starts when the vehicle is on the unstable position with zero angular velocity, and the axis of rotation runs through the wheel-ground contact points. To pass the requirements of this regulation, the structure should not intrude into the residual space during and after the rollover process.

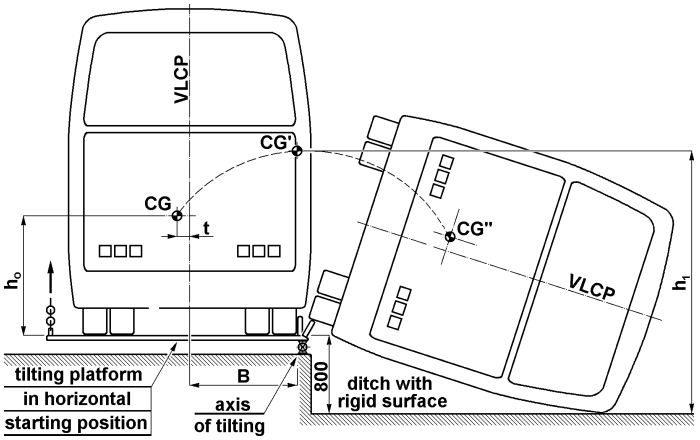

Figure 3.2 Specification for bus rollover test according to ECE-R66 [72].

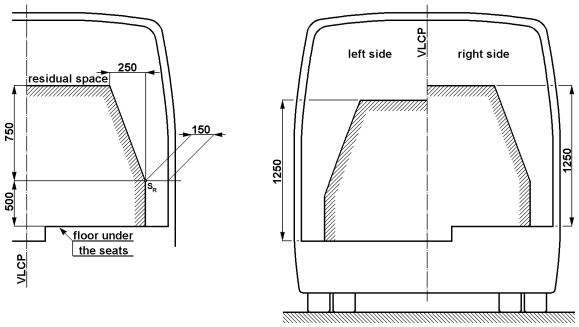

Figure 3.3 Specification of residual space [72].

The ECE-R66 rev. One allows five methods of rollover test, i.e., rollover test of the complete vehicle, rollover test of body sections, quasi-static loading test of body sections, quasi-static calculation based on testing of components and an additional test by using computer simulation of rollover test on the complete vehicle. Computer simulation allows

the manufacturers to significantly save time and money as it allows designs to be tested virtually, and modifications of various parts of the structure can be made early in the design process. This method is thus the main interest of this work.

3.3 Topology Optimization of Bus Structure

The current status of the research on bus optimization was concerned and combined all three loading conditions (described in Section 3.2) into the optimization process. The topology optimization technique was first employed to determine the optimal material distribution for the bus structure, which represents the members of the superstructure.

Areas of the pillar, roof, side, and floor structures were assigned to the design variables and created based on the finite element model by using shell element (green areas in Fig. 3.4). A distributed load was applied at the roof and floor structures for representing the weight of air-conditioning and lighting systems and the weight of seats and passengers, respectively, in case of the bending stiffness. For torsion stiffness, a torque was applied at a shaft of chassis structure. Both bending and torsion stiffness were analyzed and investigated the optimal structure under static analysis with elastic material properties.

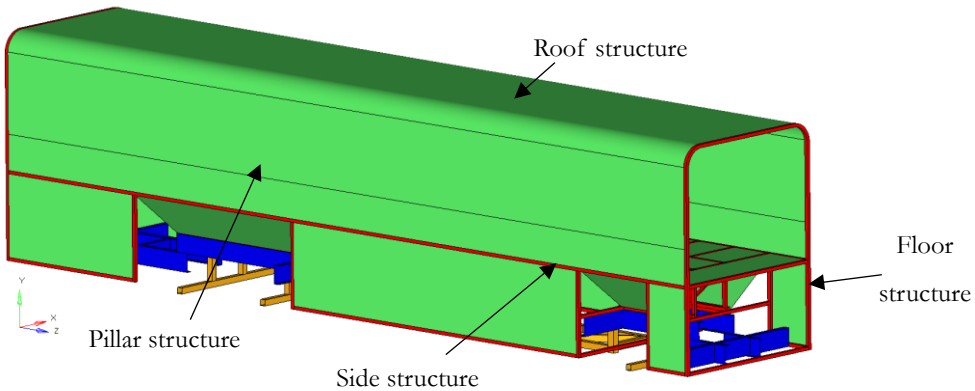

Figure 3.4 Bus structural model for topology optimization.

A real condition for the rollover test according to ECE-R66 concerns the permanent deformation of the bus structure during the test procedure. Therefore, a nonlinear analysis with material plasticity has to consider for the rollover problem by using dynamic analysis of finite element. Since dynamic rollover involves nonlinear geometric and material behaviors of the structure, finite element analysis of rollover process demands high cost of computation time and resource. To include the rollover evaluation as one of the design constraints of the optimization problem, an equivalent quasi-static load test is necessarily implemented in place of a complete dynamic analysis.

The result of topology optimization shows the material distribution of structure, which represents the locations and dimensions of the required members. Each optimization iteration stipulates the results for each part of the bus frame. An iterative optimization achieved the optimal structure for all design areas. The first optimization loop clearly shows the recommended positions of the pillar and the necessity of longitudinal beams along the bus length on top of the floor beam (figure 3.5). The upper parts of the bus structure were then modified with the location of pillars and longitudinal beams for reducing the number of design variables in the next optimization loop. The optimization process was continued with the same loading conditions. The locations of the side structure obtained in the second loop of the optimization process (figure 3.6), and the roof and floor structures displayed from the final optimization loop (figure 3.7). The final model of the bus structure (figure 3.8) was created based on all the results from the iterative topology optimization.

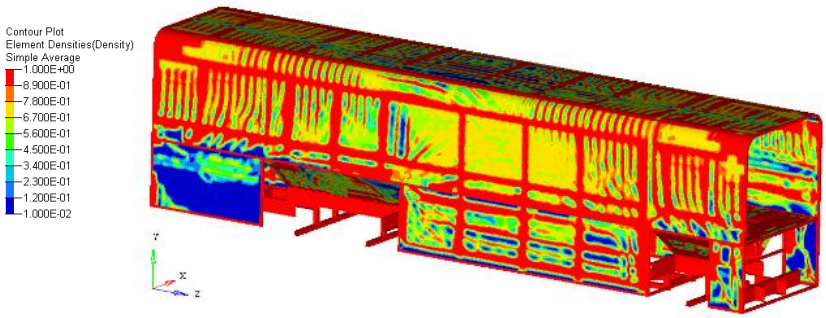

Figure 3.5 The first topology optimization loop with the results of pillar.

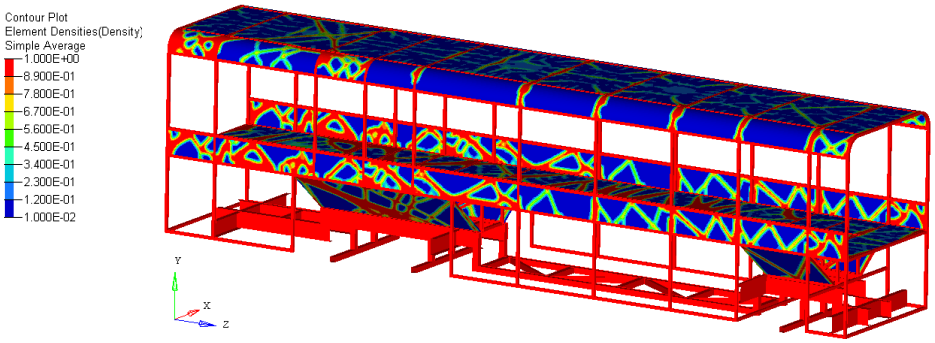

Figure 3.6 Optimization results for side structure.

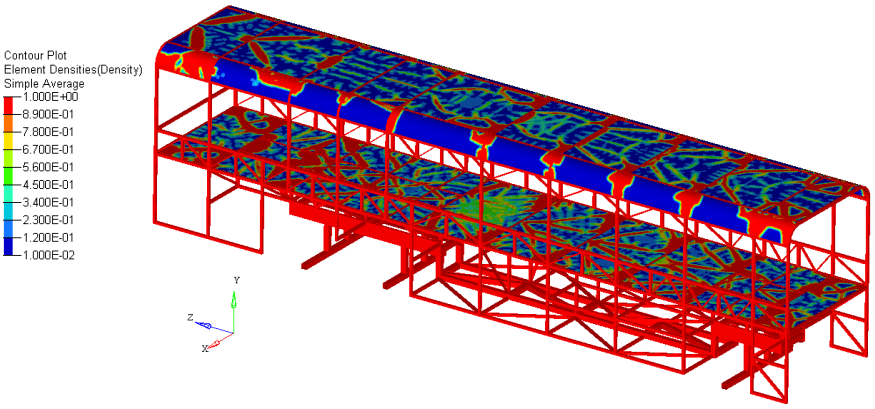

Figure 3.7 Optimization results for roof and floor structures.

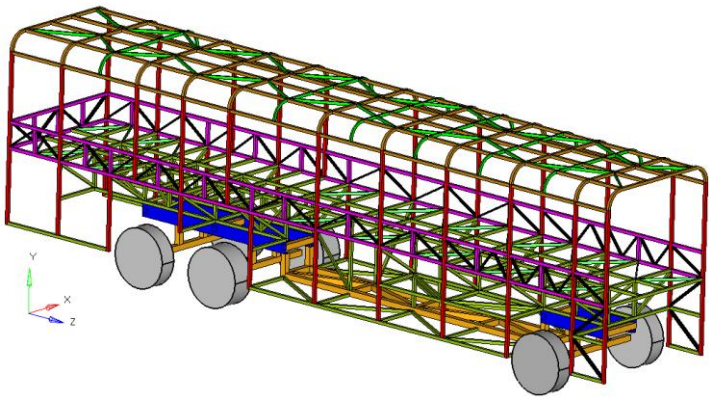

Figure 3.8 Proper model of bus structure from topology optimization.

The preliminary bus model from topology optimization was investigated the structural stiffness and strength under all safety requirements, including the rollover test according to ECE-R66. It found that the preliminary bus model passed the requirements of bending and torsion stiffness due to the deformation after the analysis was lower than the baseline model. Next, the full explicit dynamic rollover analysis considering nonlinear material and geometry was performed. The bus frame did not pass the requirement of the ECE-R66 regulation due to some of the pillar structure intruded into the assigned residual space during the rollover procedure (figure 3.9). Therefore, size optimization needs to employ for the current bus frame for implementing the structural performance.

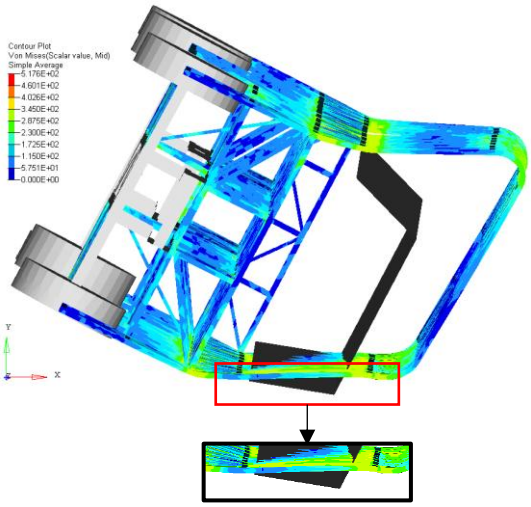

Figure 3.9 Rollover analysis of the preliminary bus frame.

3.4 Future Recommendations

Nonlinear topology optimization is an opportunity to design the bus frame under the rollover condition directly. The advantage of the nonlinear design for this problem is for optimizing the bus structure without any simplification on dynamic or nonlinear problems. Commercial software for analysis and design requires a high computational cost for the nonlinear geometrical structure and dynamic problem. Moreover, the optimization

steps can be reduced from the current process. If the nonlinear design is performed based on the topology optimization process, the size optimization does not need to employ for implementation of the structural performance in advance.

Other than those mentioned above, there are several problems that should consider the nonlinear material properties, such as crashworthiness or metal forming. Thus, this dissertation proposes a topology optimization technique, which includes nonlinear behavior into the optimization process. Furthermore, a new update procedure for nonlinear topology optimization is also introduced in the next chapter.

Chapter 4

PROPORTIONAL METHOD

The proportional method is used for updating the density value of each design variable during the optimization. The process and algorithm of this method are explained in this chapter. The criteria of fully stressed design for topology optimization also was merged for formulating the proportional algorithm.

4.1 Overview

The updated function is necessary through the topology optimization procedure due to the material interpolation of element densities needs to be intermediate updated in each iteration. Thus, there are many algorithms of the updated function proposed and adopted for the gradient based method for topology optimization such as Method of Moving Asymptotes (MMA) and Sequential Convex Programming. Among these methods, the

optimality criteria method [74-77] is the most common for updating the element density, which combines with the SIMP method. The sensitivity analysis is also required for utilizing the optimality criteria on the topology optimization process. Most topology optimization problems based on the gradient method for the linear structure have been employed the optimality criteria method to update the density of the design variable [2-4]. The sensitivity information of the objective function and optimization constraints is usually required by the derivation method to provide for the numerical algorithms when solving the topology optimization problem with the aforementioned algorithms. The sensitivity information is easily obtained for the general continuous differentiable function. However, for stress constraint problems, a calculation may bring an additional computation burden when theses sensitivities are required and are analytically complicated to derive. Thus, the optimization problem is challenging to obtain the derivation of these sensitivities without simplification for more complex problems such as mechanism synthesis using nonlinear analysis or crashworthiness design using dynamic analysis. For instance, a large number of stress constraints are imposed due to the calculation of sensitivity analyses that may become infeasible in practical applications. In another example, a structural analysis is always carried out the results in every iteration, and it causes computationally intensive when sensitivity analyses are concerned [31].

Since this dissertation aims to optimize the structure under the stress constraint problem (which describes in chapter 5), the non-sensitivity approach is necessary to apply with the optimization procedure. There are many algorithms on the non-sensitivities that have been introduced for topology optimization such as genetic algorithm, simulated annealing algorithm, and proportional topology optimization algorithm. These methods do not require the sensitivity information of the correlation functions in the design problem. Therefore, the complications associated with the sensitivity information can be avoided during the computational process. Moreover, an efficient of the non-sensitivity algorithms also has been verified in numerous published literature. To optimize the nonlinear material structure, the proportional topology optimization method is introduced in this research. It is an efficient non-sensitivity method for solving and updating the element densities

through the topology optimization with a stress constraint problem. The proportional topology optimization method is highly heuristic and searches for optimized solutions, and its performance is much better than stochastic methods [31]. In particular, it imposes constraints only globally on the entire system. Furthermore, the proportional topology optimization possesses some advantages in case of considerable efficiency and accuracy of solutions, no-requiring sensitivity information, and simplicity. It also possesses some disadvantages that relatively poor ability to approach the results of element density in 0-1 solution, poor robustness, and poor topology structure. Nevertheless, a new formulation of the proportional topology technique for updating the element densities in this work is also newly proposed by combining with the criteria for fully stressed design for topology optimization for performance improvement. The process and formulation of the proportional method are described in the following context of this chapter.

4.2 Updating Procedure

The proportional method proceeded with the updating procedure of the element density by concerning each design variable. This method requires an iterative calculation until the value of element densities converges to the termination criteria. The overall of the optimization process is illustrated in figure 4.1, in which the proportional technique is a sub-optimization loop for determining the element density only.

Every iteration of the optimization process starts from the finite element and stress analyses of an initial model. The results of each design element are then transferred as the input values for the optimization process. Material interpolation schemes are operated during the optimization process. After that, the proportional method is performed for investigating the element densities and checking with the sub-termination criteria. The element densities of the whole design area were compared with the convergence value, and the proportional process will be done if the results are convergence with the designated termination criteria. Otherwise, the proportional algorithm will be iteratively calculated and

updated the element densities until the convergence.

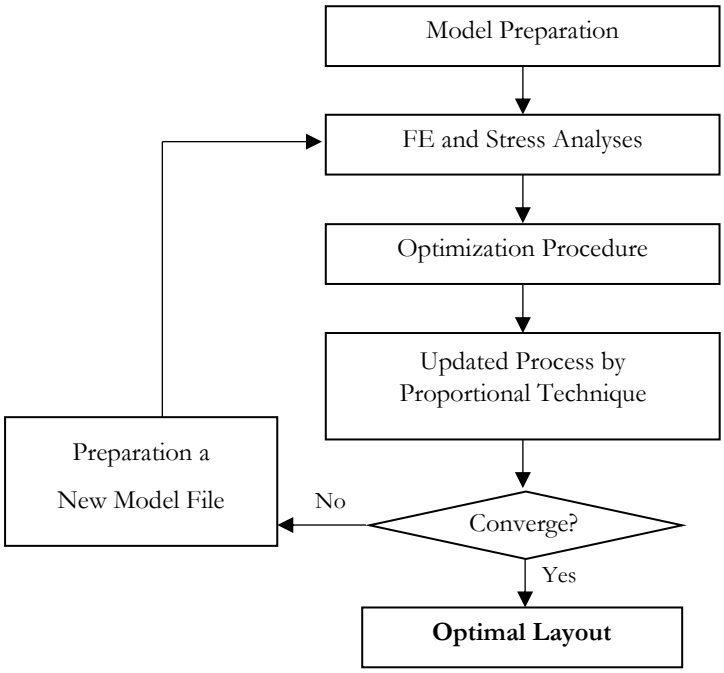

Figure 4.1 Overall process for structural topology optimization.

4.3 Proportional Algorithms

This research proposed the new proportional technique for topology optimization under stress constraint problem. So, an elemental stress of all design variables was salubrious for starting the updating process by this method. Target material amount (ρ_{target}) is first determined by investigating the elemental stress of all design variables. The value of the target material amount, which calculates by using equation 4.1 where ρ_i is element density at element i^{th} and N is a total number of design variables. This value represents the target of the total density value that should be involved in the final layout of the current optimization iteration. In other words, the current material amount will be updated to the target material amount.

$$\rho_{target} = \sum_{i=1}^{N} \rho_i \pm (total\ number\ of\ elements) \tag{4.1}$$

The valve of the target material amount depends on and investigates from the elemental stress (σ_i) when compared to the allowable stress (σ_{all}) of the design variables (figure 4.2).

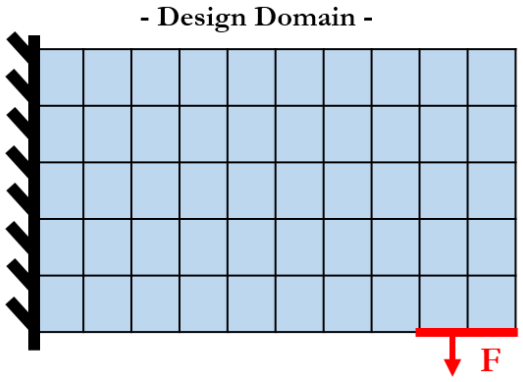

$$\sigma_i < \sigma_{all}$$

(a) All elemental stresses are lower than the allowable stress

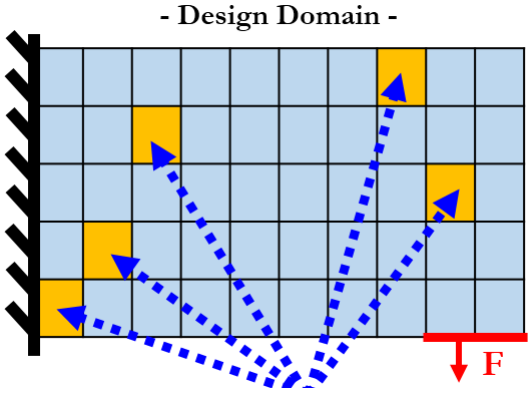

$$\sigma_i > \sigma_{all}$$

(b) Some of elemental stress is higher than the allowable stress

Figure 4.2 Investigation of the target material amount.

If the maximum elemental stress in the design area is lower than the allowable stress limit (figure 4.2a), then the current material amount is decreased by a material move amount (based on equation 4.1). Otherwise, the current material amount is increased by the same material move amount (figure 4.2b). The material move amount scales with the number of elements (0.002 x total number of elements) and, it fixes to be a constant value for all of the optimization process.

Next, the target material amount is distributed to the elements. The target material amount can be distributed iteratively because of this iterative procedure performs for the proportional algorithm. The material amount, which is distributed to the element, called the remaining material amount (ρ_{rem}). For each proportional optimization loop iteratively, the target material amount is assigned to equate to the remaining material amount.

To perform the proportional algorithm, the process is going to the inner loop for updating the optimal density value. The updated function for the proportional technique (equation 4.2) is employed for determining the optimal density value of each design variable (ρ_i^{opt}). The current element density of previous iteratively proportional optimization (ρ_i^{prev}) is a based value for evaluation of the new value of the element density. For the first iteration of the inner loop for the proportional process, the current element density of previous is set to be zero.

$$\rho_i^{opt} = \rho_i^{prev} + \frac{\rho_{rem}}{\sum_{i=1}^{N} u_i}\left(\frac{\sigma_i^q}{\sigma_{all}^q}\right)\eta_i \tag{4.2}$$

A ratio of the elemental stress and allowable stress is a criterion of the fully stressed design [78] for the topology optimization process, and it is combined to be one factor of the updated function for the proportional algorithm. An internal energy density (will be described in chapter 5) is also included to evaluate the optimal density value of each design variable. The above relation distributes the remaining material amount regardless of density limits. As a result, the actual material amount is different than the target material amount.

This difference is the reason for distributing the remaining material amount iteratively in an inner loop until the target material amount is reached. Every iteration of the inner loop starts with distributing the remaining material amount. It is followed by the application of filtering (η_i) for smooth material distribution and density limits. The proportional exponent *(q)* is recommended by the nonlinear optimization software [79] based on the *q* value should be 2.666 for suitable nonlinear optimization.

The new optimum density value is rechecked based on equation 4.3 by comparing to the first target of the material distribution (ρ_{target}), which is evaluated in the first iteration of each inner loop. The total optimal densities value of the current iteration should be a difference from the target material distribution, should not exceeded 0.001 as specified for the convergence criteria of the proportional method. The updating process of each design variable will be done if the difference value in equation 4.3 is less than the convergence criterion; if not, an iterative proportional calculation will be required until the total optimal densities value reaches the convergence. To calculate the optimal material density of the next inner loop, a new remaining material amount of the current iteration (ρ_{new}) is assigned to equate the remaining material amount (ρ_{rem}) of the next iteration. In the same way, the current optimum density (ρ_i^{opt}) is also assigned to be the element of the previous iteration (ρ_i^{prev}). After all the parameters were assigned, the iterative calculation performs again based on the propose update function (equation 4.2) until the optimal density value is converged.

$$\rho_{new} = \rho_{target} - \sum_{i=1}^{N} \rho_i^{opt} \leq 0.001 \tag{4.3}$$

4.4 Procedure Summarization

The overall process and updating details based on the proportional topology optimization method is illustrated in figure 4.3 with step by step. To find the optimal density of each design variable, the target material amount is necessary to determine for setting up

the target of all material distributions. The optimal density value is then calculated based on the updated function. All material distributions are rechecked by comparing to the first target of material for the current iteration. If the convergence is reached, the proportional topology optimization is done for the current main optimization loop.

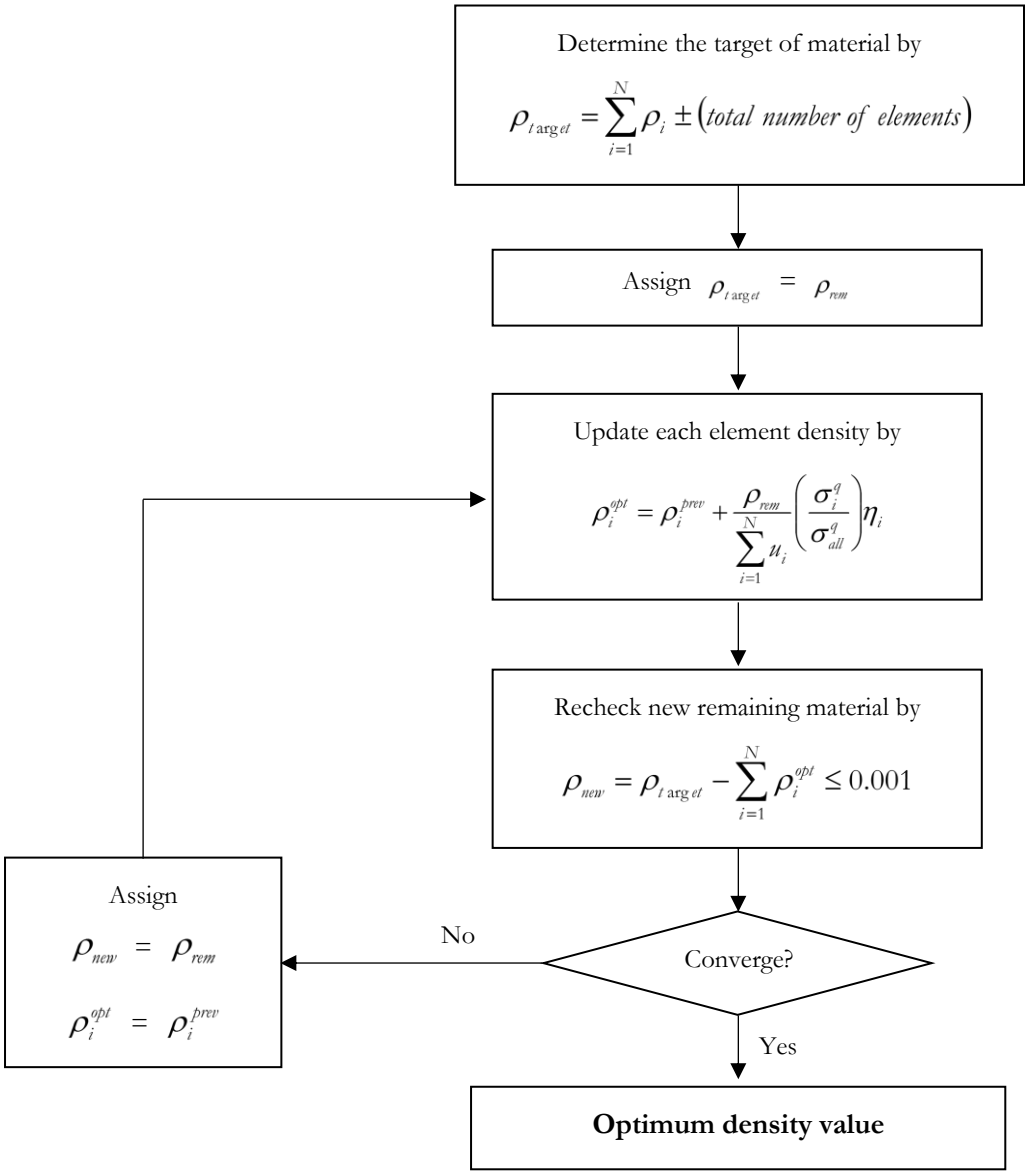

Figure 4.3 Step-by-step of the proportional topology optimization process.

The iterative calculation is performed again in case the optimal densities are not converged. The remaining material amount and the current optimal densities are transferred to be the new input parameter for the next inner loop optimization. The equation 4.2 is employed for evaluating the new value of each element density. This process repeats until all material distributions are reached to the defined convergence.

Chapter 5

MODEL VALIDATION

The validation process is used for investigating an efficiency of the proportional optimization method under nonlinear material structure. The optimal layout under the topology optimization by using the proportional technique is compared to the conventional gradient based method to evaluate the performance of this algorithm.

5.1 Optimization Model

A mechanical structure, which shown in figure 5.1, was expected to optimize under nonlinear topology optimization. This optimization process aimed to investigate the performance of the proportional algorithms when it was applied to the nonlinear material properties. This optimization model was fixed at the end of the left and right sides (cannot translation and rotation for all directions). An external load was applied at the center-top of the structure, which represented as the distributed load for 15 mm. The whole body of the structure (a gray area) was assigned to be the design domain in this problem.

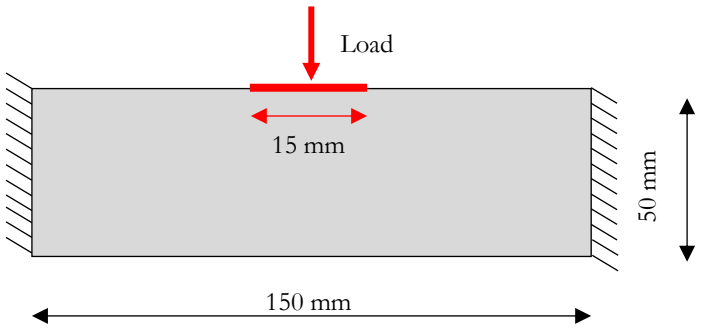

Figure 5.1 Design domain for verification model.

The discretization of the design domain performed based on LS-DYNA (a commercial finite element software). This process divided the whole design area into each element (meshing) and assigned to be the design variable. Figure 5.2 showed the finite element model for the initial design domain of the validation process. The model was created by using shell element; four nodes per one element, and each node has 6 degrees of freedom (3 translations and 3 rotations). The model consisted of 50 elements and 150 elements in the vertical and horizontal lines, respectively. Therefore, there are a total of 7,500 elements in this model as the first design variable, as implied for the total design variables.

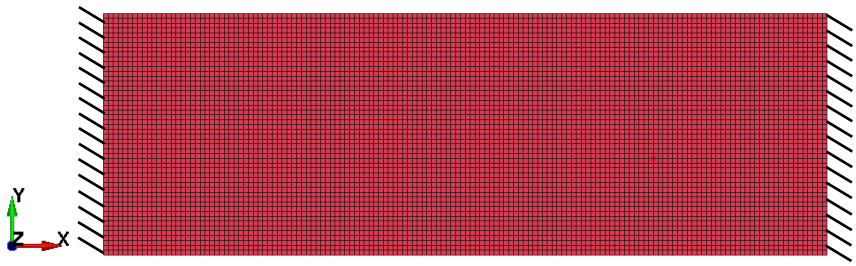

Figure 5.2 Finite element model of the initial design domain.

5.1.1 Characteristic of Material Property

To include the nonlinear behavior into the analysis and optimization process, the

characteristic of bilinear elastoplastic material properties was considered for the deformation behavior of the structure in the verification process. A relationship between stress and strain according to the bilinear elastoplastic material was displayed in figure 5.3 by excluding an unloading behavior. The behavior of the bilinear elastoplastic material shows a linear relationship between stress and strain after the yielding point until the end of ultimate tensile stress. Accordingly, 285 MPa of yield stress, 600 MPa of ultimate tensile stress, 0.3 of Poisson's ratio, and 207 GPa for Young's modulus were defined to the structure.

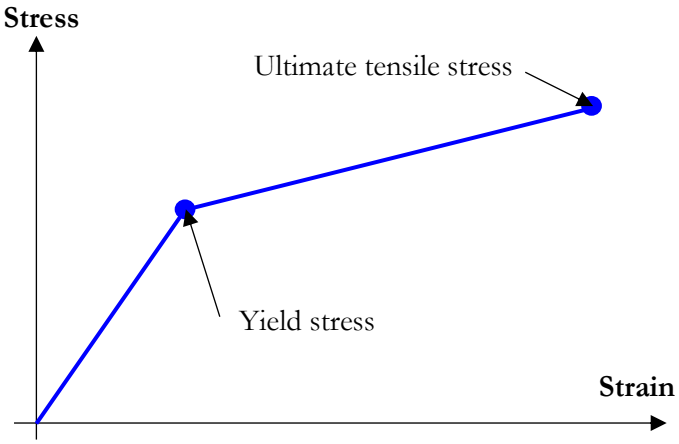

Figure 5.3 Bilinear elastoplastic material properties.

5.1.2 Analysis on Initial Design Model

The external load of 18 kN was applied to the structure as the static load case; it means the load value is not changed and varies by time during the analysis. The analysis procedure performed based on the finite element with the solver of LS-DYNA. This model sets the analysis conditions for the implicit static analysis problem for investigating the deformed shape within 1 seconds. All input and keyword commands have been done by LS-PrePost, which is a pre-processing software of the LS-DYNA. The results of deformation in the vertical direction and stress of the structure after the analysis was shown in figure 5.4 and 5.5, respectively.

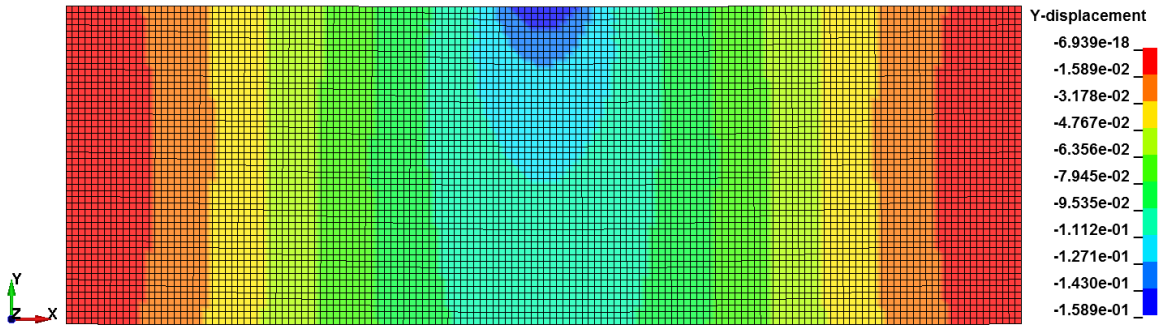

Figure 5.4 Deformation in the vertical direction of the initial design model.

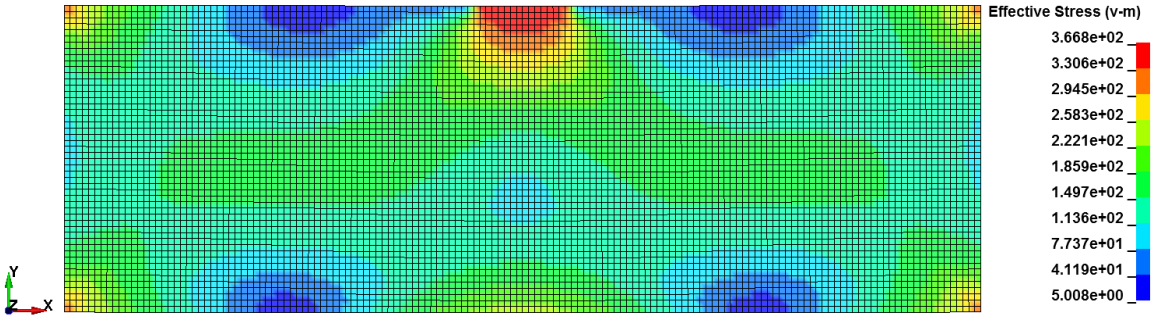

Figure 5.5 Von Mises stress in the vertical direction of the initial design model.

The maximum deformation of the initial design domain was 1.6 mm and caused 367 MPa for the maximum stress. These results implied the structure under the external load occurred the permanent deformation because the maximum stress was over the yield stress. In other words, the structure cannot be recovery its shape after the external load acted to the structure. For the application of nonlinear analysis and design, an internal energy is one parameter that indicates an ability for absorbed energy. The result of the global internal energy was displayed in figure 5.6, with the highest internal energy was 1,459 mJ. The result of internal energy showed the behavior of characteristic of nonlinear material by increasing in linear relation when the structure still was an elastic material. After the structure transformed into the plastic deformation, the internal energy kept the constant value until the end of the analysis procedure.

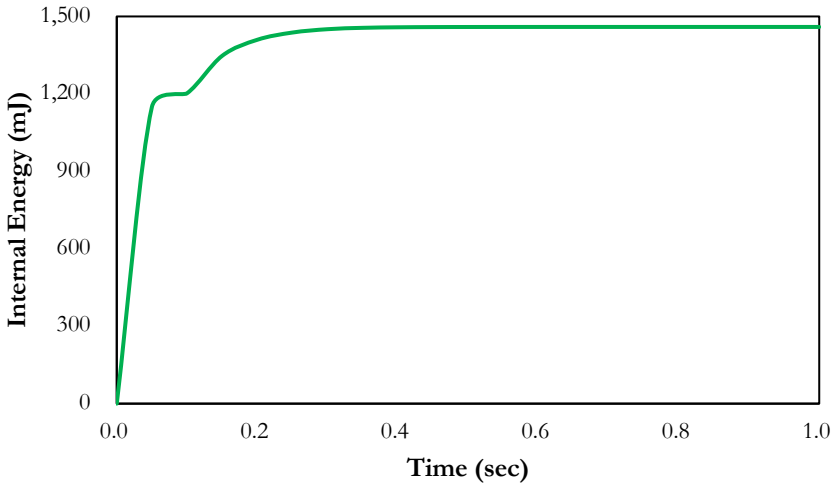

Figure 5.6 Internal energy of the initial design domain.

5.2 Filtering Density

Since the topology optimization for nonlinear mechanical structures is presented in this dissertation by using the SIMP method. The density approach or the SIMP method is usually prone the checkerboards and mesh-dependency to the problems if there is no regularization scheme. For example, four elements were considered by the surrounding one node in the finite element model. Two opposite elements were designated for the solid material, and the other two elements were a void material (circles, figure 5.7).

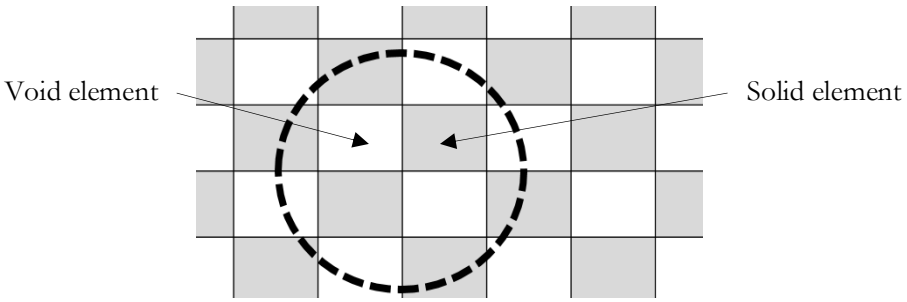

Figure 5.7 Element pattern by one-node connectivity for checkerboarding.

The element pattern arranged in the finite element model seemed to be a block pattern building. This pattern of element led to the checkerboarding problem for the design model, and it affected the numerical instability (which explained in Chapter 2) for the analysis process, which is not an obvious material distribution for the final layout. The numerical instabilities also effect to the analysis process and cannot get the results of the current model for preparing the input parameters of the next optimization loop. So, the checkerboards and mesh-dependency problems are also a big issue for the topology optimization process.

To reduce and protect the checkerboard pattern problem, there were many kinds of research have proposed and suggested different regularization schemes. The techniques for reducing the checkerboards problem were presents to use for connecting the elements with the topology optimization problem such as patch technique, perimeter control, higher-order finite element method, and filtering technique. The most popular method due to their ease of efficiency and their implementation is the density filters technique. Therefore, this dissertation also applied the filtering density technique to the nonlinear topology optimization with the proportional method.

A common filtered density for topology optimization [80] was employed for finding an optimal layout in the current process. The filtering density equations of design element i^{th} (η_i), which used for the nonlinear topology optimization with the proportional method in this dissertation, are shown as follows:

$$\eta_i = \frac{\sum_{j=1}^{N} w_{ij} d_j}{\sum_{j=i}^{N} w_{ij}} \tag{5.1}$$

$$w_{ij} = \begin{cases} \dfrac{r_0 - r_{ij}}{r_0} & for \quad r_{ij} < r_0 \\ 0 & for \quad r_{ij} > r_0 \end{cases} \tag{5.2}$$

$$r_{ij} = \sqrt{\left(x_i - x_j\right)^2 + \left(y_i - y_j\right)^2} \tag{5.3}$$

where w_{ij} is a weight filtering factor of element i^{th} and j^{th}, d_j is the non-filtering density of element j^{th}, r_0 is the prescribed filtering radius and r_{ij} is a distance between element i^{th} and j^{th}. For the validation process, the prescribed filtering radius (r_0) is defined to for determining the size of the sphere of influence (as illustrated in figure 5.8). The distance between element i^{th} and j^{th} always automatically calculates by applying equation 5.3 based on center-to-center distance between centroid of elements i^{th} (x_i, y_i) and j^{th} (x_j, y_j).

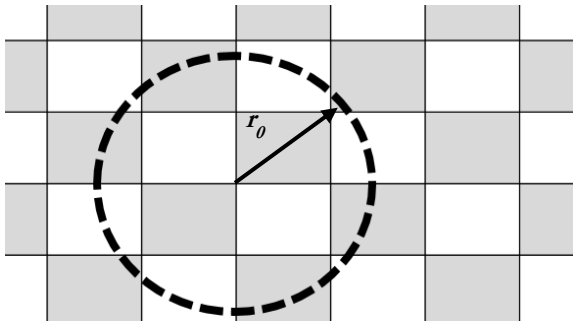

Figure 5.8 Prescribed filtering radius.

5.3 Optimization Problem

There are many types that have been introduced the problem of nonlinear topology optimization problem. Stiffness of a structure is represented by strain energy, compliance, or complementary work (figure 1.2) due to nonlinear behavior. A different function is used through the nonlinear topology optimization will be obtained different results due to the value of three parameters are unequal along with the geometrically nonlinear structure. Most studied focused on minimizing compliance for maximizing the stiffness of the structure. Meanwhile, minimizing the strain energy or the complimentary work is also performed to optimize the structure under nonlinear material geometries.

The aim of the topology optimization in this dissertation is to represent the nonlinear problem of material properties. Thus, an application of the automotive manufacturer was focused on the optimization problem for acquiring an optimal layout of the structure. In crashworthiness design, the internal energy is expected to increase for absorbing ability while keeping the loads transmitted to the occupants. This is the most common method to ensure passenger safety when it occurs an accident with the vehicle, such as a frontal crash accident. Therefore, the internal energy density of each design element was expected to maximize and defined as the objective function. A mathematical formulation of the objective function can be written as follows:

$$U(\rho) = \sum_{i=1}^{N} E_e\left(\rho_i\right) u_i \tag{5.4}$$

where $U(\rho)$ is the objective function of this optimization problem, N is total numbers of design variable, E_e is the material properties of the structure, u_i the elemental internal energy density and ρ_i is the element density at element i^{th}. The vector of all design variables is shown as follows:

$$\rho = \left\{\rho_1, \rho_2, \rho_3, \ldots, \rho_N\right\} \tag{5.5}$$

The element distortion is one more problem when highly nonlinear behavior appears during the finite element analysis. In this case, elemental stress was used to be the criteria for investigating the failure of the element. Each design element should not exceed the allowable stress through analysis and optimization processes, and it was assigned to be the optimization constraint. Moreover, the element density value for topology optimization is acceptable in the range of zero to one, which represents void and solid elements, respectively. So, all optimization constraints for the elemental stress $(g(\rho))$ and the element densities $(p(\rho))$ can be written in mathematical formulations as follows:

$$g(\rho) = \frac{\sigma_i}{\sigma_{all}} - 1 \le 0 \tag{5.6}$$

$$0 < \rho_{\min} \le \rho_i \le 1 \tag{5.7}$$

where $\rho_{\min}$ is a minimum allowable element density as 0.3 that defined for this value. The optimal results have to satisfy all conditions of the optimization constraint. If the results are not satisfactory, either one or all the optimization constraints, the optimization process will be termination.

5.4 Optimization Procedure

The whole process for doing a numerical example consists of two sections: analysis procedure and optimization procedure. Both two procedures were merged into one process for calculation and optimization automatically. For this dissertation, LS-DYNA solver performed all the nonlinear numerical analyses, while all optimization algorithms operated and executed through coding on MATLAB. To convey all analysis results from LS-DYNA to MATLAB, the coding of LS-PrePost Scripting Command Language was also employed to support the transferring results during the optimization procedure.

5.4.1 LS-DYNA Operation

The initial design model was created based on LS-PrePost and discretized the design domain into each design variable. Firstly, all design variables were assumed to be a solid element for evaluating structural performance. The material properties of bilinear elastoplastic (figure 5.3) assigned to all design elements. Due to LS-DYNA was used for structural analysis in every iteration of the optimization process, the material properties for the void element are also necessary to assign during the model file preparation. The void

element should not affect any results during the analysis procedure, so, the material properties in Table 5.1 was assigned for the void material. Boundary and loading conditions were also constructed to the initial design model in the LS-PrePost for combining all components to create the model file (input file). The model file was analyzed by LS-DYNA and collecting all the necessary results.

Table 5.1 Material properties for void material.

Mechanical Properties	Value
Young's Modulus	0.001 GPa
Density	1×10^{-6} kg/m^3
Poisson's Ratio	0.3

Results after the analysis procedure have to convey for preparing the input parameter of the optimization process. Since the automatic calculation requires for every optimization iteration, the LS-PrePost Scripting Command Language (SCL) used in this dissertation for performing data manipulation between LS-DYNA and MATLAB smoothly. The LS-PrePost SCL is likely a C computer language that is executed inside LS-PrePost. The results from the analysis, model data, and additional operations of LS-PrePost can retrieve and execute by applying the LS-PrePost SCL. So, the user needs to define the target for retrieving and coding the computer language by themselves. The structural layout for coding the LS-PrePost SCL script is shown in Table 5.2 as follows:

Table 5.2 Coding structure for LS-PrePost SCL.

Basic structure of the LS-PrePost SCL script
Definition section → *Void func()*
Global declaration section → *int a* =…
Main () function section → *define the types of result*
Subprogram section → *define the time interval for getting the results*

5.4.2 MATLAB Operation

All processes until acquiring an optimal layout (structural analysis and optimization) were controlled and coding based on MATLAB programming. The coding structure for merging operation between LS-DYNA and MATLAB is shown in Table 5.3 with an overview process. MATLAB reproduced the layout of the design variable based on the finite element model to imitate the design domain. The element density was then initialized to each design variable for initiating the topology optimization process. The results of internal energy density and elemental stress were extracted based on the LS-PrePost SCL and rearrange data by MATLAB to calculate the objective function and investigate the optimization constraints. After finished the updating process through the proportional algorithm, the structural model was analyzed to examine all the optimization conditions based on controlling by MATLAB code. If the new structural model does not satisfy, MATLAB will update the element type (solid or void element) and rewrite the new finite element input file according the format of LS-DYNA. Iterative calculation and optimization are required by MATLAB until the all conditions are satisfied. And the new layout and stress distribution of structure after optimization process are displayed by MATLAB.

Table 5.3 Overview process for coding on MATLAB.

Coding structure on MATLAB programming
Define initial parameters for optimization
Analyze the model → *using LS-DYNA solver*
Import and arrange the analysis results → *using LS-PrePost SCL*
Optimize the structure using the SIMP
Update element using element density using proportional technique
Create a new model file
Analyze the structure from new model file → *using LS-DYNA solver*
Display the optimal layout
Check the optimization criteria

The overview process for nonlinear topology optimization in this dissertation was illustrated in figure 5.9, with step by step until the optimal layout is obtained. Every step during the optimization process has to generate the results and transfer to the next step for analysis or optimization automatically. Therefore, the flow of coding in MATLAB needs to be careful. The process of rewriting the new model file according to the format of LS-DYNA is also the most important section for doing the iterative optimization process. If the format of the model file is wrong, the process will be termination.

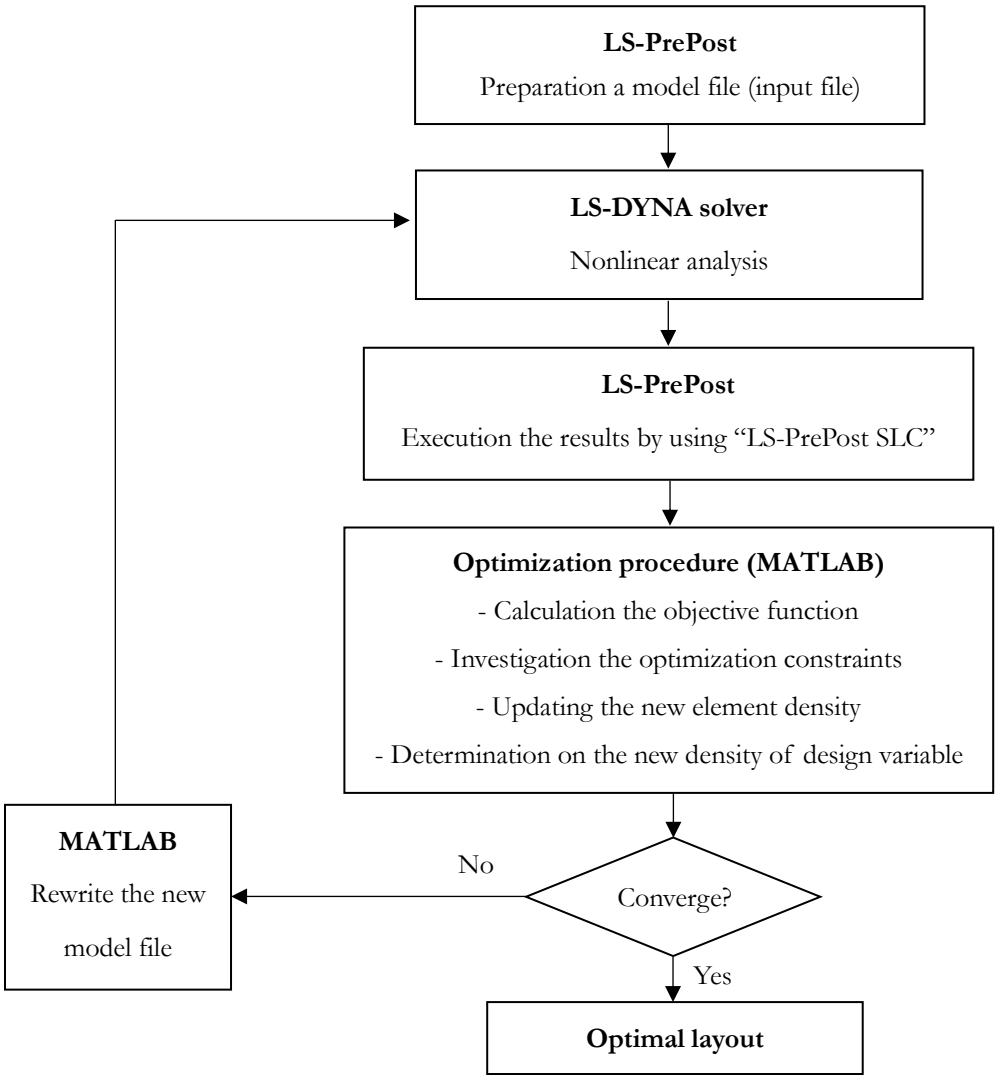

Figure 5.9 Overview the topology optimization process.

5.5 Optimization Results

The optimal layout was acquired by using the topology optimization technique with the proportional method. The objective function and optimization constraints followed equation 5.4, 5.6, and 5.7, respectively. The optimization and optimal layout are divided into two parts: linear and nonlinear material properties. Design variables were defined as in question 5.5, which is the whole area of the design domain (figure 5.2).

5.5.1 Linear Material Property

Linear analysis with elastic material properties (figure 5.10) was considered in this section. Therefore, the structure is allowable to recover to the initial shape after deformation under applied the external load. The topology optimization with the proportional technique based on a characteristic of linear material aims to compare the optimal layout with the analytic results. The yield stress is assigned to the structure as 285 MPa with 207 GPa of Young's modulus. The optimization results expected to observe on material distributions of the structure during the optimization process. An iterative optimal layout on linear material structure showed in figure 5.11.

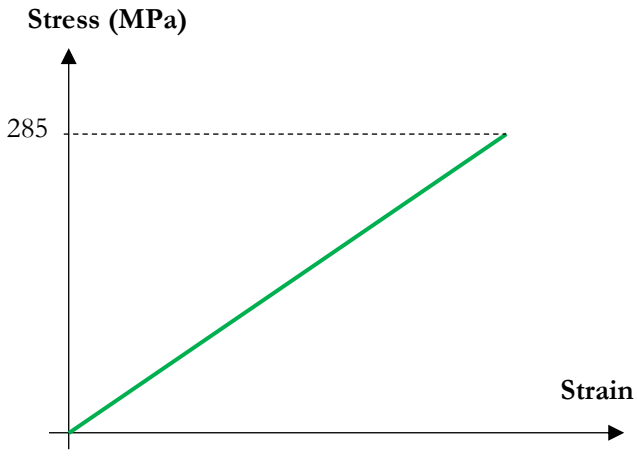

Figure 5.10 Characteristic of elastic material.

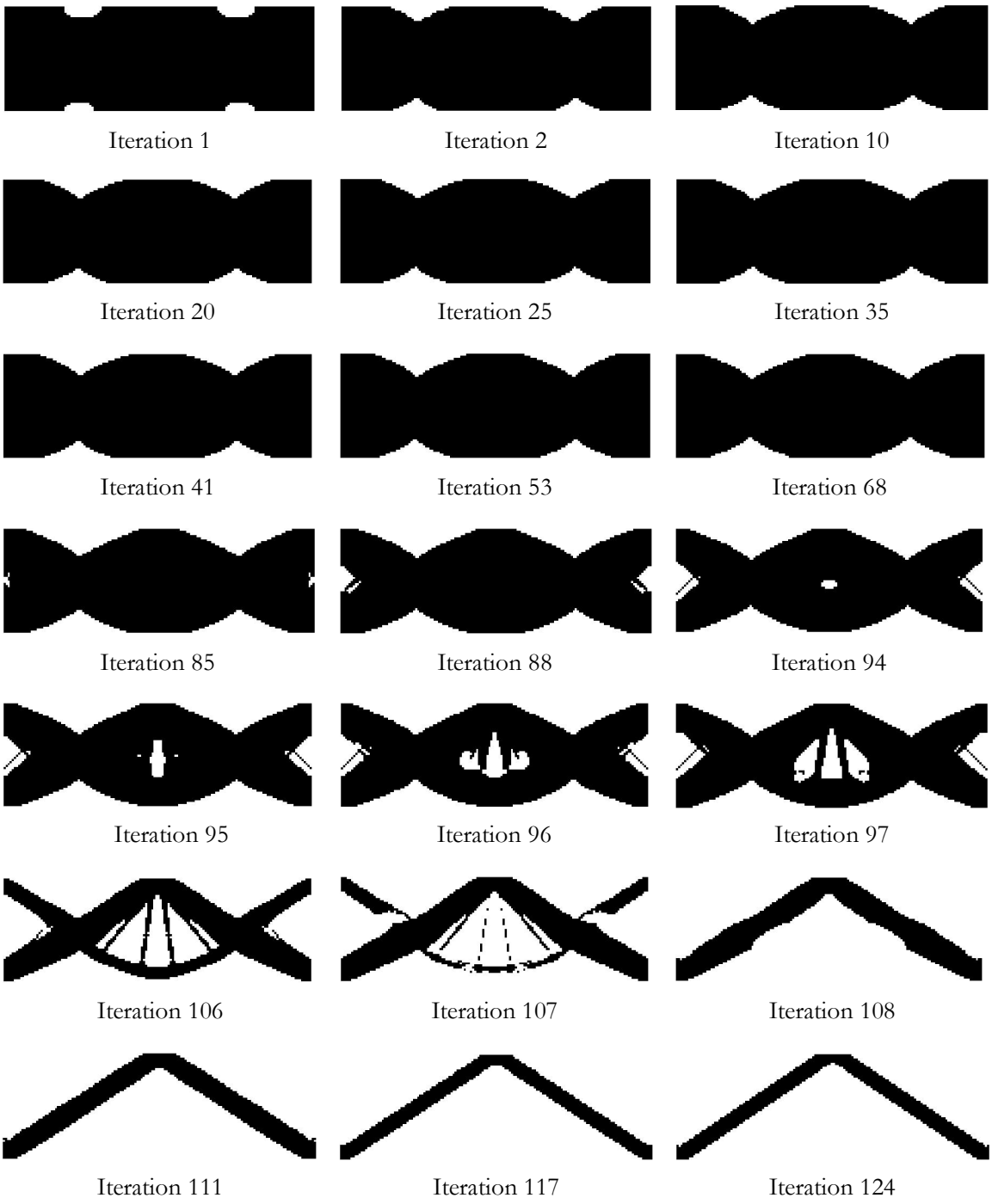

Figure 5.11 Iterative material distribution for the validation process based on linear material structure.

The optimal layout obtained at iteration 124 (figure 5.12) with stress distribution does not over the stress limit (figure 5.13). During the optimization process, the layout changed slowly since the process started until iteration 93. After that, the major change of the design domain displayed from iteration 94 by removing the unnecessary elements from the design domain. The maximum stress occurred at the bottom part of the structure (right and left sides) with 123 MPa and the stress distributed at members of the structure around 73 MPa. The structural layout of the optimal design showed the proportional technique performed to optimize the structure based on the linear material properties because the final layout acquired as same as the analytic results.

Figure 5.12 Final layout on linear structure for the verification model.

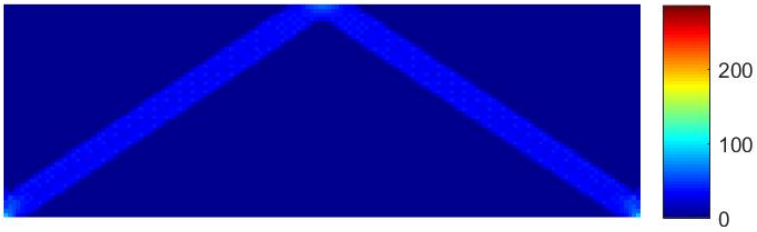

Figure 5.13 Stress distribution of the final layout for the linear verification model.

5.5.2 Nonlinear Material Property

The characteristic of bilinear elastoplastic material (section 5.1.1) was assigned to the structure for validating the topology optimization method. For nonlinear topology design, the stress limit (equation 5.6) was assigned to 600 MPa for the optimization constraint. The material and stress distributions of the optimal structure during the nonlinear design were shown in figure 5.14 and 5.15, respectively.

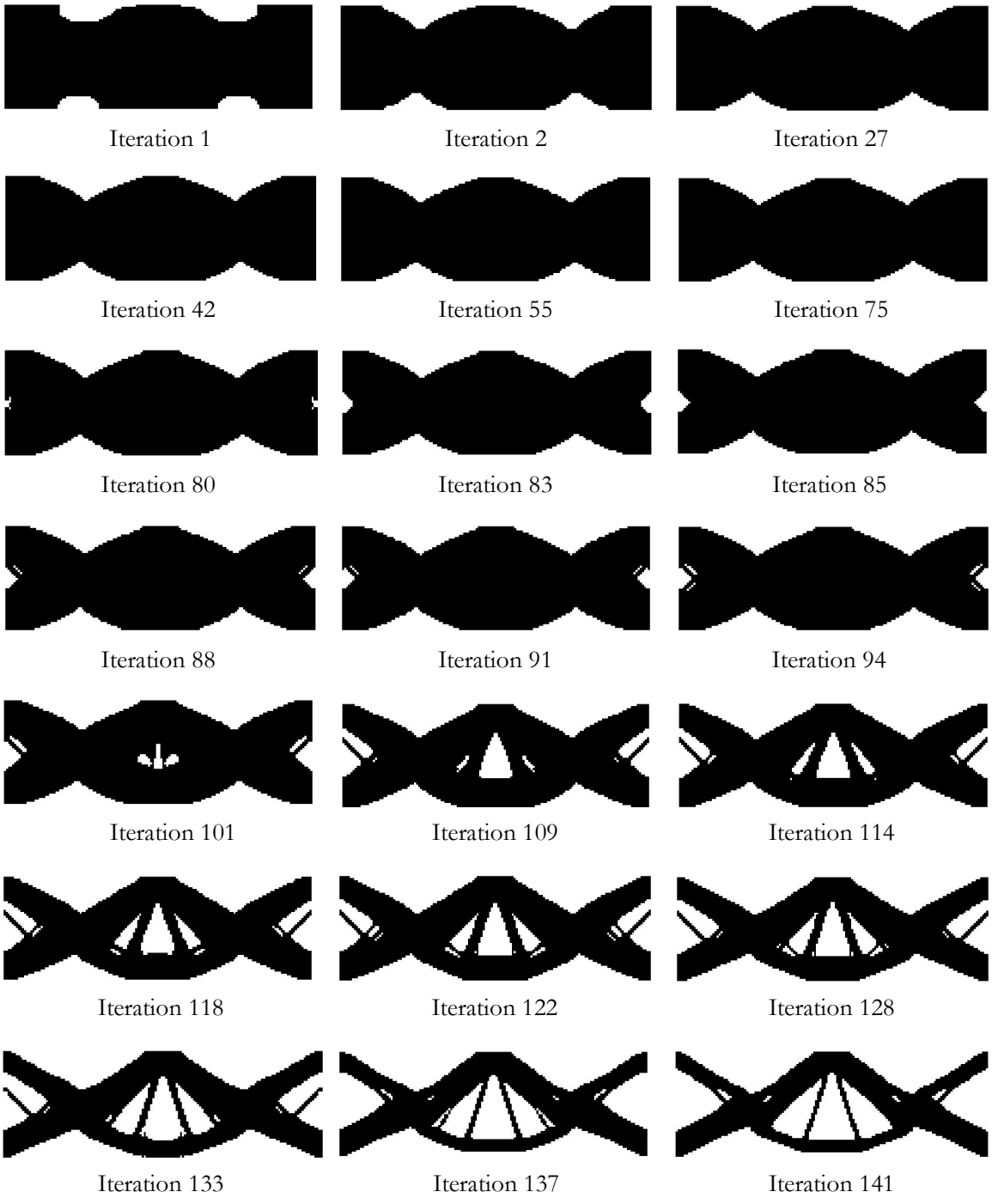

Figure 5.14 Iterative material distribution for the validation process based on nonlinear material structure.

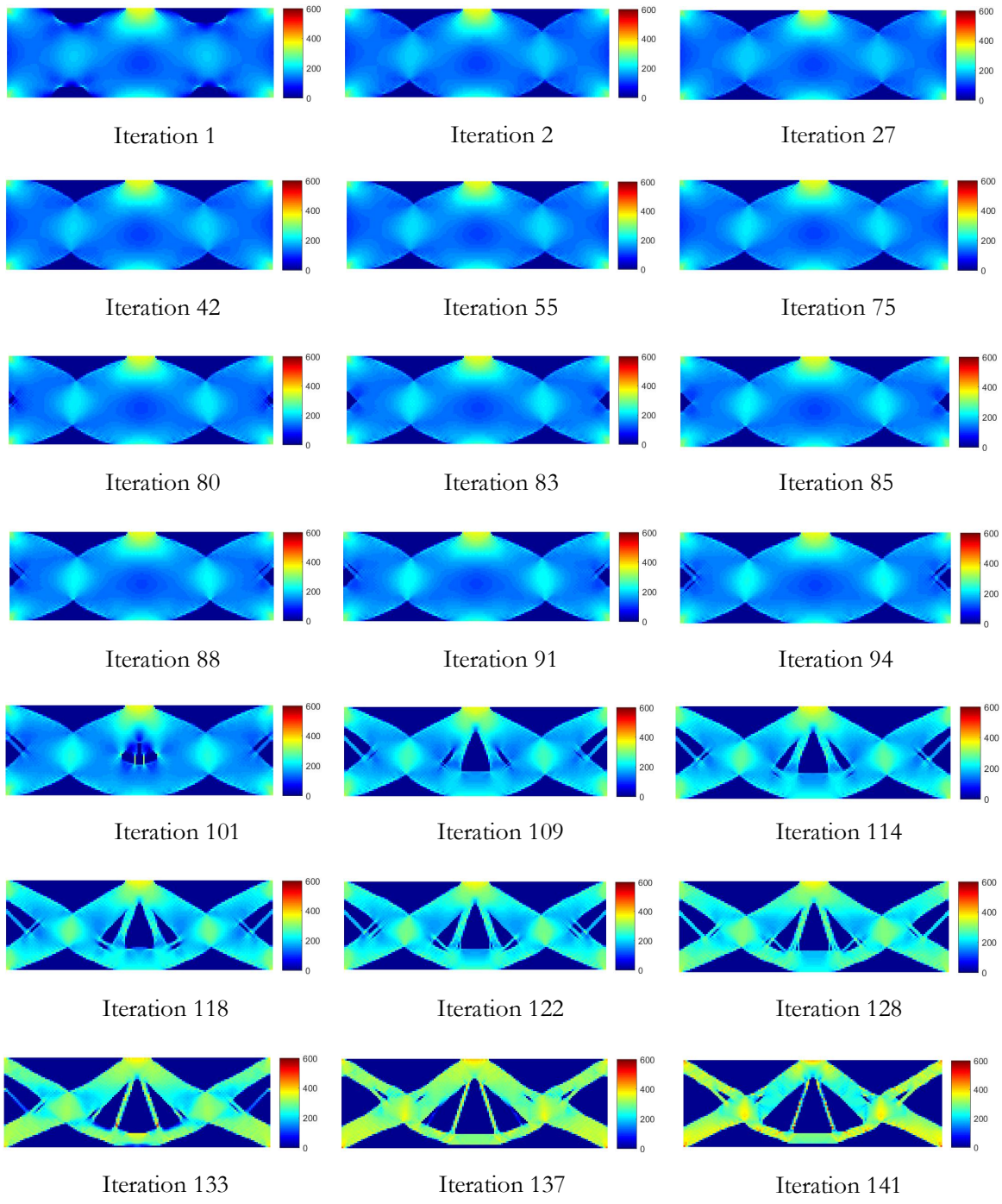

Figure 5.15 Iterative stress distribution for the validation process based on nonlinear material structure.

The final layout based on nonlinear topology optimization acquired at iteration 141, with the result showed fully stressed distribution inside the members of the structure (figure 5.16). The top and bottom areas were removed since iteration 1. The end left and right sides of the structure were also deleted around iteration 80. The hollow area occurred by eliminating the un-want design variables at the center of the structure around iteration 100, and the layout changed until it obtained the final layout continuously. The maximum stress of the final layout was 490 MPa, which is not over limit of the stress design. The material distribution of the final layout will be compared to the layout from the gradient method in the next section for investigating the performance of this algorithm.

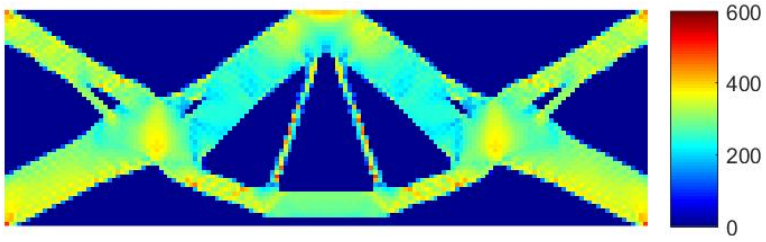

Figure 5.16 Stress distribution of the final layout for the nonlinear verification model.

5.6 Results Comparison

The optimal layout based on nonlinear topology optimization will be compared only in this section due to the linear topology optimization acquired the final design as same as the analytic result. The final design of the gradient method [81] was employed to compare with the result from topology optimization with the proportional method. The final layout from the gradient and proportional topology method were compared by displaying in figure 5.17a and 5.17b, respectively. The results showed that the optimal layout from the proportional technique was similar to the gradient method. The material distributions after the topology optimization process were similar to obtain the layout of each member and can predict the same real model. There are some limitations in this dissertation to verify this model to be the exact results with the gradient method based on dimensions of the

design domain, material properties, and the objective and optimization constraint. This dissertation defined the object function and optimization constraints which differed from the reference model. But the characteristic of material properties was the same. So, it is not easy to verify the same optimization conditions due to the optimal layout based on nonlinear topology optimization are sensitive to an external response.

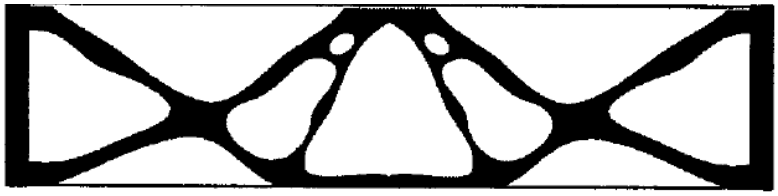

(a) Topology optimization with gradient method [81].

(b) Topology optimization with proportional method.

Figure 5.17 Comparisons on the optimal layouts for the bilinear elastoplastic material.

5.7 Conclusion

The nonlinear optimization with the proportional topology method was performed for acquiring the final layout, both linear and nonlinear material properties. The proportional algorithm formulated by combining the criteria of topology optimization on fully stress design for updating the element densities in each optimization iteration. Collaborative action between the analysis process under LS-DYNA solver and optimization procedure by coding on MATLAB was implemented to move the whole process smoothly.

The optimization of the linear material structure showed the final layout could be obtained as same as the analytic problem. To verify the optimization of the nonlinear problem, the main limitations are objective function and optimization constraints due to there are various types to define the problem, and it is sensitive to the material properties. The final layout from topology optimization, according to bilinear material properties, showed material distribution inside the design domain similar to the result from the gradient method. Moreover, the stress of the final model fully distributed on structural members. Thus, the proportional technique can be performed the topology optimization on the nonlinear mechanical structure.

Chapter 6

OPTIMIZATION ON STATIC LOADING

This chapter investigates numerical examples for both linear and nonlinear structural designs by topology optimization based on the proportional method. Over-relaxation factor is applied for improving the convergence of the updated function during the optimization procedure. The numerical examples on the over-relaxation are also examined.

6.1 Optimization Model

An imitation of a cantilever beam (figure 6.1) was defined to be the design model for nonlinear topology optimization problems. A dimension of 50 mm high and 150 mm wide constructed the initial design model with applied a downward direction of the external load. The structural model was fixed at the end left side of the structure for all directions (cannot translation and rotation for all directions).

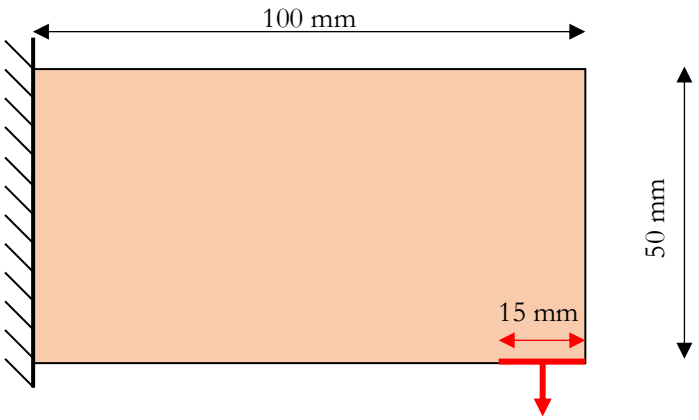

Figure 6.1 Initial model for nonlinear topology optimization with static loading.

The design domain was focused on the two-dimensional model, which assuming the shear stress was minimal and assigned 5 mm for the thickness. The model created by using shell element, which is four nodes per one element; one node has 6 degrees of freedom (3 translations and 3 rotations). The model creation was according to the dimension of figure 6.1. The design area was created and discretized to assign the design variable by using LS-PrePost. The element size of the design area was specified to 1 mm per each side, 100 elements along the vertical line, and 50 elements along the horizontal line (figure 6.2). Therefore, the finite element model totally consisted of 5,000 elements, and it assigned to be all the design variables during the topology optimization process.

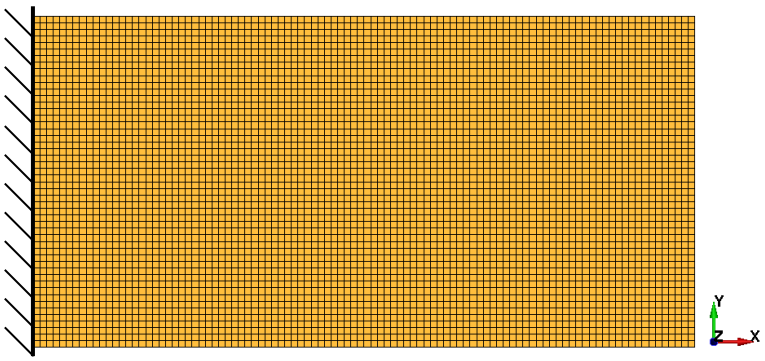

Figure 6.2 Finite element model of the initial design on static loading.

The finite element model of the initial design domain (figure 6.2) was firstly analyzed to investigate the structural performance with 8 kN of the external load. The bilinear elastoplastic material properties (figure 5.3) was considered for structural behavior after deformation. The problem also analyzed based on implicit static. The material properties were defined as the same as the optimization process in section 5.5.2. Analysis procedure performed by using LS-PrePost and LS-DYNA solver. The results were displayed in figure 6.3 and 6.4 for displacement in the y-direction and von mise stress, respectively. The maximum displacement occurred 0.28 mm, while 320 MPa caused for the maximum stress. From these results, the structure after the external load acted to the model became the permanent deformation period, which cannot recover to the initial shape, because the maximum stress was over the yield stress.

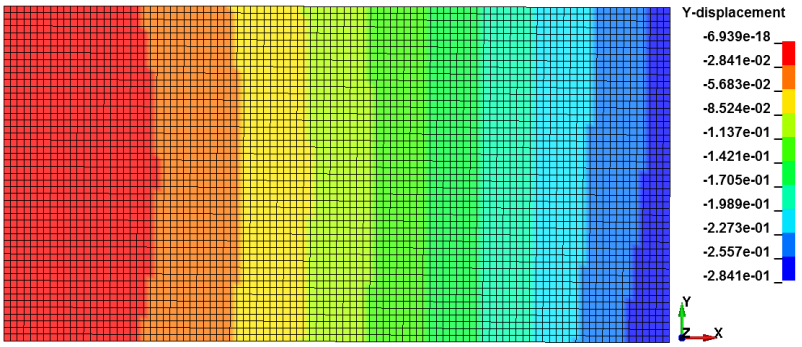

Figure 6.3 Vertical displacement of the initial design model on static loading.

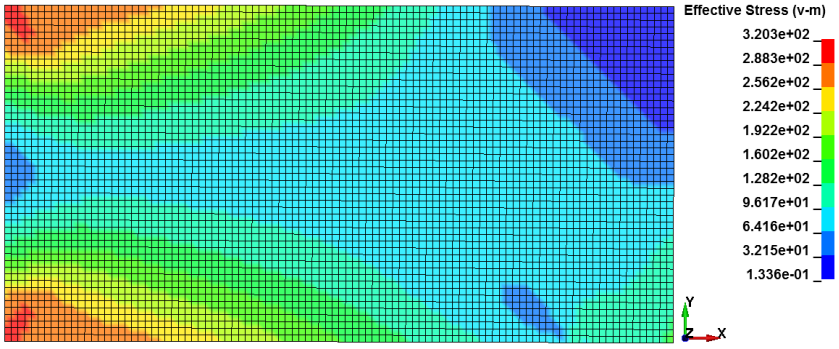

Figure 6.4 Stress distribution of the initial design model on static loading.

6.2 Optimization Results

The topology optimization performed with an updated function based on the proportional method (in chapter 4). All element densities of the design area updated their density values according to the update function in equation 4.2 by applying equation 5.1 and 5.2 for the filtering density technique. The structures were expected to maximize internal energy (equation 5.4) as defined as the objective function. There are two sections for investigating the optimization algorithm performance: linear and nonlinear material models. Analysis and optimization procedures operated based on the overview of the topology optimization process, which described in section 5.4.2 (figure 5.9). The optimization results and conditions are shown in the following section.

6.2.1 Linear Material Model

A characteristic of the linear material model, which showed in figure 5.10, was employed for the topology optimization process with linear static analysis. The elemental stress of all design variables should not exceed 285 MPa as assigned as the optimization constraint (equation 5.6). According to 207 GPa of Young's modulus and 0.3 of Poisson's ratio were also assigned to each design element. Iterative optimization results were shown in figure 6.5 and 6.6 for material and stress distributions during the optimization process, respectively.

The optimization process started to remove the design variables in the low-stress area of the design domain (middle-left and top-right areas). After that, the design elements at the center area were eliminated since iteration 30. The pre-layout of the structure was displayed around iteration 80. At iteration 126, the optimal layout acquired based on the elastic material model and linear static analysis. The maximum stress occurred at the top-left and down-left side of the structure with 220 MPa. This value can be confirmed that the optimization process is a convergence problem because the maximum stress of the stress is not over the stress limit during the optimization process.

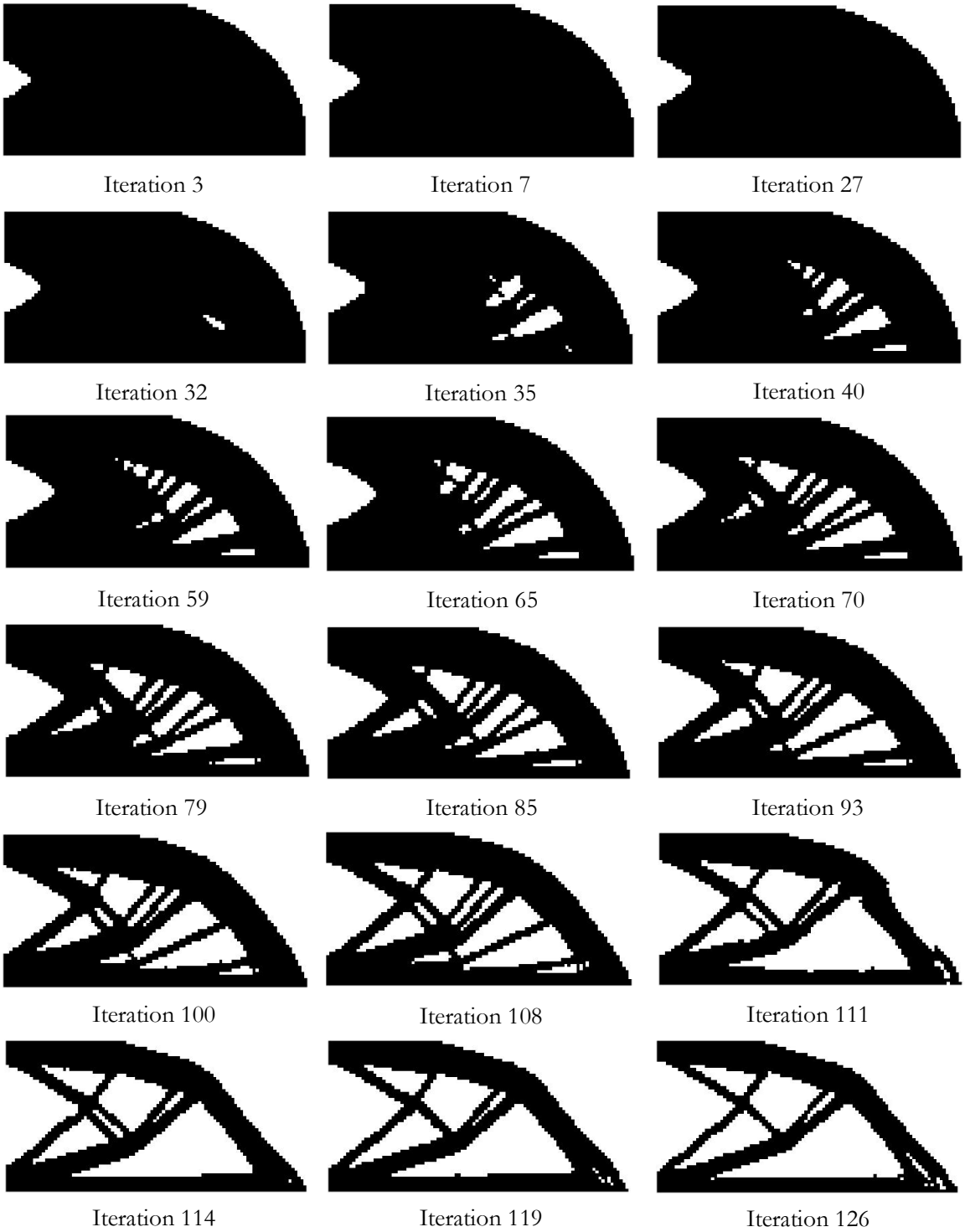

Figure 6.5 Iterative material distribution for static loading on linear analysis.

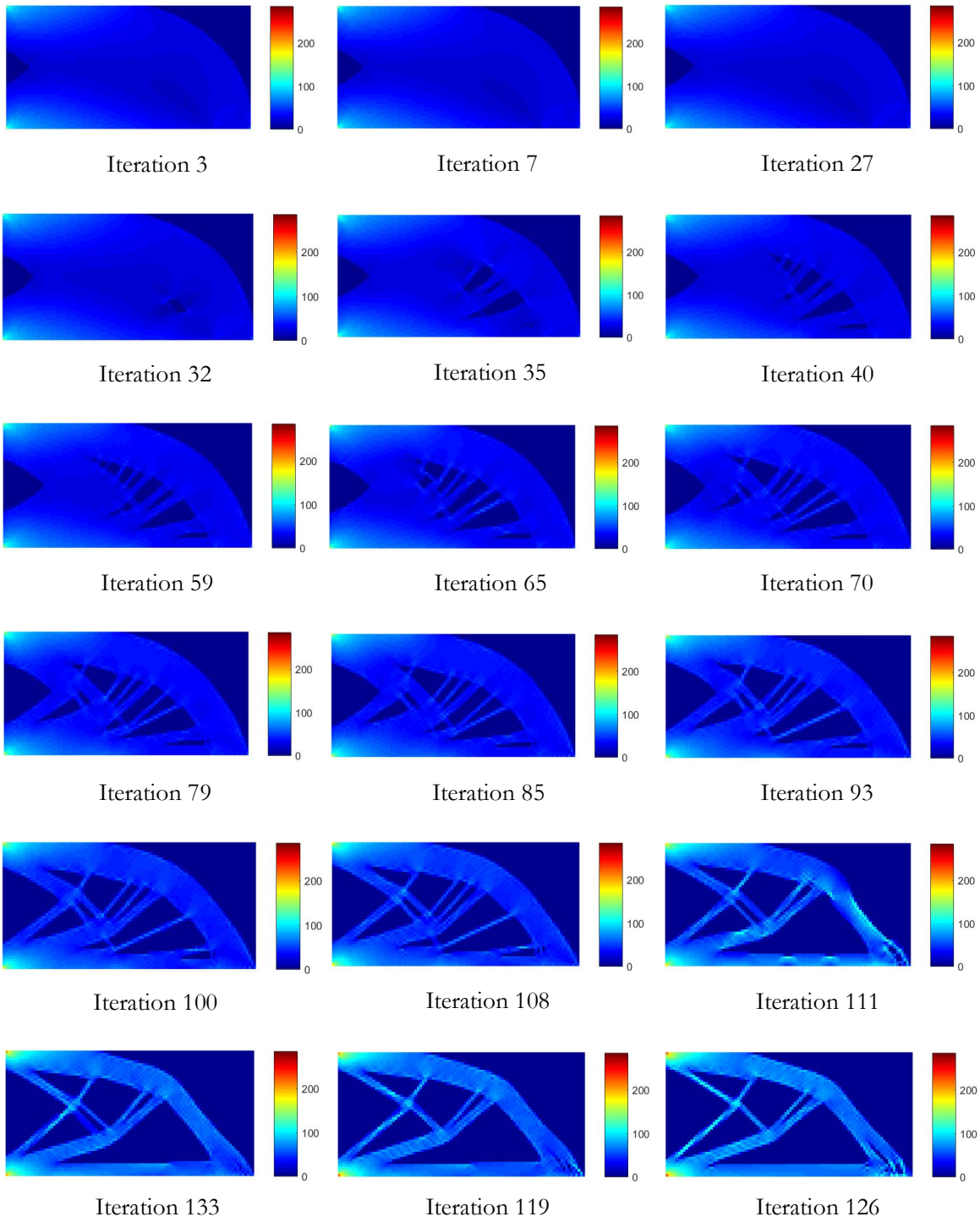

Figure 6.6 Iterative stress distribution for static loading on linear analysis.

6.2.2 Nonlinear Material Model

The topology optimization proceeded to find an optimal layout based on the nonlinear behavior of the characteristic of bilinear elastoplastic material property (figure 5.3). The maximum stress of 600 MPa was also assigned to be the optimization constraint (equation 5.6) for all design variables during the optimization process, as same as the verification procedure.

The maximum stress during the topology optimization process (measured from the maximum element in each iteration) was displayed in figure 6.7 for investigating the convergence. The stress history led to the stress limit (600 MPa) and not over the limit. Therefore, the optimization process was the convergence problem for nonlinear material property. An iterative material and stress distributions for nonlinear topology optimization were shown in figure 6.9 and 6.9, respectively. The optimization process also started by removing a low-stress area from the design domain until obtained the final layout at iteration 151. Moreover, the final layout showed fully stressed distribution in all members and no failure occurred during the optimization procedure.

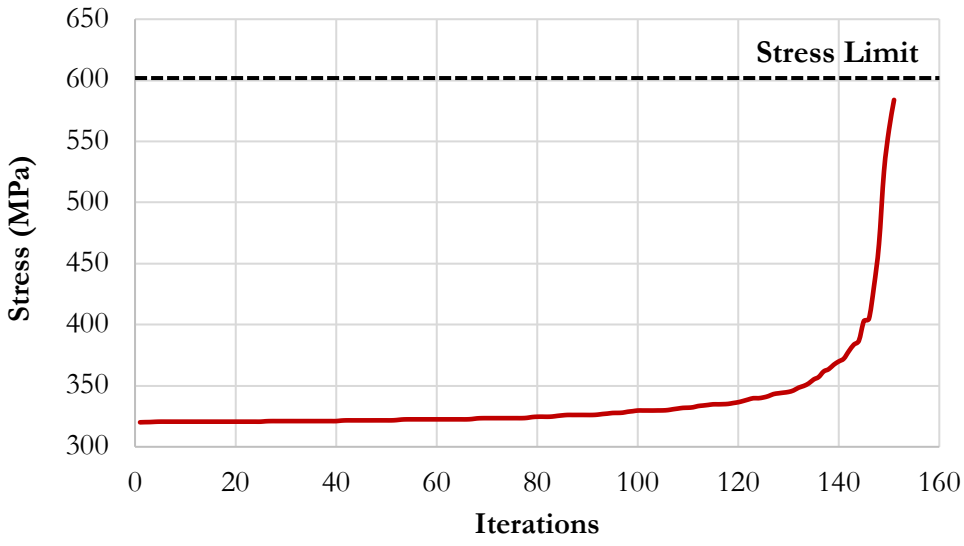

Figure 6.7 Maximum stress during the optimization process.

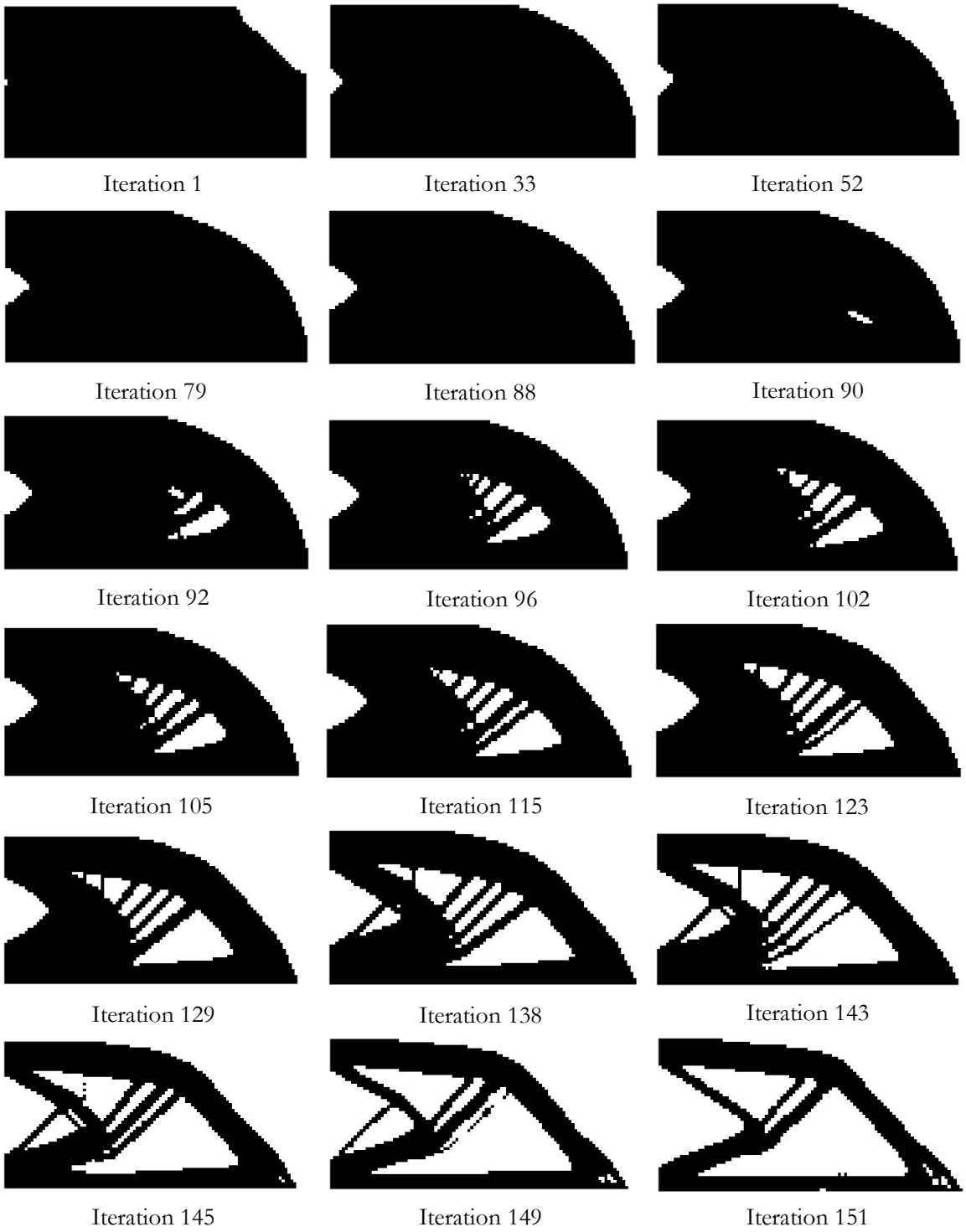

Figure 6.8 Iterative material distribution for static loading on nonlinear analysis.

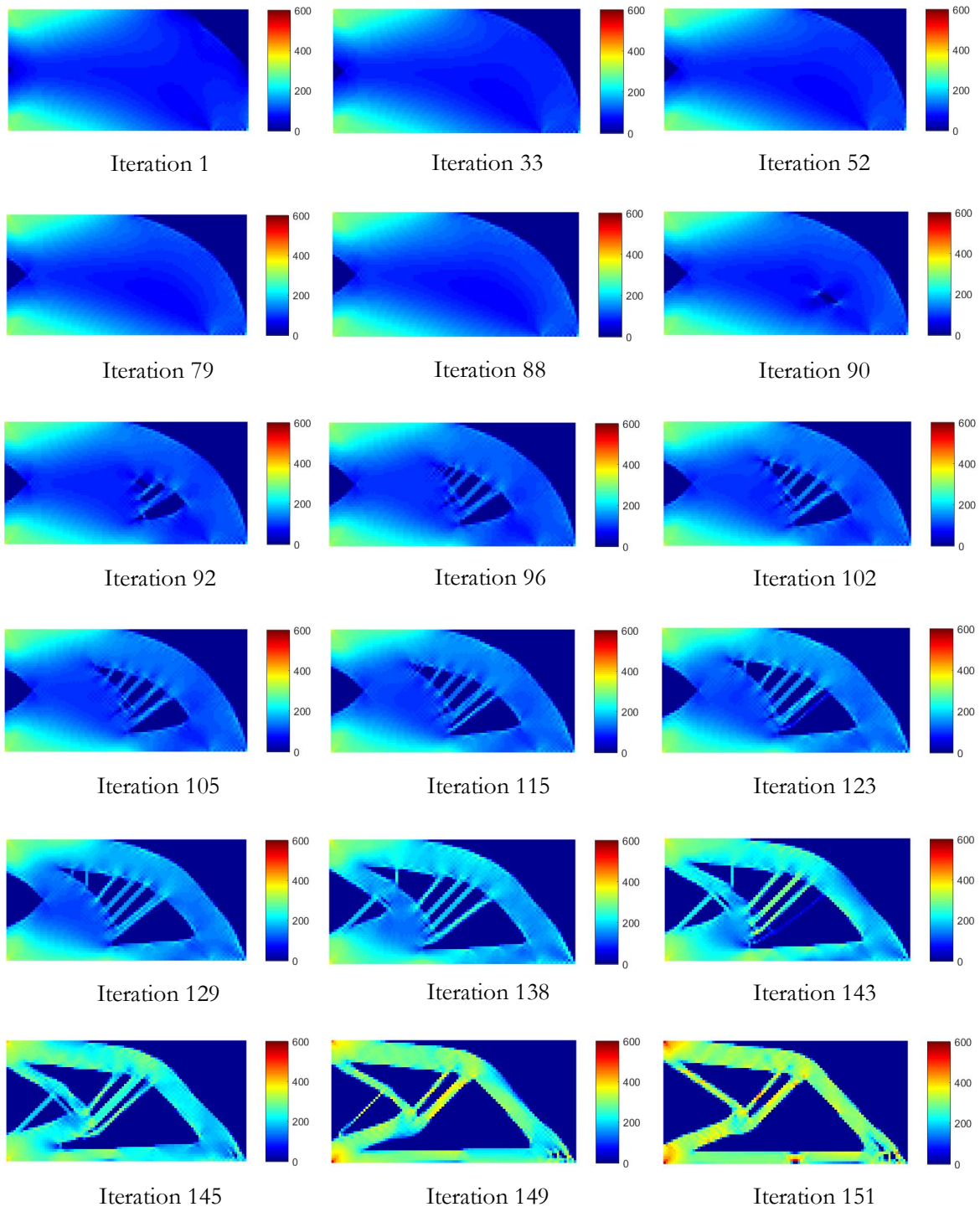

Figure 6.9 Iterative stress distribution for static loading on nonlinear analysis.

Nonlinear analysis requires high computational costs to solve the nonlinear equation of each time increment and affects to calculation time for each iterative optimization process. To reduce the computational costs, the over-relaxation factor is proposed for the optimization process by expecting to reduce the number of iteration and computational time for the nonlinear problem.

6.3 Over-relaxation Factor

The over-relaxation factor is a technique for expediting the global convergence of the topology optimization problem according to the objective function and optimization constraints. As mentioned above, the aim of the over-relaxation factor is to reduce the computational cost by relating to the number of optimization iteration and global convergence. Therefore, this dissertation proposed the over-relaxation technique based on the over-relaxation factor and applied it to the process of the proportional algorithm. According to the proportional method for updating the element densities, the criteria of fully stressed design based on topology optimization was newly implemented to formulate the update function for nonlinear topology optimization in this dissertation. So, the over-relaxation technique indicated the update function for all design elements based on the value of stress ratio in equation 4.2 by applying the over-relaxation factor. The new update function based on the over-relaxation factor was re-formulated as follows:

$$\rho_i^{opt} = \rho_i^{prev} + \frac{\rho_{rem}}{\sum_{i=1}^{N} u_i} \left(\frac{\sigma_i^q}{\sigma_{all}^q} \right)^v \eta_i \tag{6.1}$$

where v is the over-relaxation factor which applied to the stress ratio. The value of the over-relaxation factor (v) should assign to be higher than one ordinally. Thus, the numerical examples are necessary to investigate the performance of the over-relaxation factor (v) when it applied to the update function based on equation 6.1.

6.3.1 Optimization Results with Over-relaxation Factor

This section investigated the performance of the over-relaxation factor for nonlinear topology optimization. The optimization model was created and defined based on the mechanical structure, which shown in figure 6.1 and discretized to each design variable by using the finite element method (as illustrated in figure 6.2). The objective function of the optimization problem is to maximize the internal energy with assigned 600 MPa of the stress limit to be the optimization constraint.

The numerical examples evaluated the performance of the over-relaxation factor by varying the value from 1.0 to 1.8, and the results of the number of iterations and computational time were displayed in figure 6.10 for each case. For the over-relaxation was equate 1.0 means the optimization process, the element densities were updated by using the regular update function (equation 4.2) of the proportional technique. Histories on optimization results showed that the number of iterations decreased when the value of the over-relaxation factor was increased until value 1.7 of the over-relaxation factor. The high computational costs were required when applied the value 1.8 of the over-relaxation factor. So, the value of the over-relaxation factor from 1.1 to 1.7 was considered to determine the optimal layout.

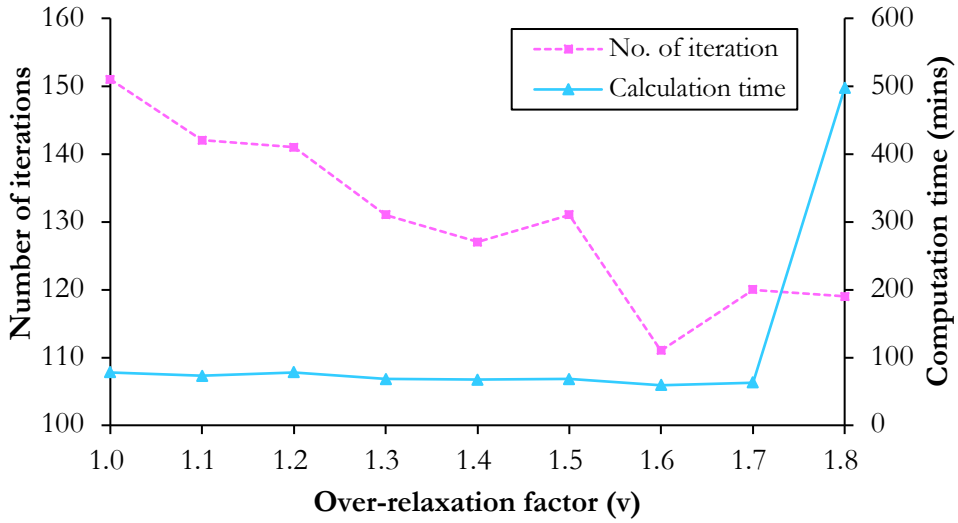

Figure 6.10 Histories on topology optimization with the over-relaxation factor.

The optimal layouts and stress distributions were shown in Table 6.1 for each over-relaxation factor from 1.0 to 1.7. All layouts have to compare to the baseline model (which the over-relaxation factor is 1.0) for investigating the optimization performance. The results showed the value of over-relaxation factor effects to improve the convergence and the final layout of the structure. Actually, the over-relaxation factor of 1.6 should be the best results and layout due to acquiring the minimum number of the optimization iteration. However, the final layout on value 1.6 of the over-relaxation factor was completely different from the baseline model. On the other hand, the over-relaxation of 1.5 obtained the final layout, which is the most similar to the final layout from the reference model when compared with the other over-relaxation factors. So, the over-relaxation of 1.5 was suitable for this dissertation to employ the over-relaxation technique.

Table 6.1 Comparisons on optimal layout based on the over-relaxation factor.

Over-relaxation factor	Optimal layout	Stress distribution
1.0		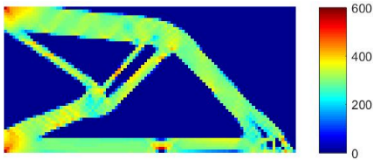
1.1		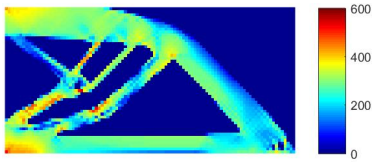
1.2		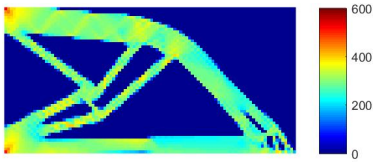
1.3		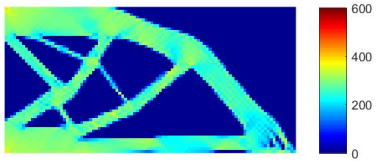

Table 6.1 Comparisons on optimal layout based on the over-relaxation factor (*continued*).

Over-relaxation factor	Optimal layout	Stress distribution
1.4		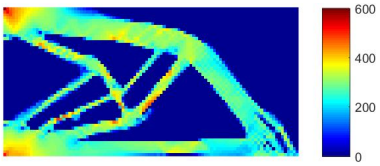
1.5		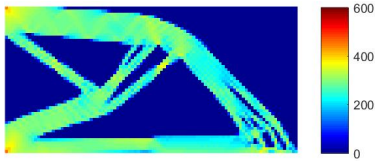
1.6		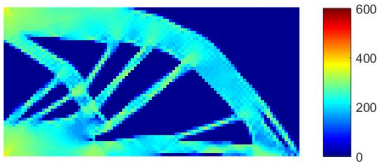
1.7		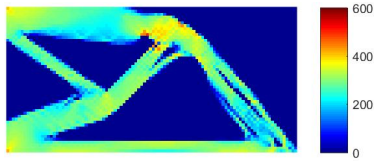

The final layouts and stress distribution of the over-relaxation factor 1.0 and 1.5 were shown in figure 6.11 and 6.12, respectively, for comparing the optimization results. The final layout from over-relaxation faction 1.0 obtained at iteration 151, while the final layout can be obtained at iteration 131 when the over-relaxation factor 1.5 was applied.

(a) over-relaxation 1.0

(b) over-relaxation 1.5

Figure 6.11 Comparisons of the final layout for over-relaxation factor.

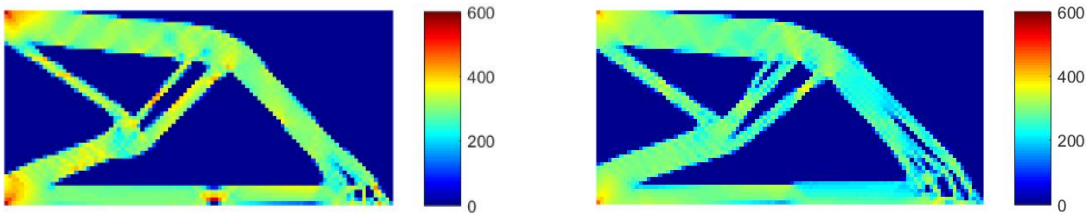

(a) over-relaxation 1.0 (b) over-relaxation 1.5

Figure 6.12 Comparisons of the stress distribution for over-relaxation factor.

Moreover, the maximum stress inside the final layout from the over-relaxation factor is lower than the reference model, and even the layout is similar. The baseline model (over-relaxation factor 1.0) caused the maximum stress of 560 MPa, while the final layout from the over-relaxation factor showed 455 MPa for the maximum stress. Stress distribution can be an implied safety factor of the structure. So, the over-relaxation can increase the safety factor by decreasing the maximum stress. Comparisons on internal energy and maximum stress during the optimization for each over-relaxation factor was shown in figure 6.13 and 6.14, respectively.

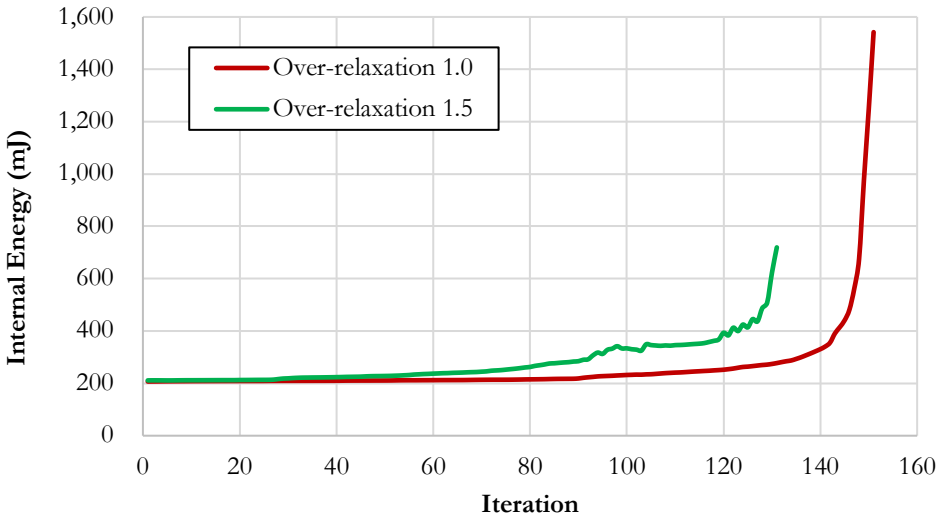

Figure 6.13 Comparisons of the internal energy for over-relaxation factor.

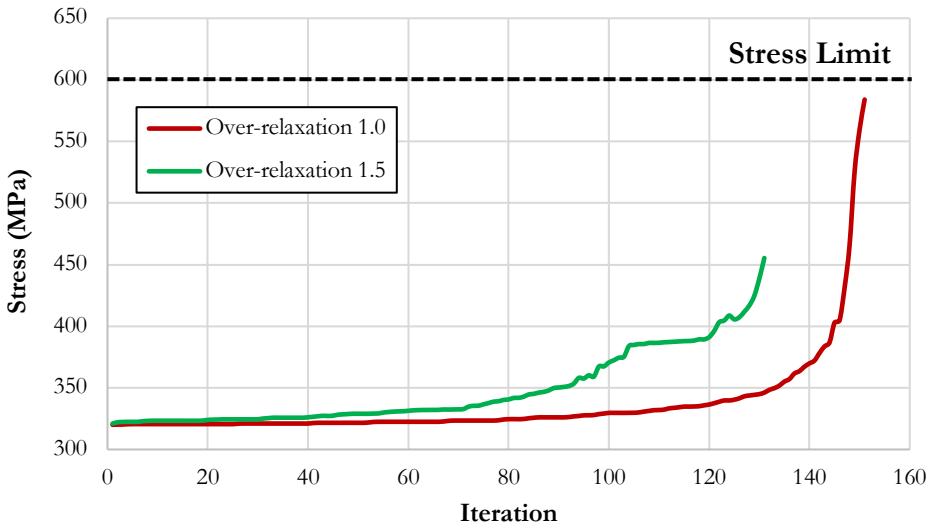

Figure 6.14 Comparisons of the maximum stress during the optimization process for over-relaxation factor.

Iterative internal energy and maximum stress during the optimization process of the over-relaxation factor 1.5 were higher than the normal update function. However, the final layout acquired both values smaller than the 1.0 of the over-relaxation factor. Therefore, the user has to concern the purpose of each optimization procedure. There are some contrasts for applying the normal and over-relaxation factor to the update function. Both techniques can generate an optimal layout based on the topology optimization process with results that are also quite different.

6.4 Conclusion

The performance of nonlinear topology optimization was investigated by using numerical examples. The final layout can be obtained based on the update function of the proportional technique. The objective function is to maximize the internal energy and defined the maximum stress limit for the optimization constraint. Optimal layouts from

linear and nonlinear material properties showed differences in material distribution inside the design domain. The layout from linear and nonlinear optimization procedures showed the convergence to the optimization problem because the maximum stress of each optimization iteration is not over the stress limit. The over-relaxation factor was proposed to reduce the computational costs and expedite the global convergence of the optimization process. Thus, the over-relaxation factor (ν) was included in the update function of the proportional technique for indicating the stress ratio. The numerical examples were also examined for investigating the performance of the over-relaxation factor. Finally, the final layout which applied the over-relaxation factor can be reduced the maximum stress inside the structure; in other words, this technique increases the safety factor into the design process.

Chapter 7

OPTIMIZATION ON CYCLIC LOADING

This chapter described a structural behavior when applied an external cyclic load. Moreover, a new weight filtering equation is proposed for optimization process under the cyclic loading. The results on analysis and optimization under the cyclic loading are showed different layout under both bilinear elastoplastic and isotropic and kinematic hardening materials.

7.1 Optimization Model

The initial design domain for analysis and optimization under cyclic loading used the model as same as the optimization under static loading (figure 6.1) and discretized the design area by using the finite element method based on LS-PrePost (figure 6.2). Firstly, the model is analyzed to investigate the difference of the stress distributions inside the

structure between static and cyclic loads. The material behavior of bilinear elastoplastic (figure 5.3) is assigned to the structure for investigating process with 285 MPa of yield stress, 600 MPa of ultimate tensile stress, 207 GPa of Young's modulus, and 0.3 of Poisson's ratio. The behavior of the bilinear elastoplastic material shows a linear relationship between stress and strain after yielding. This effect of load behavior should effectively show the stress distribution distinction.

7.1.1 Cyclic Loading

The behavior of cyclic load is demonstrated in figure 7.1, and it is applied as the external load to the structure for utilizing the analysis process. The characteristic of the cyclic load behavior indicates both tension and compression loads through the analysis procedure. A negative factor of the cyclic loading means the upward direction of the cyclic loading, while a positive factor denotes the downward direction of the cyclic loading. The unloading point is represented when the load factor equals to zero. For comparison, the stress distribution of the structure under the cyclic loading should show similar results with the static loading at the time instance 2.5 seconds because the load factor equals to one represents the load value as same as the static load case.

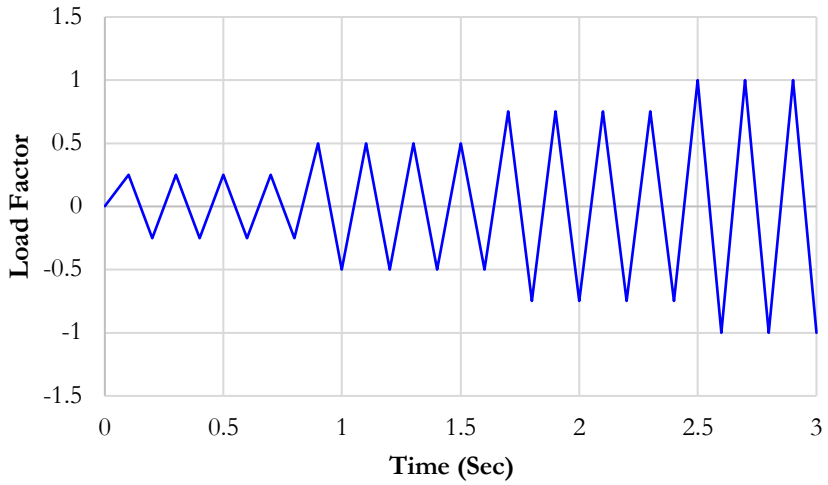

Figure 7.1 Cyclic loading behavior.

7.1.2 Analysis Results on Initial Design Domain

The analysis procedure is performed based on the LS-DYNA solver by interesting for 3 seconds throughout the process. There are two cases for this analysis: static load and cyclic load cases. The bilinear elastoplastic material behavior was assigned to both cases and similarly defined all boundary conditions. The results are focused on elemental stress, which measured at the same element number for both cases in the comparison process. The analysis results of the static and cyclic loads were displayed in figure 7.2 based on the maximum elemental stress.

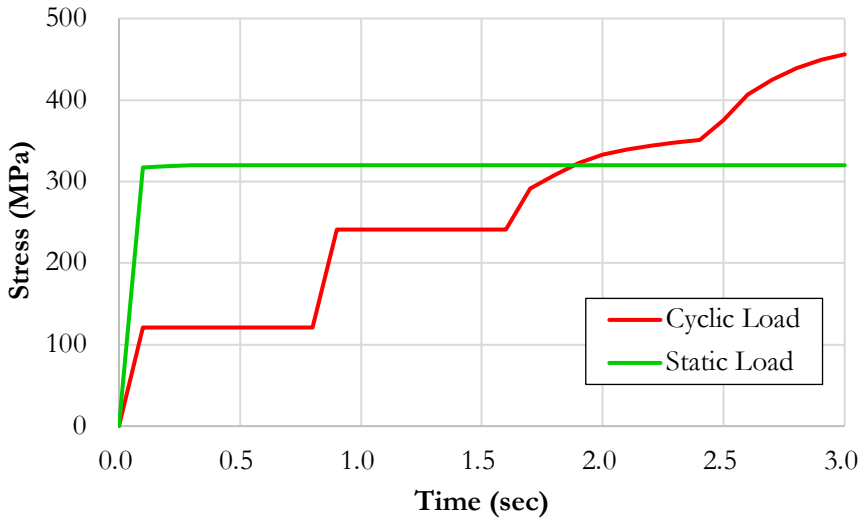

Figure 7.2 Maximum stress based on the static and cyclic load cases.

The results showed the constant of maximum elemental stress under the static load case since the first-time step. The maximum elemental stress based on the cyclic loading was affected, and different from the static load case with the stress was varied by the time during the analysis. For the cyclic load, the stress values were constant according to the load factor within the elastic deformation until the yielding point. After that, the tendency of the stress value is increased even though the load factor value was similar in the same period of the cyclic loading. Moreover, the stress values of the cyclic loading are higher than the

static load case; even the load factor is equal to one, and it equal to the static load value. Therefore, the cyclic load behavior affected the stress distribution when the structure becomes the permanent deformation (inelastic period) even though the load value and material properties are similar to the static load case.

7.2 Weight Filtering Factor for Optimization under Cyclic Loading

As described in chapters 2 and 5, the filtering technique is used for avoiding the numerical instability, which causes by the checkerboard pattern based on the topology optimization process under the SIMP approach. A common filtered density equation for the topology optimization process was shown in equations 5.1 and 5.2, which used by many pieces of research. However, those researches have been focused on the static load case as applied as the external load. As this chapter of this dissertation investigates an optimal layout of the structure under topology optimization with the cyclic loading. Thus, a new wight filtering factor is proposed for the optimization process to gain a smooth density of the design variables. The new weight filtering factor (w_{ij}) for topology optimization under the cyclic loading is shown as follows:

$$w_{ij} = \max\left(1 - r_0 - r_{ij}, 0\right) \tag{7.1}$$

where r_0 is the prescribed filtering radius and r_{ij} is the distance from center-to-center between element i^{th} and j^{th}, which automatically measured from centroid of each element based on equation 5.3. The performance of the new weight filtering factor in equation 7.1 will be discussed in Section 7.5 based on the results of numerical examples. The optimal layout from the new weight filtering factor is also compared with the other weight filtering factors under the optimization on the cyclic loading and material nonlinearities.

7.3 Isotropic and Kinematic Hardening Material

The characteristic of bilinear elastoplastic material (which describe in chapter 5) was employed to optimize the structure for the nonlinear problem. Besides, the characteristic of isotropic and kinematic hardening material also used and assigned to the structure for topology optimization with nonlinear material behavior in this dissertation. The stress-strain relation based on the characteristic of isotropic and kinematic hardening material is illustrated in figure 7.3 with differed from the bilinear elastoplastic material.

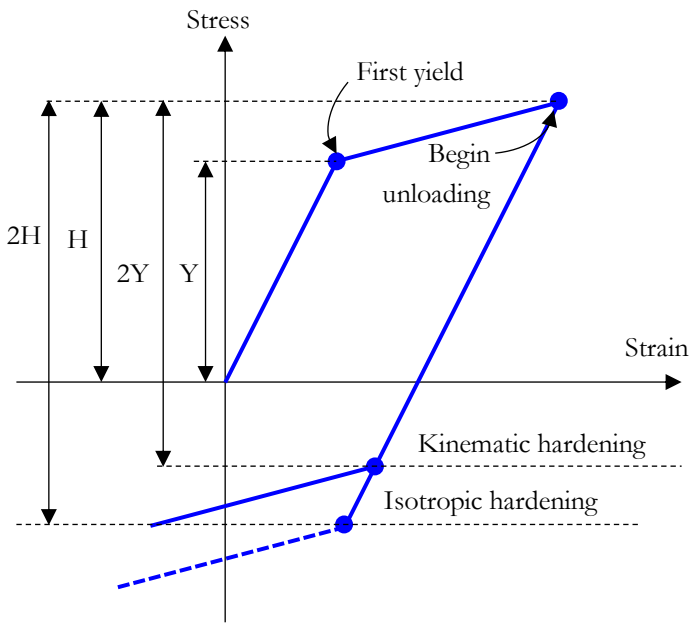

Figure 7.3 Isotropic and kinematic hardening material properties.

The unloading effect is concerned in this material property, which shows by stress reduction after the unloading point. The stress interval after the unloading point of two times of yield stress (2Y) represents kinematic hardening. Meanwhile, isotropic hardening behavior is showed by two times of ultimate tensile stress (2H) for the stress interval after the unloading point. In this dissertation, the behavior of kinematic hardening properties

was considered for investigating the optimal layout under nonlinear topology optimization with cyclic loading. Furthermore, the kinematic hardening also used for investigating the performance of the new weight filtering factor.

7.4 Optimization Results

The topology optimization under cyclic loading was investigated to acquire an optimal layout in this section. The proportional techniques (as explained in chapter 4) was also used to update all element densities according to equation 4.2 during the nonlinear optimization process. For the optimization problem, the objective function is defined for maximizing the internal energy of the whole design domain (equation 5.4), and it is subjected to the stress limit for avoiding the failure of the structure during the analysis process (equation 5.6). All analyses and optimization procedures were operated by following the process in figure 5.9 (as described in section 5.4.2). The process of nonlinear analysis was performed based on LS-DYNA solver, while the optimization procedure was operated by coding on MATLAB. As the aim of this section is to investigate the performance of the new weight filtering factor. So, there are three weight filtering factors, which used for comparing the optimal layout based on nonlinear topology optimization.

The first weight filtering factor depicted the standard weight filtering factor for topology optimization and was applied in [17]. The second weight filtering factor was defined as a ratio of the prescribed filtering radius (r_0). The last weight filtering factor is the new weight filtering factor, which proposed for optimization under cyclic loading (equation 7.1). The first, second, and third weight filtering factors were supposed to model A, model B, and model C, respectively for the simplification. The weight filtering factor of the model A and B are expressed in equation 7.2 and 7.3, respectively. The filtered density (η_i) in equation 5.1 were used for investigating with all weight filtering factors (w_{ij}).

$$w_{ij} = \max\left(0, r_0 - r_{ij}\right) \tag{7.2}$$

$$w_{ij} = \max\left(1 - \frac{r_0}{r_{ij}}, 0\right) \tag{7.3}$$

The numerical examples were divided into two sections: bilinear elastoplastic material and isotropic and kinematic hardening material. Accordingly, 285 MPa of yield stress, 600 MPa of ultimate tensile stress (as assigned to be the optimization constraints for both cases of material properties), 0.3 of Poisson's ratio, and 207 GPa for Young's modulus were defined for both cases of material properties. Each section will investigate an optimal layout for all wight filtering factors under topology optimization with the characteristic of cyclic loading (figure 7.1).

7.4.1 Bilinear Elastoplastic Material

The characteristic of bilinear elastoplastic material (figure 5.3) was employed to optimize the structure under cyclic loading for three weight filtering factors. An optimal iterative layout and stress distribution were illustrated for each model (on each weight filtering factor).

The results on optimal iterative layout and stress distribution of model A, model B, and model C were shown in figure 7.4 to 7.9, respectively. Model A obtained the final layout at iteration 138 with 592 MPa for the maximum stress of the design structure. Iteration 123 displayed the final layout in case of model B with stress distribution 519 MPa for the maximum stress. While the model C, which is the new weight filtering factor, the final layout was obtained at iteration 134 with the maximum stress was 557 MPa. As observed in the stress distribution of all models, the maximum stress caused at the top and bottom of the left-side structure, which is the point for causing the stress concentration of the cantilever beam model. Therefore, this is one point for confirming the optimization algorithm and optimization procedure.

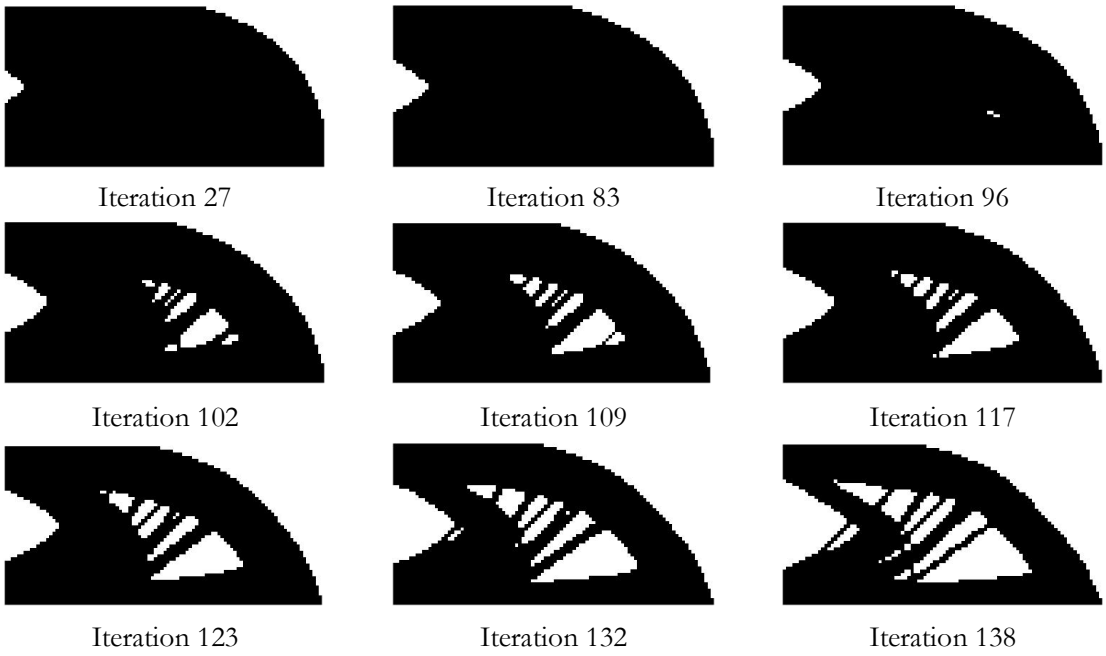

Figure 7.4 Iterative material distribution on bilinear elastoplastic material with cyclic loading of Model A.

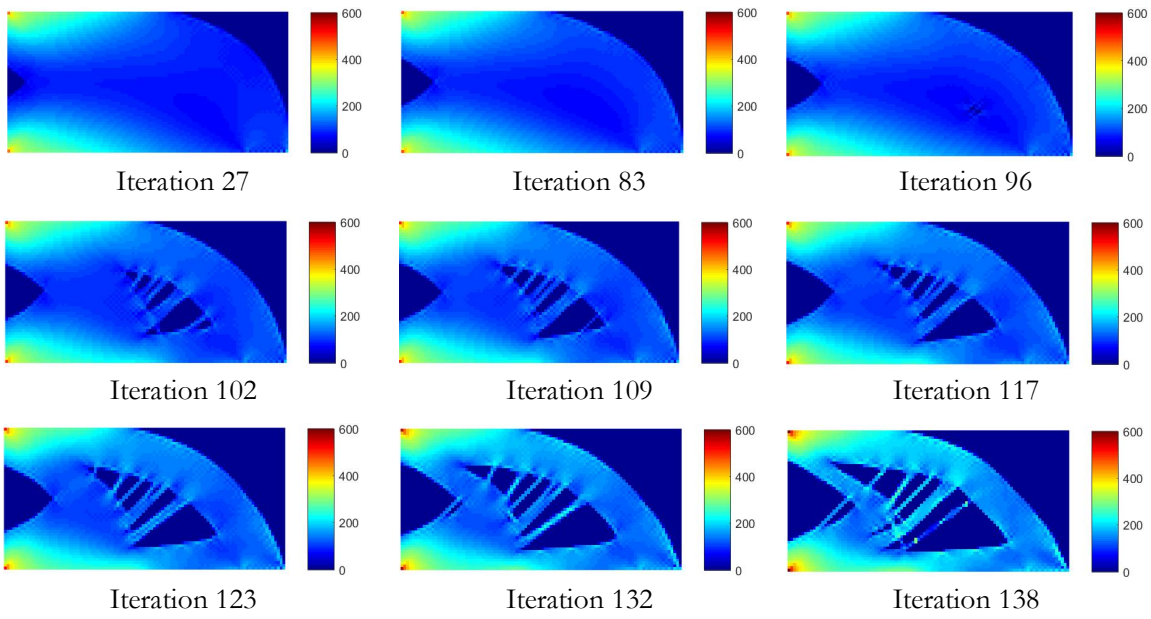

Figure 7.5 Iterative stress distribution on bilinear elastoplastic material with cyclic loading of Model A.

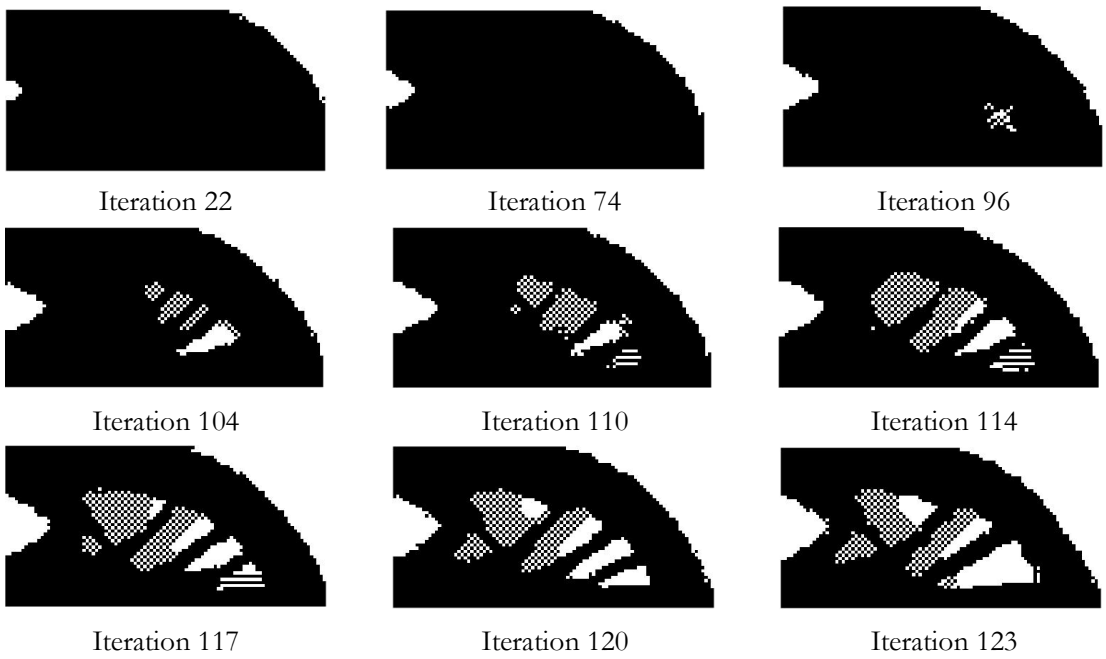

Figure 7.6 Iterative material distribution on bilinear elastoplastic material with cyclic loading of Model B.

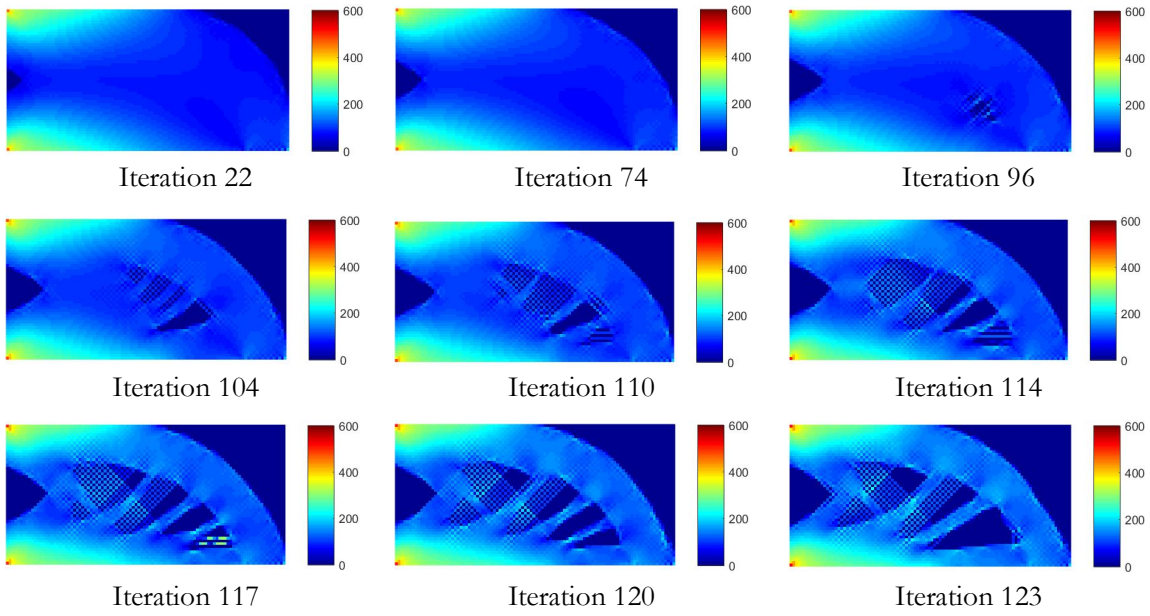

Figure 7.7 Iterative stress distribution on bilinear elastoplastic material with cyclic loading of Model B.

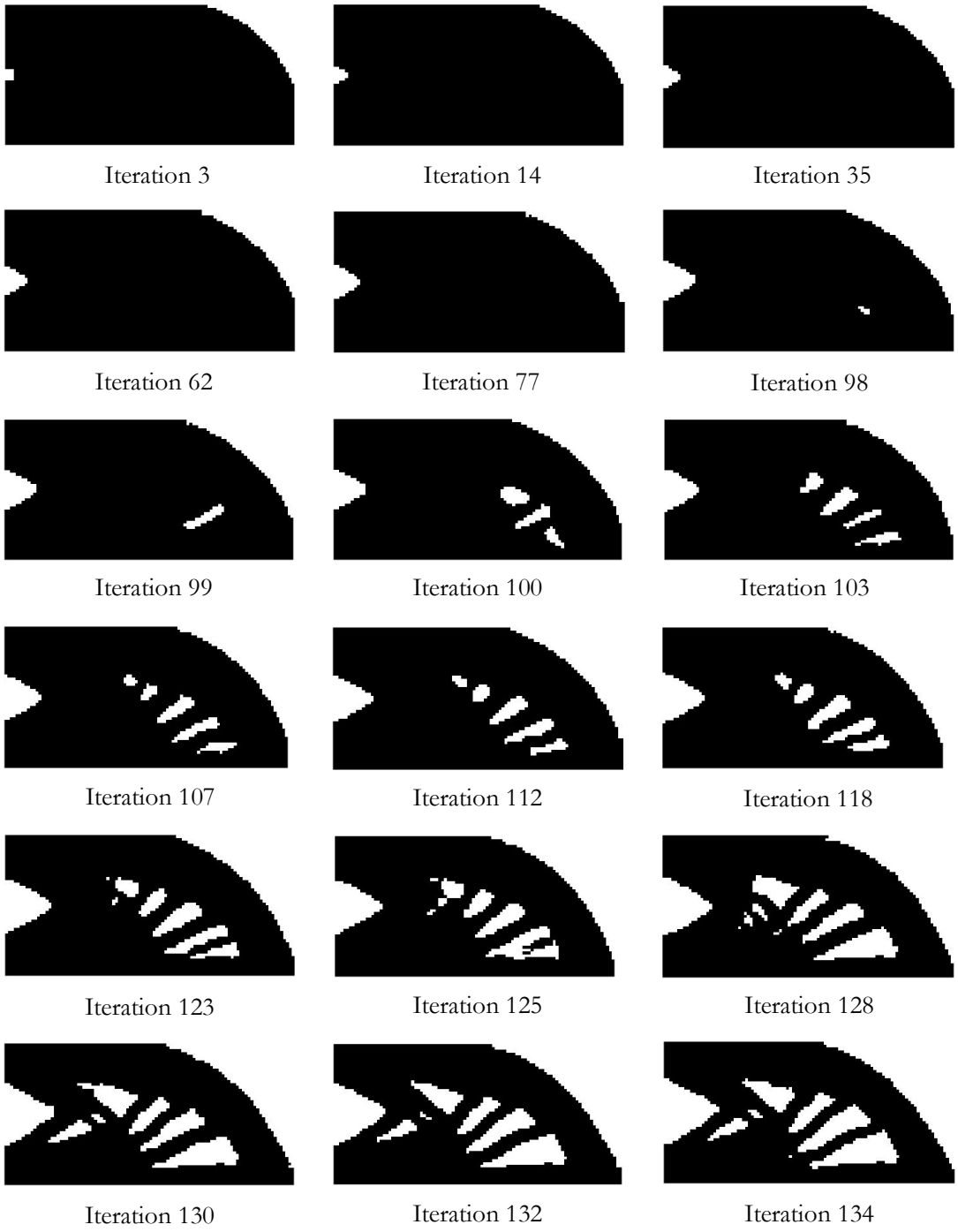

Figure 7.8 Iterative material distribution on bilinear elastoplastic material with cyclic loading of Model C.

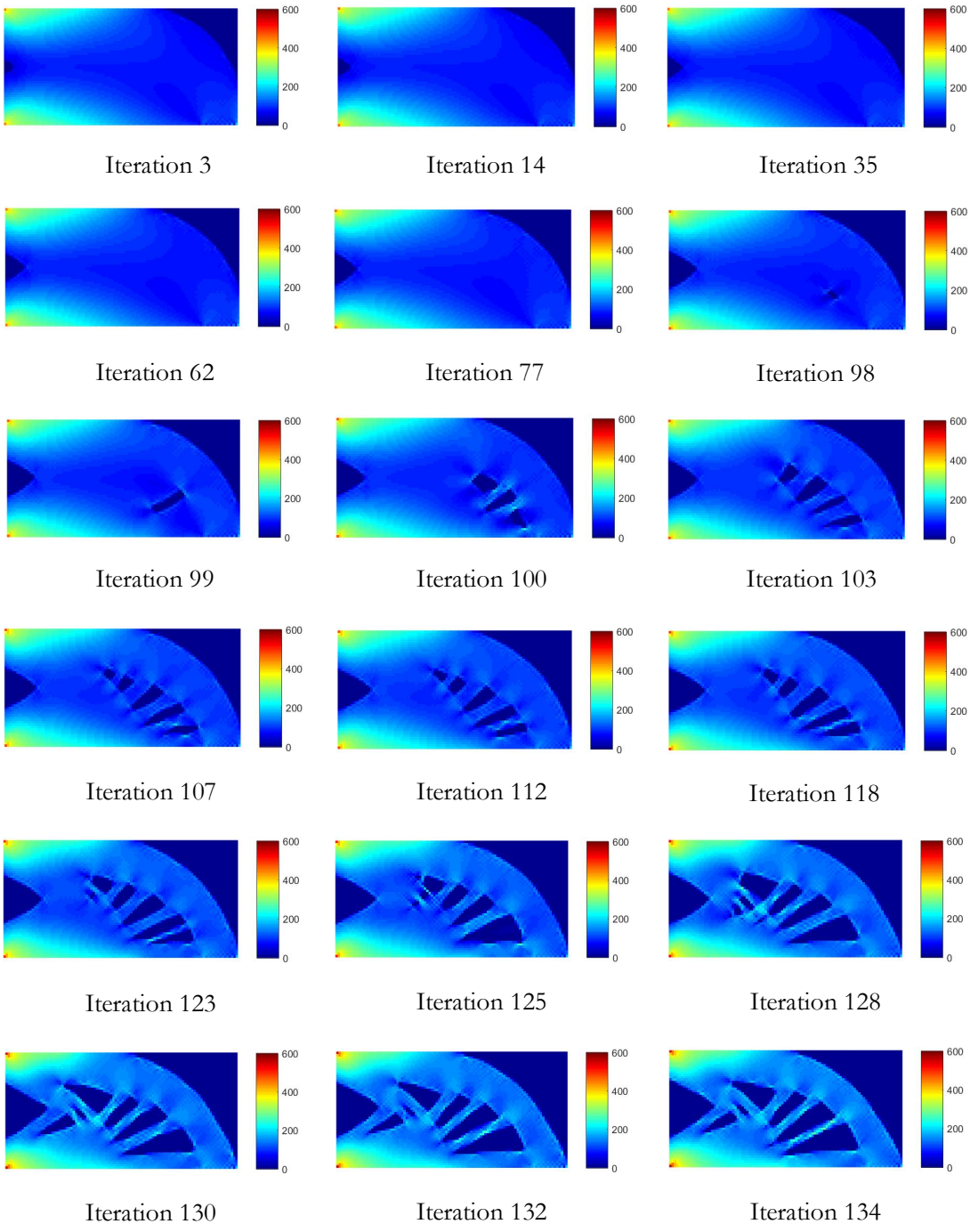

Figure 7.9 Iterative stress distribution on bilinear elastoplastic material with cyclic loading of Model C.

During the optimization process, stress histories of each weight filtering factor were illustrated in figure 7.10 for comparing the three optimization models. The results were plotted based on the elemental stress, which caused the maximum value at each iteration of each optimization model. The stress distribution of all three models showed the maximum stress increased for each iteration since the first iteration until terminated into the parabolic tendency by removing the material amount of the design area. Moreover, the optimization process terminated when the stress on each model closed to the stress limit (600 MPa), which assigned as the optimization constraint. According to the application of crashworthiness design, a deformation of the whole model increased to maximize the internal energy density, which defined to be the objective function. Therefore, the stress value is increased to converge the optimization constraint and not over the stress limit for avoiding the failure of the structure.

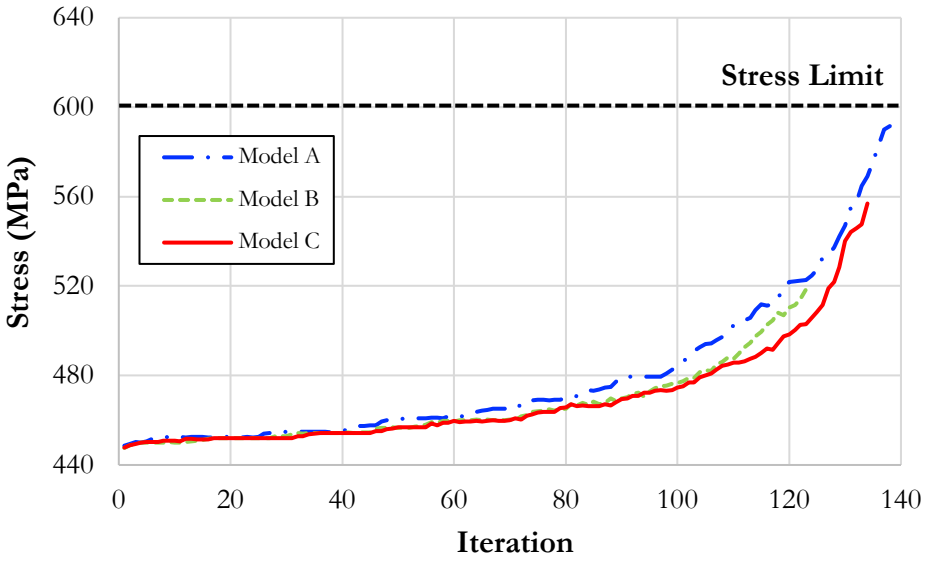

Figure 7.10 Maximum stress of the three models during the optimization process based on the bilinear elastoplastic material.

The internal energy at each iteration during the optimization process was also plotted in figure 7.11 for three models. The results showed that the internal energy was increased

during the optimization until causing the termination. Furthermore, the internal energy of all optimization models was increased to converge the optimization problem corresponding to the assigned objective function for maximizing the internal energy.

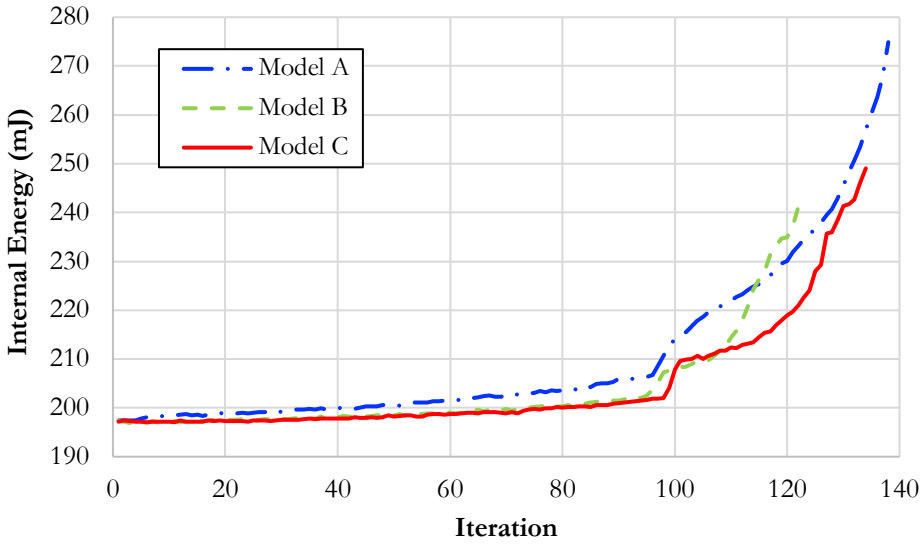

Figure 7.11 Internal energy of the three models during the optimization process based on the bilinear elastoplastic material.

The optimal layout of the three models was compared, as showed in Table 7.1, for investigating the performance of the weight filtering factor. The result of Model A showed the complicated structural members, and it was quite challenging to predict the real structure by observing from this structural layout. The weight filtering factor of Model B caused the checkerboard pattern of the optimal layout, which was not efficient for designing the structure. Model C acquired the clear optimal layout by comparing it with the other two models, even though the internal energy was only 9% lower than Model A. The material distribution of Model C was removed 33% from the initial design domain. In this case, the proposed weight filtering factor was effectively performed to obtain the final layout under the cyclic load, which is the clearest layout. Furthermore, the results showed that stress was not affected by the cyclic load behavior.

Table 7.1 The optimal layout of structure based on the bilinear elastoplastic model.

Model	Weight Filtering Factor	Final Layout	Stress Distribution of Final Layout
A	$w_{ij} = \max(0, r_0 - r_{ij})$	 Iteration 138	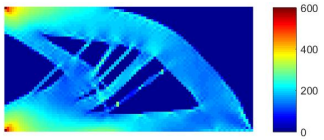 Max. stress 592 MPa
B	$w_{ij} = \max\left(1 - \frac{r_0}{r_{ij}}, 0\right)$	 Iteration 123	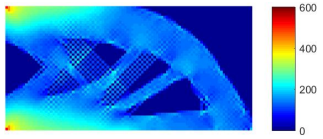 Max. stress 519 MPa
C	$w_{ij} = \max(1 - r_0 - r_{ij}, 0)$	 Iteration 134	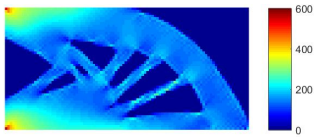 Max. stress 557 MPa

7.4.2 Isotropic and Kinematic Hardening Material

The characteristic of isotropic and kinematic hardening material properties (figure 7.3) was assigned to the initial design structure for acquiring the optimal layout under cyclic loading. This material behavior differs from the bilinear elastoplastic material in case of the effect of unloading is considered. Three weight filtering factors were similarly investigated as the bilinear elastoplastic material based on the nonlinear topology optimization.

An iterative on material and stress distributions of optimization results on Model A, Model B, and Model C was illustrated in figure 7.12 to 7.17, respectively. The final layout of Model A acquired at iteration 187, which caused 492 MPa for the maximum stress. Iteration 164 showed the final layout of Model B with the maximum stress of 414 MPa. Finally, the proposed Model C was obtained from the final layout at iteration 184, and it caused 499 MPa inside the optimal structure.

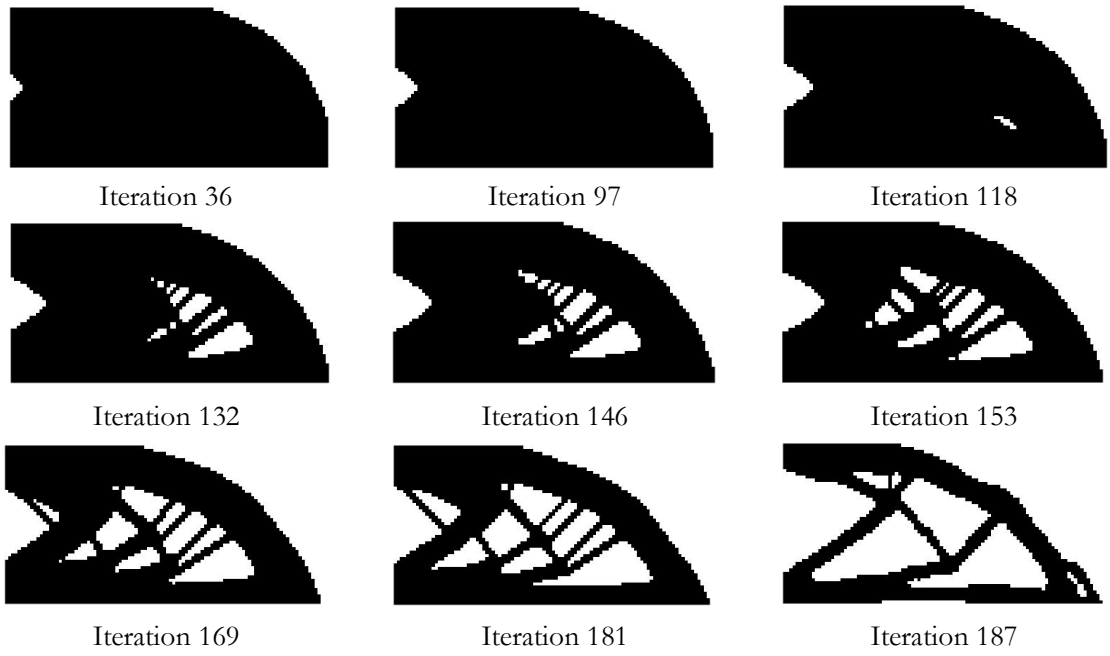

Figure 7.12 Iterative material distribution on isotropic and kinematic hardening material with cyclic loading of Model A.

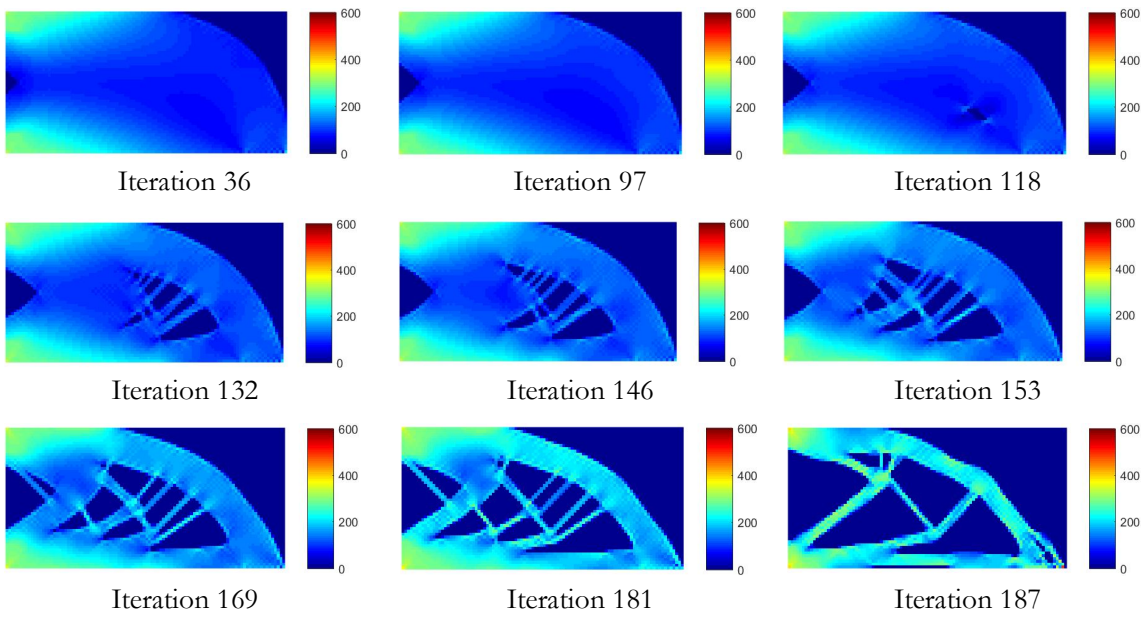

Figure 7.13 Iterative stress distribution on isotropic and kinematic hardening material with cyclic loading of Model A.

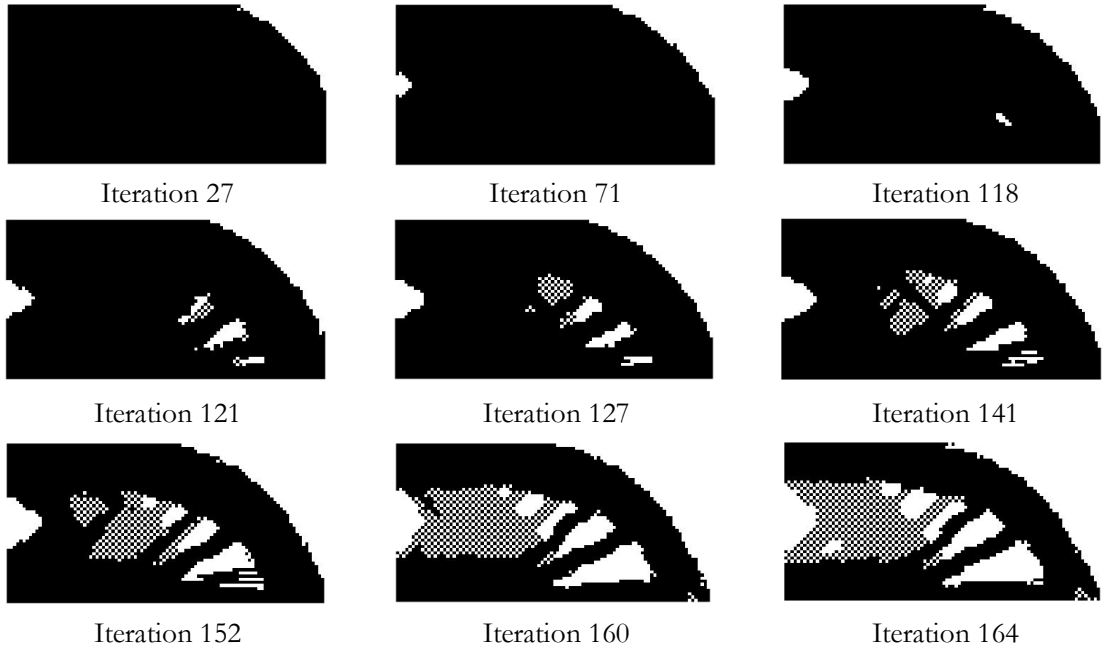

Figure 7.14 Iterative material distribution on isotropic and kinematic hardening material with cyclic loading of Model B.

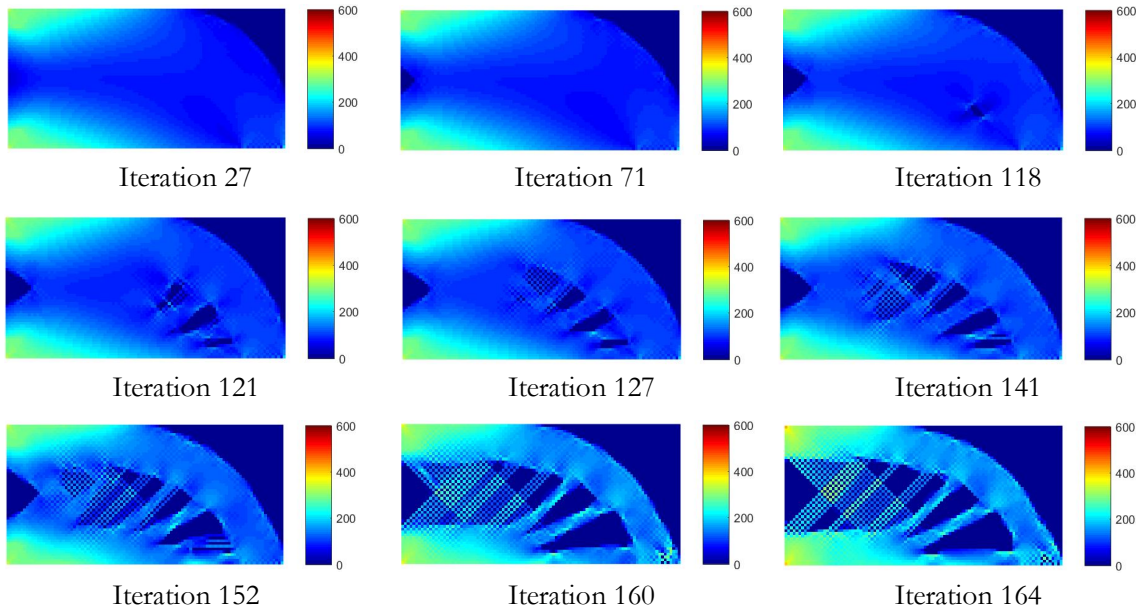

Figure 7.15 Iterative stress distribution on isotropic and kinematic hardening material with cyclic loading of Model B.

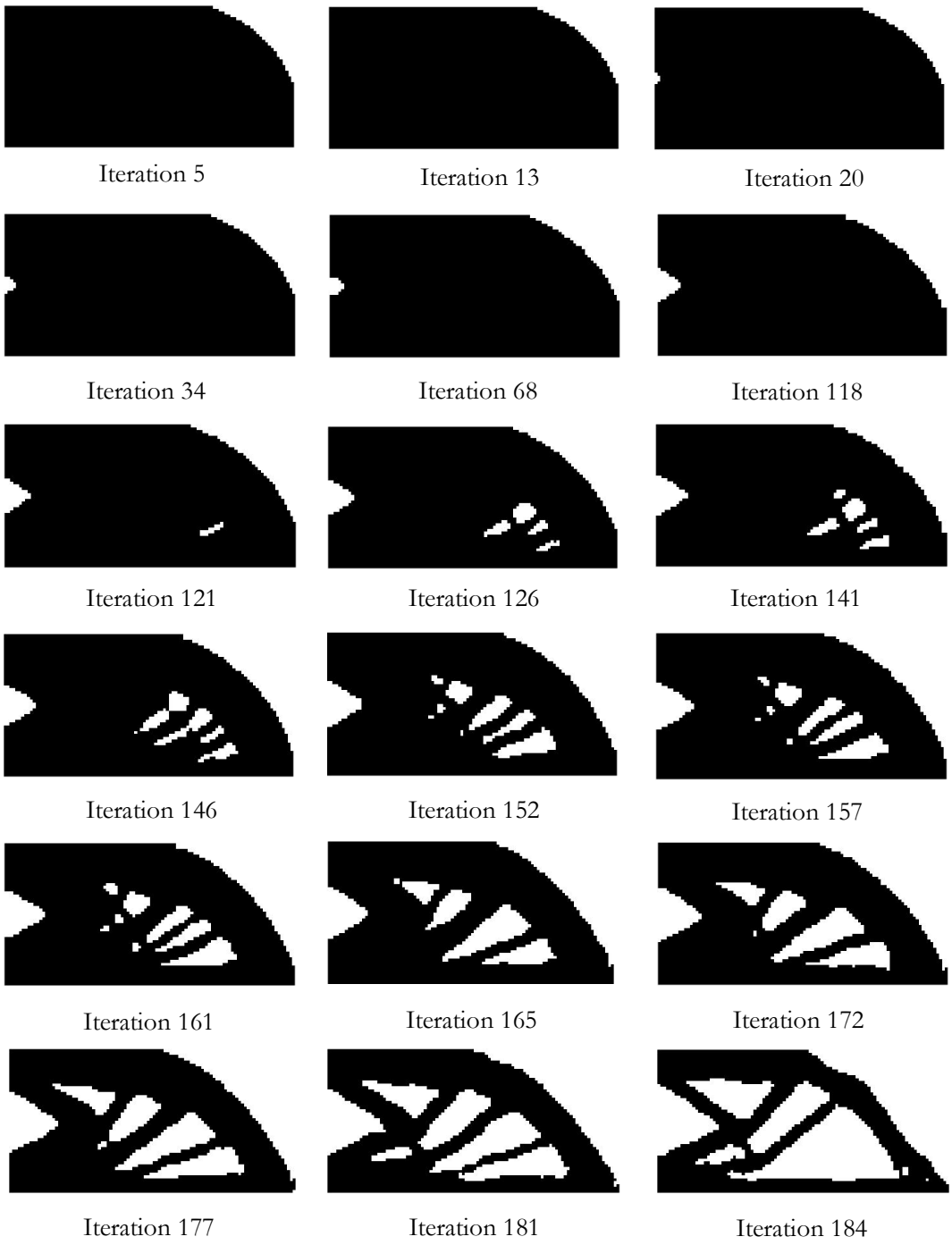

Figure 7.16 Iterative material distribution on isotropic and kinematic hardening material with cyclic loading of Model C.

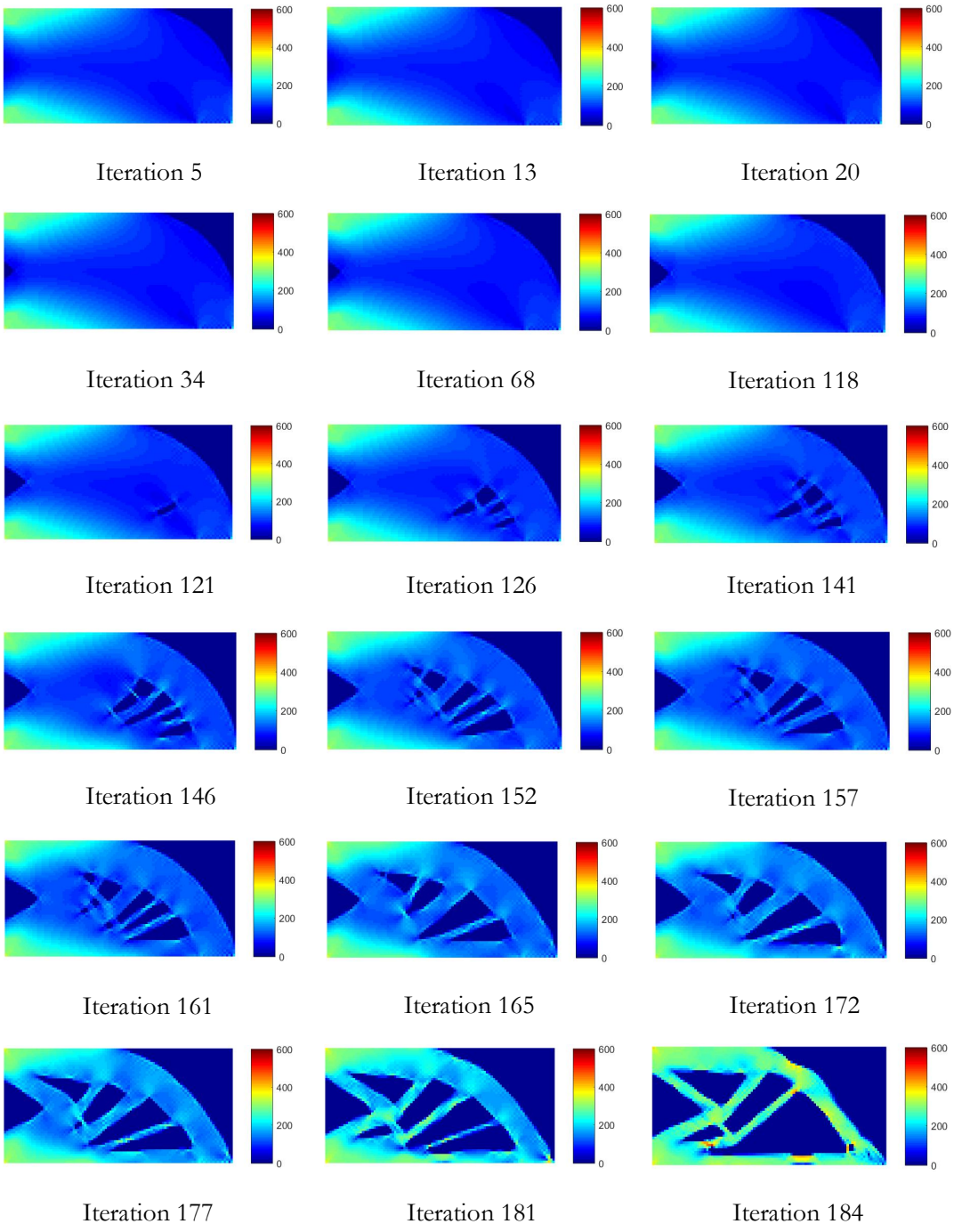

Figure 7.17 Iterative stress distribution on isotropic and kinematic hardening material with cyclic loading of Model C.

The internal energy at each iteration for all three models was plotted as figure 7.18 to investigate the convergence of the optimization problem. A tendency of all three models had increased the internal energy when the optimization iteration was increased. Only the proposed Model C was increased the internal energy smoothly, while Model A and C caused a fluctuation at iteration instance 160 due to the effect of unloading behavior. From these results, the optimization process for three models was preliminary confirmed the convergence under cyclic loading.

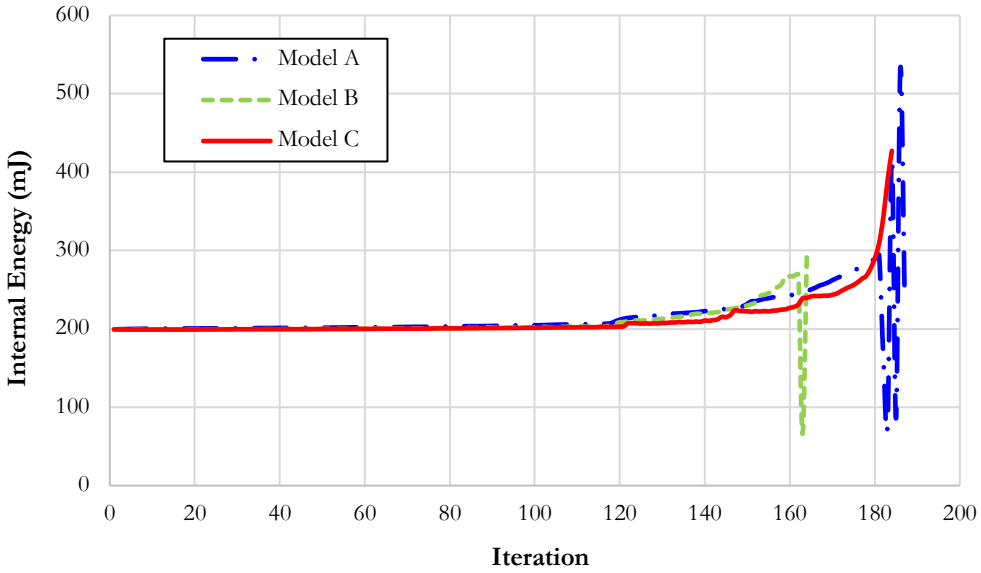

Figure 7.18 Internal energy of the three models during the optimization process based on the isotropic and kinematic hardening material.

Table 7.2 showed a comparison on the final layout of three optimization models with the definition of each model being specified as the same as the bilinear elastoplastic material case. The weight filtering factor, which applied to Model B, repeatedly obtained the final layout in the checkerboard pattern. Since the value of weight filtering factor in Model B usually indicates zero. On the other hand, the weight filtering factor of Model A and Model C are positive values and higher that zero. Therefore, the equation of Model B was not beneficial in optimizing the structure under the cyclic load and the nonlinear material

properties. The final layouts of Model A and Model C obtained were quite similar lay-outs, and both layouts were not complicated to conjecture the real structure. Thus, the stress constraint of each model during the optimization process was crucial with further considerations to decide on a more effective weight filtering factor.

Table 7.2 The optimal layout of structure based on the isotropic and kinematic hardening model.

Model	Weight Filtering Factor	Final Layout	Stress Distribution of Final Layout
A	$w_{ij} = \max(0, r_0 - r_{ij})$	 Iteration 187	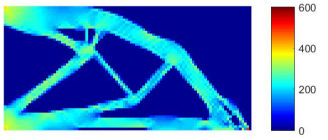 Max. stress 492 MPa
B	$w_{ij} = \max\left(1 - \frac{r_0}{r_{ij}}, 0\right)$	 Iteration 164	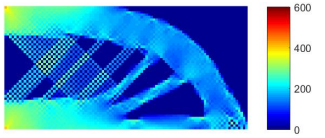 Max. stress 414 MPa
C	$w_{ij} = \max(1 - r_0 - r_{ij}, 0)$	 Iteration 184	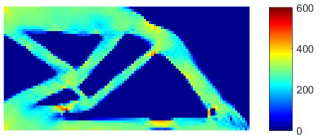 Max. stress 499 MPa

The maximum stress during the optimization process, which measured maximum elemental stress at each iteration, was displayed in figure 7.19 for comparing all three weight filtering factors. The stress constraint of the three models was the similar tendency at the beginning of the optimization process. Moreover, the stress histories were divergent from the bilinear elastoplastic material model due to the effect of cyclic loading and unloading point of the isotropic and kinematic hardening material. These effects caused a high interval of stress during the optimization process.

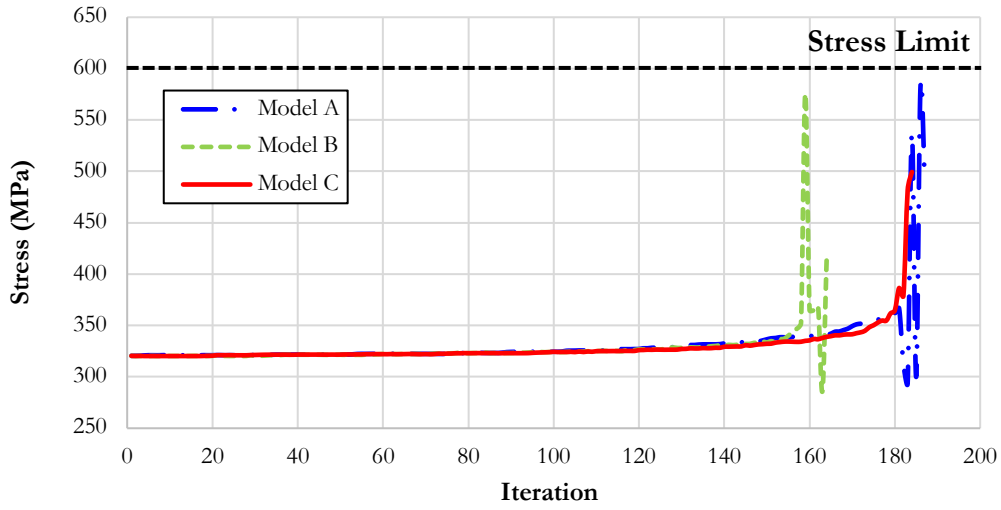

Figure 7.19 Maximum stress of three models during optimization process based on isotropic and kinematic hardening material.

The fluctuation of the stress occurred at the iteration instance 150, and the stress histories were plotted in figure 7.20 until the termination process. Model A and Model B occurred the swing effect of stress during the optimization process due to the cyclic load that forces the problem into tension and compression loads, and the unloading point of kinematic hardening material. The unloading point of the external load appeared when the load factor was equal to zero. The stress fluctuation of Model A and B obviously showed the high-stress interval between the maximum and minimum peaks, while Model C was optimized without the swing effect. The final layout of Model A and Model C occurred the maximum stress of 429 MPa and 414 MPa, respectively, which was lower than the maximum peaks of the optimization constraints. Model C caused the maximum stress of 499 MPa on the final layout, which is the maximum peak of the optimization constraints because Model C did not fluctuate. Moreover, the stress distribution on the final layout of Model C clearly demonstrated the fully stressed distribution when compared with the other two models. Therefore, the proposed weight filtering factor (Model C) was suitable for nonlinear topology optimization under the cyclic loading. Finally, 54% of the material amount can be removed from the initial design domain on Model C.

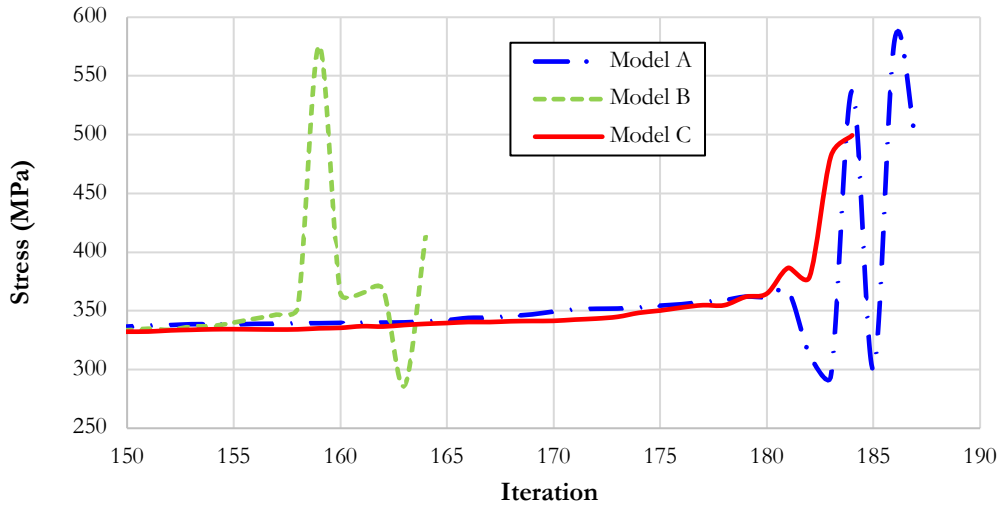

Figure 7.20 Stress fluctuation during the optimization process based isotropic and kinematic hardening material.

7.5 Conclusion

The nonlinear topology optimization was performed by applying an external cyclic loading. The proportional method was also employed to update an element density on each optimization iteration. An optimization process was investigated for acquiring an optimal layout on two material models: bilinear elastoplastic and isotropic and kinematic hardening properties. The characteristic of the cyclic load was specified based on the load factor value, which forced the problem into both tension and compression external loads. The objective of the optimization process is to maximize the internal energy of the whole design area and specified the allowable stress for the optimization constraint.

To acquire the optimal layout based on nonlinear topology optimization with cyclic loading, the new weight filtering factor was proposed to avoid the effects of cyclic loading, which increased the elemental stress of the plastic deformation period and were not constant throughout the analysis. The final layout was clearly obtained in the case of

bilinear elastoplastic material properties, with 33% removing the material from the initial design domain. While the isotropic and kinematic hardening material behavior, a stress fluctuation was observed during the topology optimization process. The new weight filtering factor can reduce the effect of stress fluctuation, and the final layout remained 46% of the material distribution of the design area.

Chapter 8

SUMMARY AND RECOMMENDATIONS

8.1 Summary

The aim of this dissertation is to implement and develop the algorithm for topology optimization with nonlinear material behaviors. The whole process to acquire an optimal layout consists of two subsections: structural analysis and optimization processes. An analysis by using LS-DYNA software and the optimization algorithm by coding on MATLAB were merged as illustrated in figure 8.1 to perform the problems on topology design smoothly. An application of crashworthiness design was concerned for nonlinear topology optimization. Thus, maximizing the internal energy of the design model was defined as the objective function of the optimization problem. Likewise, the optimization constraint was specified by allowable stress, which assigned for avoiding structural failure during the analysis process.

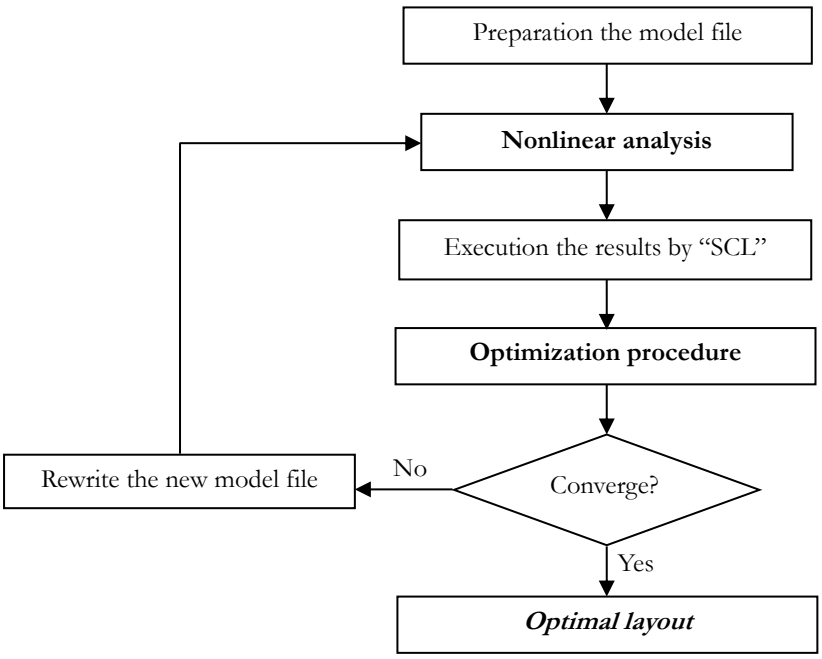

Figure 8.1 Summarization on the topology optimization process.

An updated procedure is necessary and important for the topology optimization process. This study proposed the proportional method, which is a non-sensitivity method and employed the update procedure during the nonlinear topology optimization process. Moreover, the criteria of fully stressed design for topology optimization were combined and formulated the update function based on the proportional technique. Firstly, the proportional method has verified the accuracy of the optimization algorithms by comparing the results with the conventional gradient-based method. The results from the optimization process showed that the final layout from the proportional procedure is significantly effective by comparing it with the sensitivity method. After that, the topology optimization was performed with applied external static loading to the structure based on the characteristic of bilinear elastoplastic material properties. The difference between the optimal layouts from linear and nonlinear material behaviors distinctly acquired based on the updating process of element densities with the proportional technique. Furthermore, the cyclic loading, in which the load value is not constant through the analysis procedure, was applied to optimize the structure under nonlinear topology design. The effects of cyclic

loading caused stress fluctuation during the optimization process when the unloading behavior was concerned with isotropic and kinematic hardening material properties. Finally, the new weigh filtering equation was proposed to optimize the structure under cyclic loading, and it can reduce the effects of stress fluctuation. The optimal layout with employing the new weight filtering factor was clearly obtained with the fully stress distribution inside the final structure. In summary, this dissertation provides the major contributions as following subsection.

8.1.1 Major Contributions

1. This study presented the nonlinear topology optimization based on the nonlinear material behaviors. A structure was analyzed by using the nonlinear analysis, and structural behaviors in permanent deformation (stress after the yielding point) were included in the optimization procedure. Stress distribution of the final layout demonstrated that the problem becomes a nonlinear problem. To support this contribution, numerical examples in chapter 5-7 showed findings for the nonlinear topology optimization.

2. This dissertation proposed an update function for nonlinear structural design by using the proportional method, which is a non-sensitivity method and formulated by combining the fully stressed design criteria. The elemental stress of the structure in the current optimization iteration was used to investigate and update the element densities of each design variable. The following information is finding to support this contribution.

   2-I) Chapter 5: The validation process of the proportional algorithms confirmed the accuracy of the update function and the updated procedure for nonlinear topology optimization problems. Furthermore, the optimal layout obtained a similar material distribution with a sensitive method.

   2-II) Chapter 6 and Chapter 7: Numerical examples were examined to confirm that the final layouts were acquired based on the proportional method.

3. This study investigated the nonlinear topology optimization process when the cyclic load was applied as an external load. Optimal layouts were differently obtained between applying the external static and cyclic loads. However, the cyclic loading caused the stress fluctuation during the optimization process when the unloading point was concerned with the optimization problems (chapter 7).

4. To reduce the stress fluctuation from the effects of cyclic loading, this dissertation proposed the new weight filtering equation for designing the structure under topology optimization. Numerical examples in chapter 7 were also examined the performance of the proposed weight filtering factor by comparing it with other filtering equations. Finally, the new weight filtering equation showed it was suitable for optimization with the cyclic load.

8.2 Future Recommendations

In addition to this dissertation, there are various points to develop and implement the performance for optimization on nonlinear topology design. So, several suggestions for implementing the nonlinear topology optimization are described as follows:

1. An optimization model can implement to three-dimensional model for the designing process. Due to this dissertation focused on optimizing the two-dimensional model only. So, this is one recommendation to carry out this study and examining the optimal layout under the nonlinear topology optimization process.

2. An optimization method can define by using other approaches, such as the level set method or evolutionary algorithm. If the different optimization approaches are applied to the nonlinear topology optimization process, there are other points to develop for increasing the performance. For example, the level set method is used for optimizing the structure, an implement on a level set function should be studied and proposed instead of the update function for nonlinear problems.

3. The development of the update function is one choice for implementing this dissertation. A characteristic of nonlinear material properties is very complex to anticipate a behavior on plastic deformation. So, an implementation of the update function should be interested in finding a suitable solution for each nonlinear optimization problem.

References

[1] Olason, A. and Tidman, D. (2010). ***Methodology for topology and shape optimization in the design process*** (Master's thesis). Retrieved from Chalmers University of Technology, Sweden.

[2] Sigmund, O. (2001). A 99 line topology optimization code written in Matlab. ***Structural and Multidisciplinary Optimization***, 21, 120-127.

[3] Andreassen, E., Clausen, A., Schevenels, M., Lazarov, B.S. and Sigmund, O. (2011). Efficient topology optimization in MATLAB using 88 lines of code. ***Structural and Multidisciplinary Optimization***, 43, 1-16.

[4] Liu, K., Tovar, A. (2014). An efficient 3D topology optimization code written in Matlab. ***Structural and Multidisciplinary Optimization***, 50, 1175-1196.

[5] Challis, V.J. (2010). A discrete level-set topology optimization code written in Matlab. ***Structural and Multidisciplinary Optimization***, 41, 453-464.

[6] Otomori, M., Yamada, T., Izui, K. and Nishiwaki, S. (2015). Matlab code for a level set-based topology optimization method using a reaction diffusion equation. ***Structural and Multidisciplinary Optimization***, 51, 1159-1172.

[7] Sethian, J.A. and Weigmann, A. (2000). Structural boundary design via level set and immersed interface methods. ***Journal of Computational Physics***, 163(2), 489-528.

[8] Yamada, T., Izui, K., Nishiwaki, S. and Takezawa, A. (2010). A topology optimization method based on the level set method incorporating a fictitious interface energy,

Computer Methods in Applied Mechanics and Engineering, 199(45-48), 2876-2891.

[9] Deng, S. and Suresh, K. (2016). Multi-constrained 3D topology optimization via augmented topological level-set. ***Computers and Structures***, 170, 1-12.

[10] Chen, T.Y. and Chiou, Y.H. (2013). Structural topology optimization using genetic algorithms. ***In the World Congress on Engineering 2013***, London, U.K.

[11] Hoshi, N. and Hasegawa, H. (2018). Aco topology optimization: the pheromone control for considering the mechanical Kansei, ***In 17th International Conference on Modeling and Applied Simulation***, Budapest, Hungary, 168-172.

[12] Zuo, Z.H. and Xie, Y.M. (2015). A simple and compact Python code for complex 3D topology optimization, ***Advances in Engineering Software***, 85, 1-11.

[13] Kurdi, M. (2015). A structural optimization framework for multidisciplinary design. ***Journal of Optimization***, 2015, 1-14.

[14] Kongwat, S., Jongpradist, P. and Kamnerdtong, T. (2016). Optimization of bus body based on structural stiffness and rollover constraints. ***In Asian Congress of Structural and Multidisciplinary Optimization 2016***, 22-26 May 2016, Nagasaki, Japan.

[15] Kongwat, S., Jongpradist, P., Kamnerdtong, T. and Hasegawa, H. (2016). Application of topology and size optimization to design of lightweight bus superstructure. ***In Japan Society of Mechanical Engineers, 12th Optimization Symposium***, 6-7 December 2016, Hokkaido, Japan.

[16] Hailu, G.S., Dereje, W.E. and Frkhuruldin, H.M. (2017). A comparative study on stress and compliance based structural topology optimization, **P*roc. of IOP Conf. Series: Materials Science and Engineering***, 24, 1-7.

[17] Xia, L., Fritzen, F. and Breitkopf, P. (2017). Evolutionary topology optimization of

elastoplastic structures. ***Structural and Multidisciplinary Optimization***, 55(2), 569-581.

[18] Huang, X. and Xie, Y.M. (2008). Topology optimization of nonlinear structures under displacement loading. ***Engineering Structures***, 30, 2057-2068.

[19] Gomes, F.A.M. and Senne, T.A. (2014). An algorithm for the topology optimization of geometrically nonlinear structures, ***International Journal for Numerical Methods in Engineering***, 99(6), 391-409.

[20] Castro, S.L.C., Gomes, F.A.M. and Santos S.A. (2016). Level set-based topology optimization using nonlinear programming: a preliminary study. ***Proc. of the XXXVII Iberian Latin-American Congress in Computational Methods in Engineering***, Brazil, 6-9 November 2016.

[21] Xia, Q. and Shi, T. (2016). Stiffness optimization of geometrically nonlinear structures and the level set based solution. ***International Journal for Simulation and Multidisciplinary Design Optimization***, 7(A3), 1-13.

[22] Yamada, T., Manabe, M., Izui, K. and Nishiwaki, S. (2013). A topology optimization method for geometrically nonlinear problems incorporating level set boundary expressions and a particle method. ***Journal of Advanced Mechanical Design, Systems, and Manufacturing***, 7(4), 630-643.

[23] Xia, L. and Breitkopf, P. (2014). A reduced multiscale model for nonlinear structural topology optimization. ***Computer Methods in Applied Mechanics and Engineering***, 280, 117-134.

[24] Eom, Y.-S. and Han, S.-Y. (2014). A new topology optimization scheme for nonlinear structures. ***Journal of Mechanical Science and Technology***, 28 (7), 2779-2786.

[25] Chang, D.-H., Yoo, K.-S., Park, J.-Y. and Han, S.-Y. (2012). Optimum design for nonlinear problems using modified ant colony optimization. ***Proc. in 2012 International Conference on Software and Computer Applications***, Singapore,

45-49.

[26] He, Q., Kang, Z. and Wang, Y. (2014). A topology optimization method for geometrically nonlinear structures with meshless analysis and independent density field interpolation. ***Computational Mechanics***, 54, 629-644.

[27] Yoon, G.-H. and Kim, Y.-Y. (2007). Topology optimization of material-nonlinear continuum structures by the element connectivity parameterization. ***International Journal for Numerical Methods in Engineering***, 69(10), 2196-2218.

[28] Yoon, G.-H., Joung, Y.-S. and Kim, Y.-Y. (2007). Optimal layout design of three-dimensional geometrically non-linear structures using the element connectivity parameterization method. ***International Journal for Numerical Methods in Engineering***, 69(6), 1278-1304.

[29] Gea, H.C. and Luo. J. (2001). Topology optimization of structures with geometrical nonlinearities. ***Computers and Structures***, 79, 1977-1985.

[30] Buhl, T., Pedersen, C. and Sigmund, O. (2000). Stiffness design of geometrically nonlinear structures using topology optimization. ***Structural and Multidisciplinary Optimization***, 19, 93-104.

[31] Biyikli, E. and To, A.C. (2015). Proportional topology optimization: a new non-sensitivity method for solving stress constrained and minimum compliance problems and its implementation in MATLAB. ***PLoS ONE***, 10(12), 1-23.

[32] Zhifang, F., Junpeng, Z. and Chunjie, W. (2016). Robust topology optimization under loading uncertainty with proportional topology optimization method. ***Proc. in 2016 Eight International Conference on Measuring Technology and Mechatronics Automation***, Macau, China, 584-588.

[33] Cui, M., Zhang, Y., Yang, X. and Luo, C. (2018). Multi-material proportional topology optimization based on the modified interpolation scheme. ***Engineering with Computers***, 34(2), 287-305.

[34] Sigmund, O. (2007). Morphology-based black and white filters for topology optimization. ***Structural and Multidisciplinary Optimization***, 33(4-5), 401-424.

[35] Guest, J.K., Prévost, J.H. and Belytschko, T. (2004). Achieving minimum length scale in topology optimization using nodal design variables and projection functions. ***International Journal for Numerical Methods in Engineering***, 61(2), 238-254.

[36] Guest, J.K. (2009). Topology optimization with multiple phase projection. ***Computer Methods in Applied Mechanics and Engineering***, 199(1-4), 123-135.

[37] Babuška, I. (1976). Solution of interface problems by homogenization. I. ***SIAM Journal on Mathematical Analysis***, 7(5), 603-634.

[38] Cioranescu, D. and Paulin, J.S.J. (1979). Homogenization in open sets with holes. ***Journal of Mathematical Analysis and Applications***, 71(2), 590-607.

[39] Bendsøe, M.P. and Kikuchi, N. (1988). Generating optimal topologies in structural design using a homogenization method. ***Computer Methods in Applied Mechanics and Engineering***, 71, 197-224.

[40] Abdi, M. (2015). ***Evolutionary topology optimization of continuum structure using X-FEM and isovalues of structural performance***. (Doctor's dissertation). Retrieved from University of Nottingham, England.

[41] Yang, X.Y., Xie, Y.M., Steven, G.P., and Querin, O.M., (1999). Bidirectional evolutionary method for stiffness optimisation. ***AIAA***, 37(11), 1483-1488.

[42] Querin, O.M., Steven, G.P. and Xie, Y.M. (2000). Evolutionary Structural optimization using an additive algorithm. ***Finite Element in Analysis and Design***, 34, 291-308.

[43] Huang, X. and Xie, Y.M. (2013). Convergent and mesh-independent solutions for the bi-directional evolutionary structural optimization method. ***Finite Elements in Analysis and Design***, 43, 1039-1049.

[44] Querin, O.M., Young V., Steven, G.P. and Xie, Y.M. (2000). Computational Efficiency and validation of bi-directional evolutionary structural optimization. ***Computer Methods in Applied Mechanics and Engineering***, 189(2), 559-573.

[45] Huang, X. and Xie, Y. M. (2010). A further review of ESO type methods for topology optimization. ***Structural and Multidisciplinary Optimization***, 40(1-6), 409-416.

[46] Zhou, M. and Rozvany, G.I.N. (2001). On the validity of ESO type methods in topology optimization. ***Structural and Multidisciplinary Optimization***, 21(1), 80-83.

[47] Holland, J.H. (1975). ***Adaptation in national and artificial systems***. University of Michigan Press, Ann Arbor, USA.

[48] Goldberg, D. E. (1989). ***Genetic algorithms in search, optimization and machine learning***. Reading: Addison-Wesley.

[49] Jakiela, M., Chapman, C., Duda, J., Adewuya, A., Saitou, K. (1999). Continuum structural topology design with genetic algorithms. ***Computer Methods in Applied Mechanics and Engineering***, 186(2), 339-356.

[50] Chapman, C.D. and Jakiela, M.J. (1996). Genetic algorithm-based structural topology design with compliance and topology simplification considerations. ***Journal of Mechanical Design***, 118(1), 89-98.

[51] Wang, S.Y. and Tai, K. (2005). Structural topology design optimization using genetic algorithms with a bit-array representation. ***Computer Methods in Applied Mechanics and Engineering***, 194(36-38), 3749-3770.

[52] Kane, C. and Schoenauer, M. (1997). Topological optimum design using genetic algorithms. ***Control and Cybernetics***, 25(5), 1059-1088.

[53] Jakiela, M., Chapman, C., Duda, J., Adewuya, A. and Saitou, K. (1999). Continuum structural topology design with genetic algorithms. ***Computer Methods in Applied***

Mechanics and Engineering, 186(2-4), 339-356.

[54] Osher, S. and Sethian, J.A. (1988). Fronts propagating with curvature-dependent speed: algorithms based on Hamilton-Jacobi formulations. ***Journal of Computational Physics***, 79(1), 12-49.

[55] Allaire, G., Jouve, F. and Toader, A.M. (2004). Structural optimization using sensitivity analysis and a level-set method. ***Journal of Computational Physics***, 194(1), 363-393.

[56] Wang, M.Y., Wang, X. and Guo, D. (2003). A level set method for structural topology optimization. ***Computer Methods in Applied Mechanics and Engineering***, 192(1-2), 227-246.

[57] Osher, S. and Fedkiw, R.P. (2001). Level set methods: an overview and some recent results. ***Journal of Computational Physics***, 169(2), 463-502.

[58] Sethian, J.A. (2001). Evolution, implementation, and application of level set and fast marching methods for advancing fronts. ***Journal of Computational Physics***, 169(2), 503–555.

[59] Osher, S. and Fedkiw, R.P. (2003). ***Level set methods and dynamic implicit surfaces***, vol 153. Springer, New York.

[60] Sethian, J.A. (1999). ***Level set methods and fast marching methods: evolving interfaces in computational geometry, fluid mechanics, computer vision, and materials science***. Cambridge University Press, Cambridge.

[61] Petersson, J. and Sigmund, O. (1998). Slope constrained topology optimization. ***International Journal for Numerical Methods in Engineering***, 41(8), 1417–1434.

[62] Bendsøe, M.P. and Sigmund, O. (2004). ***Topology optimization-theory, methods and applications***. Springer, Berlin

[63] Lee, E. (2012). ***Stress-constrained structural topology optimization with design-dependent loads*** (Master's thesis). Retrieved from Graduate Department of Institute for Aerospace Studies, University of Toronto.

[64] Bendsøe, M.P. and Sigmund, O. (1999). Material interpolation schemes in topology optimization. ***Archive of Applied Mechanics***, 69, 635-654.

[65] Sigmund, O. and Petersson, J. (1998). Numerical instabilities in topology optimization: A survey on procedures dealing with checkerboards, mesh-dependencies and local minima. ***Structural Optimization***, 16, 68-75.

[66] Aremu, A., Ashcroft, I., Wildman, R, Hague, R., Tuck, C., Brackett, D. (2013). The effects of bidirectional evolutionary structural optimization parameters on an industrial designed component for additive manufacture. ***Proc. of the Institution of Mechanical Engineers, Part B: Journal of Engineering Manufacture***, 227(6), 794-807.

[67] Diaz, A. and Sigmund, O. (1995). Checkerboard patterns in layout optimization. ***Structural Optimization***, 10, 40-45.

[68] Bathe, K.-J. (1996). ***Finite Element Procedure***. United States of America: Prentice-Hall International, Inc.

[69] Hallquist, J.-O. (2006). ***LS-DYNA Theory Manual***. California: Livermore Software Technology Corporation.

[70] Goyal, C.-R. (2017). ***Uncertainty Quantification in Non-linear Seismic Wave Propagation*** (Master's thesis). Retrieved from University of Ottawa, Canada.

[71] U.S. Department of Transportation, National Highway Traffic Safety Administration (NHTSA). (2012). ***Traffic Safety Facts 2012*** Retrieved from https://crashstats.nhtsa.dot.gov/Api/Public/ViewPublication- /812032.

[72] United Nations Economic Commission for Europe. (2006). ***Large Passenger***

Vehicles with Regard to the Strength of their Superstructure, United Nations, Vol. 1.

[73] Sinabuth, D., Benyajati, C., Lapapong, S. and Pimsarn, M. (2012, October). Finite Element Analysis of an Electric Bus Body Structure in Real Driving Conditions. ***The 3rd TSME International Conference on Mechanical Engineering***, Chiang Rai, Thailand.

[74] Khot, N.S. (1982). ***Optimality criterion methods in structural optimization*** (Technical report AFWAL-TR-81-3124). Analysis & Optimization Branch and Structures & Dynamics Division.

[75] Patnaik, S.N., Guptill, J.D. and Berke, L. (1993). ***Merits and limitations of optimality criteria method for structural optimization*** (NASA technical paper 3373). National Aeronautics and Space Administration, Office of Management, Scientific and Technical Information Division.

[76] Shukla, A. and Misra, A. (2013). Review of optimality criterion approach scope, limitation and development in topology optimization. ***International Journal of Advances in Engineering & Technology***, 6(4), 1886-1889.

[77] Chiandussi, G., Codegoneb, M. and Ferrero, S. (2009). Topology optimization with optimality criteria and transmissible loads. ***Computers and Mathematics with Applications***, 57, 772-788.

[78] U. Kirsch (1993). ***Structural Optimization: Fundamentals and Applications***. New York, Springer-Verlag.

[79] Livermore Software Technology Corporation: ***The LS-TaSC topology and shape computation***, Theory manual, version 3.2, 2006.

[80] Burns, T.E. and Tortorelli, D.A. (2001). Topology optimization of non-linear elastic structures and compliant mechanisms. ***Computer Methods in Applied Mechanics and Engineering***, 26-27, 3443-3459.

[81] Maute, K., Schwarz, S. and Ramm, E. (1998). Adaptive topology optimization of elastoplastic structures. ***Structural Optimization***, 15, 81-91.

Appendix A

List of Publications

A.1 International Journal Paper

[J.1] **Kongwat, S.** and Hasegawa, H., 2020, "New weight filtering factor of nonlinear design for topology optimization under cyclic loading based on proportional technique", ***Journal of Mechanical Science and Technology***, Vol. 34, No. 4, pp. 1635 – 1644.

[J.2] **Kongwat, S.** and Hasegawa, H., 2020, "A study on proportional topology optimization for nonlinearities material with cyclic load", ***International Journal of Materials Science and Engineering***, Vol. 6, No. 2, pp. 7 – 14.

[J.3] **Kongwat, S.** and Hasegawa, H., 2019, "Optimization on mechanical structure for material nonlinearity based on proportional topology method", ***Journal of Advanced Simulation in Science and Engineering***, Vol. 6, No. 2, pp. 354 – 366.

A.2 International Conference (peer-reviewed)

[C.1] **Kongwat, S.** and Hasegawa, H., 2019, "A proportional algorithm of topology design by considering nonlinear material geometry", ***23rd International Conference on Computer Methods in Mechanics***, 8-12 September 2019, Krakow, Poland.

[C.2] **Kongwat, S.** and Hasegawa, H., 2019, "A study on proportional topology optimization for nonlinearities material with cyclic load", ***Proceeding of 6th International Conference on Mechanical, Electronics and Computer Engineering***, 25-27 August 2019, pp. 16, Hong Kong.

[C.3] **Kongwat, S.** and Hasegawa, H., 2018, "Structural optimization for mechanical structure under linear and nonlinear geometry by using topological technique", ***Proceedings of the 13th World Congress in Computational Mechanics***, 22-27 July 2018, pp. 1552, New York, USA.

[C.4] **Kongwat, S.** and Hasegawa, H., 2018, "Topology optimization of mechanical structure under nonlinear geometry with power law of plasticity", ***Asian Congress of Structural and Multidisciplinary Optimization 2018***, 21-24 May 2018, Dalian, China.